

ABSTRACT

Title of Dissertation: MICROPLASTIC INTERACTIONS AND EFFECTS ON *Crassostrea virginica* LARVAE

Christine Marissa Knauss, Doctor of Philosophy, 2021

Dissertation directed by: Professor Jeffrey C. Cornwell, Marine Estuarine Environmental Science

Professor Alba Torrents, Civil and Environmental Engineering

Microplastic pollution is a complex global issue, with millions of tons of plastic reaching marine ecosystems yearly. Oysters are keystone species, providing vital ecosystem services and, as filter feeders, they encounter high numbers of suspended particles. Therefore, oysters are highly susceptible to microplastic pollution exposure. Although microplastic effects on adult life stages of filter feeding bivalves have been studied, effects on larval life stages have fewer observations. This research examined the interactions and effects of microplastic ingestion on the larval stage of *Crassostrea virginica* and developed a method to manufacture standardized microfibers to make laboratory exposure experiments more environmentally relevant. Initial experiments addressed factors affecting larval microplastic ingestion, microplastic ingestion capacity, and egestion. In subsequent experiments, I exposed

oyster larvae to microplastics of various sizes, particle types, and polymers, at ingestion threshold concentrations, using physiological effects from ingestion to determine early life stage effects.

Larval oysters readily ingested microplastics. Food availability was not a factor for microplastic ingestion but microplastic concentrations of exposure solutions were important. Microplastic ingestion followed a saturation curve model, with saturation occurring at extremely high concentrations. As microplastic pollution increases in the environment, larval oysters will increase their ingestion of plastic particles. However, microbead ingestion did not cause significant physiological effects and experiments on microfiber ingestion suggested minimal effects on physiology. Therefore, microplastics likely pose minimal risks to larval oysters with current and near future environmental microplastic pollution levels. In this dissertation, I provide the first observations regarding the interactions and effects of microplastic pollution on the larval life stage of bivalve filter feeders.

MICROPLASTIC INTERACTIONS AND EFFECTS ON *Crassostrea virginica*
LARVAE

by

Christine Marissa Knauss

Dissertation submitted to the Faculty of the Graduate School of the
University of Maryland, College Park, in partial fulfillment
of the requirements for the degree of
Doctor of Philosophy
2021

Advisory Committee:

Dr. Jeffrey Cornwell, Co-Chair

Dr. Alba Torrents, Co-Chair

Dr. James Pierson

Dr. Lance Yonkos, Committee Member and Dean's Representative

Dr. Sherri Mason, The Pennsylvania State University Behrend

© Copyright by
Christine Marissa Knauss
2021

Dedication

To my sister, you are a constant reminder to let the music dance to me.

Acknowledgements

First, I would like to thank my advisors, Jeff Cornwell and Alba Torrents for your gentle guidance and support over the last years. You were like lighthouses guiding me when I lost my way. Thank you for your unwavering trust, knowing that I would work hard to conduct good science. You gave me the freedom to follow my passions and test my creativity, and allowed me to find my own scientific voice. Your continued positivity and support helped me through the most difficult challenges of my dissertation.

I want to thank my committee, Lance Yonkos, Jamie Pierson, and Sam Mason, for helping me on this journey. You have provided valuable guidance, advice, and mentorship. Lance, thank you for our long discussions on microplastic methods and details. I have learned so much from you about approaching research questions in a thorough and methodical way. Jamie, thank you for all of your help sorting out what my messy ingestion data mean and for always lending an ear when I needed it. Sam, I am forever grateful for our serendipitous meeting at the International Marine Debris Conference. I was there by myself and you and Amy immediately took me under your wings. I have learned so much about the field and about life from you.

I want to extend a very special thank you to the current and past HPL Oyster Hatchery staff: Steph, Jeff, Alex, Lisa, Julie, Alicia, Stacey, Bob, Shannon, Steven, Dakota, and Alan. You welcomed me so graciously in 2014 and never looked back. Without you, none of this work would have been possible. All of you were always willing to help me by sharing your knowledge, talking through problems, answering my questions, teaching me how to do things, lending a helping hand, and having fun when I needed it. I am so appreciative of your time, effort, support, and friendship.

Also, a very big thank you to Katie McFarland. You came to HPL at the most difficult time of my dissertation and became, not just mine but, all HPL grad students' biggest supporter. You are one of the best mentors I have ever had and, even though you are constantly busy doing amazing research, you always make time for me. I would not have finished my research without you. Thank you for your unconditional support and friendship.

I want to thank Hannah Morrisette for our consistent morning zoom writing sessions. This dissertation would not have come together without them or you. I am grateful for your support in the final months of this dissertation and for your friendship.

Thank you to my first advisor, Dr. Mutt Merritt. You provided me with an amazing opportunity to follow my passion of plastic pollution research and believed in me from the beginning.

Thank you to the Izaak Walton League of America, the Cooperative Institute for the North Atlantic Region, and the HPL Education Committee for providing funding

which allowed me to share my research at international conferences and learn from the best scientists in the field.

I want to thank the HPL maintenance crew, Ralph Kimes, Gordy Dawson, and Chris Farnell, for always helping me make things work, especially when I broke them. Thank you to Jacob Cram and Klaus Huebert for your help with statistics and R.

I want to thank my friends for all of their encouragement over the years. There was only ever support when I had to leave early or come late to important events because the oysters would die without me!

I want to thank my family, especially my grandparents. I will cherish all the time that we got to spend together, with us living so close. Late afternoon pool breaks and cocktails always helped me get through extremely challenging and long summer experiment seasons.

Lastly, I would like to thank my parents for always encouraging me to be whatever I wanted to be and giving me space to explore my passions. Without your support, I would not be here.

Table of Contents

Dedication	ii
Acknowledgements	iii
Table of Contents	v
List of Tables	vii
List of Figures	viii
Chapter 1: Introduction and Overview	1
Plastic Pollution	1
<i>Crassostrea virginica</i>	7
Dissertation overview	10
Chapter 2: The effects of food availability and microplastic availability on the uptake of polystyrene microbeads in Eastern oyster larvae	12
Abstract	12
Introduction	13
Methods	17
Results	22
Method 1	23
Method 2	25
Discussion	32
Conclusion	36
Supporting Information	37
Chapter 3: Physiological Effects of Microbeads on <i>Crassostrea virginica</i> Larvae....	41
Abstract	45
Introduction	46
Methods	50
Experimental design	51
Respiration rate measurements	54
Discussion	62
Supporting Information	67
Chapter 4: Physiological Effects of Microfibers on <i>Crassostrea virginica</i> Larvae....	71
Abstract	71
Introduction	72
Methods	75
Subsampling and larval growth measurements	80
PET fiber exposure	86
Nylon fiber exposure	90
Discussion	94
Supporting Information	99
Chapter 5: A Paraffin Microtomy Method for Improved and Efficient Production of Standardized Plastic Microfibers	103
Abstract	103
Introduction	104
Materials and Methods	108
Fiber selection	108

Fiber winding and paraffin embedding.....	108
Microfiber cutting	110
Post-microtomy processing.....	111
Microfiber analysis	112
Statistical analysis.....	113
Proof of application.....	113
Results.....	114
Discussion	118
Paraffin method assessment.....	118
Proof of application.....	123
Conclusions.....	124
Supporting Information.....	126
Chapter 6: Conclusions	132
Bibliography	137

List of Tables

- Table 1.1 Previous microplastic studies using the bivalves *Crassostrea gigas* (*C. gigas*) and *Crassostrea virginica* (*C. virginica*).
- Table 2.2 Design parameters used in Method 1 feeding experiments of *Crassostrea virginica* larvae. Larvae were exposed to a full-factorial design of different polystyrene (PS) microbeads and *Isochrysis galbana* (*I. galbana*).
- Table 2.3 Design parameters used in Method 2 feeding experiments. *Isochrysis galbana* (*I. galbana*) and polystyrene (PS) microbead concentrations used for each days-post-fertilization (dpf) of *Crassostrea virginica* larvae. *I. galbana* concentrations represent either 0%, 50%, or 100% of optimal larval diet (based on dpf) and microbead concentrations represent 0%, 0.1%, or 10% of optimum algal cell concentration.
- Table S2.1: Modified Artificial Seawater
- Table 3.1 Design parameters used for *Crassostrea virginica* (*C. virginica*) larval exposures to polystyrene (PS) microbeads and fed with *Isochrysis galbana* (*I. galbana*).
- Table 3.2 *Crassostrea virginica* (*C. virginica*) larval lengths ($\mu\text{m} \pm \text{SD}$) before and after 4- and 6- day polystyrene (PS) microbead exposures.
- Table S3.1 Modified Artificial Seawater
- Table S3.2 Data means (\pm SE) for physiological measurements of *Crassostrea virginica* (*C. virginica*) larvae after exposure to polystyrene (PS) microbeads.
- Table 4.1 Design parameters used for *Crassostrea virginica* (*C. virginica*) larval exposures to nylon 6, 6 and polyethylene terephthalate (PET) microfibers and fed with *Chaetoceros muelleri* (CHGRA) and *Tetraselmis chuii* (PLY429).
- Table S4.1 Modified Artificial Seawater
- Table S4.2 Data means (\pm SE) for physiological measurements of *Crassostrea virginica* (*C. virginica*) larvae after exposure to polyethylene terephthalate (PET) or nylon 6,6 microfibers.
- Table 5.1 Microfiber target lengths and mean cut lengths for polyethylene terephthalate (PET) and nylon 6, 6.

List of Figures

- Figure 2.1 Polystyrene microbeads in *Crassostrea virginica* larvae after a 24-hour exposure to 2 μm microbeads at 2×10^3 beads mL^{-1} treatment (A, B, 1 day-post-fertilization) and 6 μm microbeads at 5×10^3 beads mL^{-1} treatment (C, D, 5 day-post-fertilization).
- Figure 2.2 Average number of polystyrene (PS) microbeads in *Crassostrea virginica* larvae after ingestion for each microbead solution. A) 2 μm microbeads B) 6 μm microbeads. The experiment consisted of a full factorial design of four concentrations of *Isochrysis galbana* algal cells and five concentrations of PS microbeads (0, 10, 20 $\times 10^3$ cells mL^{-1} ; 0, 0.02, 2, 10, 20 $\times 10^3$ beads mL^{-1}). Larvae were exposed to the solutions for 24 hours. Each combination of feeding conditions was replicated across three broods for 2 μm (n=450) and two broods for 6 μm (n=300). A box plot for 6 μm data was not used because microbead ingestion was so low that the interquartile range was too small to show boxes. Statistical differences in the average number of beads ingested ind^{-1} are indicated by letters (two-way ANOVAs and Tukey's post hoc tests, $p < 0.05$). Note the differences in y-axis scales between A and B.
- Figure 2.3 Polystyrene (PS) microbead ingestion saturation in *Crassostrea virginica* larvae (1-day-post-fertilization) for exposures to 2 μm PS beads and all algal concentrations. Trendline represents the model fit of the Holling's Type II functional response equation: $y = y_{\max} \frac{[x]}{[x] + x_{\text{half}}}$ with $R^2 = 0.885$, $y_{\max} = 10.145$ beads ingested ind^{-1} , and $x_{\text{half}} = 5,295$ beads mL^{-1} .
- Figure 2.4 *Crassostrea virginica* larval (1-day post-fertilization) average polystyrene (PS) microbead ingestion after 24-hour exposure. Statistical differences in the average number of beads ingested ind^{-1} are indicated by letters (two-way ANOVA and Tukey's post hoc tests, $p < 0.05$). Error bars represent standard deviation.
- Figure 2.5 *Crassostrea virginica* larval (1-day post-fertilization) egestion of 2 μm polystyrene (PS) microbeads for A) 20 beads mL^{-1} and B) 2,000 beads mL^{-1} . Note the differences in y-axis scales between A and B. Error bars represent standard deviation. Larvae exposed to 2,000 beads mL^{-1} and 0 cells mL^{-1} had significantly more microbeads ind^{-1} than the other two algal treatments at 6- and 24-hour time points (two-way ANOVAs with Tukey's post hoc tests, $p < 0.05$). Statistical significance of average beads ingested ind^{-1} within algal treatments over time were excluded for clarity.
- Figure 2.6 *Crassostrea virginica* larval (5-days-post-fertilization) average polystyrene (PS) microbead ingestion after 24-hour exposure. Statistical differences in the average number of beads ingested ind^{-1} are indicated by letters (two-

way ANOVA and Tukey's post hoc tests, $p < 0.05$). Error bars represent standard deviation.

Figure 2.7 *Crassostrea virginica* larval (5-days-post-fertilization) egestion of 2 μm polystyrene (PS) microbeads for A) 50 beads mL^{-1} and B) 5,000 beads mL^{-1} . Note the differences in y-axis scales between A and B. Error bars represent standard deviation. No statistical significance was observed between the average number of beads ingested ind^{-1} for each time point (two-way ANOVAs with Tukey's post hoc tests, $p < 0.05$).

Figure 2.8 *Crassostrea virginica* larval (1-day-post-fertilization) average polystyrene (PS) microbead ingestion after 24-hour exposure. Statistical differences in the average number of beads ingested ind^{-1} are indicated by letters (two-way ANOVA and Tukey's post hoc tests, $p < 0.05$). Error bars represent standard deviation.

Figure 2.9 *Crassostrea virginica* larval (1-day-post-fertilization) egestion of 6 μm polystyrene (PS) microbeads for 2,000 beads mL^{-1} . Error bars represent standard deviation. No statistical significance was observed between the average number of beads ingested ind^{-1} for each time point (two-way ANOVA with Tukey's post hoc tests, $p < 0.05$).

Figure 2.10 *Crassostrea virginica* larval (5-days-post-fertilization) average polystyrene (PS) microbead ingestion after 24-hour exposure. Statistical differences in the average number of beads ingested ind^{-1} are indicated by letters (two-way ANOVA and Tukey's post hoc tests, $p < 0.05$). Error bars represent standard deviation.

Figure 2.11 *Crassostrea virginica* larval (5-days-post-fertilization) egestion of 6 μm polystyrene (PS) microbeads for A) 50 beads mL^{-1} and B) 5,000 beads mL^{-1} . Note the differences in y-axis scales between A and B. Error bars represent standard deviation. Larvae exposed to 50 beads mL^{-1} and 50,000 cells mL^{-1} had a significantly higher average number of beads ingested ind^{-1} compared to the 0 cells mL^{-1} treatment at 6 hours (two-way ANOVAs with Tukey's post hoc tests, $p < 0.05$). Larvae exposed to 5,000 beads mL^{-1} and 50,000 cells mL^{-1} had significantly higher average numbers of beads ingested ind^{-1} compared to 0 and 25,000 cells mL^{-1} treatments at 6 hours and the 0 cells mL^{-1} treatment at 1 and 24 hours (two-way ANOVAs with Tukey's post hoc tests, $p < 0.05$). Statistical significance of average beads ingested ind^{-1} within algal treatments over time were excluded for clarity.

Figure S2.1 Polystyrene (PS) microbead ingestion saturation in *Crassostrea virginica* larvae (1-day-post-fertilization) for exposures to 6 μm PS beads and all algal concentrations. Trendline represents the model fit of the Holling's

Type II functional response equation: $y = y_{max} \frac{[x]}{[x] + x_{half}}$ with $R^2 = 0.868$, $y_{max} = 0.765$ beads ingested ind^{-1} , and $x_{half} = 65,297$ beads mL^{-1} .

Figure S2.2 Histogram depicting 2 μm polystyrene microbead burden for each larva (1 day-post-fertilization) for three algal concentrations used in Method 2 (0, 10, 20 10^3 cells mL^{-1}) over the egestion period. Time zero is after a 24-hour ingestion exposure to 20 microbeads mL^{-1} and egestion subsamples were taken 1, 6, and 24 hours after placement in microbead free water. Microbead burden was assessed by observing the number of microbeads in each individual.

Figure S2.3 Histogram depicting 2 μm polystyrene microbead burden for each larva (1 day-post-fertilization) for three algal concentrations used in Method 2 (0, 10, 20 10^3 cells mL^{-1}) over the egestion period. Time zero is after a 24-hour ingestion exposure to 2,000 microbeads mL^{-1} and egestion subsamples were taken 1, 6, and 24 hours after placement in microbead free water. Microbead burden was assessed by observing the number of microbeads in each individual.

Figure S2.4 Histogram depicting 2 μm polystyrene microbead burden for each larva (5 days-post-fertilization) for three algal concentrations used in Method 2 (0, 25, 50 10^3 cells mL^{-1}) over the egestion period. Time zero is after a 24-hour ingestion exposure to 50 microbeads mL^{-1} and egestion subsamples were taken 1, 6, and 24 hours after placement in microbead free water. Microbead burden was assessed by observing the number of microbeads in each individual.

Figure S2.5 Histogram depicting 2 μm polystyrene microbead burden for each larva (5 days-post-fertilization) for three algal concentrations used in Method 2 (0, 25, 50 10^3 cells mL^{-1}) over the egestion period. Time zero is after a 24-hour ingestion exposure to 5,000 microbeads mL^{-1} and egestion subsamples were taken 1, 6, and 24 hours after placement in microbead free water. Microbead burden was assessed by observing the number of microbeads in each individual.

Figure S2.6 Histogram depicting 6 μm polystyrene microbead burden for each larva (1 day-post-fertilization) for three algal concentrations used in Method 2 (0, 10, 20 10^3 cells mL^{-1}) over the egestion period. Time zero is after a 24-hour ingestion exposure to 2,000 microbeads mL^{-1} and egestion subsamples were taken 1, 6, and 24 hours after placement in microbead free water. Microbead burden was assessed by observing the number of microbeads in each individual.

Figure S2.7 Histogram depicting 6 μm polystyrene microbead burden for each larva (5 days-post-fertilization) for three algal concentrations used in Method 2

(0, 25, 50 10^3 cells mL^{-1}) over the egestion period. Time zero is after a 24-hour ingestion exposure to 50 microbeads mL^{-1} and egestion subsamples were taken 1, 6, and 24 hours after placement in microbead free water. Microbead burden was assessed by observing the number of microbeads in each individual.

Figure S2.8 Histogram depicting 6 μm polystyrene microbead burden for each larva (5 days-post-fertilization) for three algal concentrations used in Method 2 (0, 25, 50 10^3 cells mL^{-1}) over the egestion period. Time zero is after a 24-hour ingestion exposure to 5,000 microbeads mL^{-1} and egestion subsamples were taken 1, 6, and 24 hours after placement in microbead free water. Microbead burden was assessed by observing the number of microbeads in each individual.

Figure 3.1 Conceptual diagram of treatment sampling for the 4- and 6-day exposures. The 6-day exposure began 13 days post fertilization (dpf), while the 4-day exposure began 15 dpf. On day 19, both experiments were terminated and larvae were concentrated and subsampled for physiological measurements. Green boxes indicate all time points where larvae were subsampled for analysis.

Figure 3.2 Filter manifold used to separate and collect *Crassostrea virginica* (*C. virginica*) larvae and *Isochrysis galbana* (*I. galbana*) for analysis in the liquid scintillation analyzer. Samples are poured through the blue 40 μm sieves on top of the steel cylinders. Glass fiber filters (Whatman 0.7 μm pore size) catch ^{14}C labelled algal cells at the bottom of the steel cylinders.

Figure 3.3 Physiological responses of *Crassostrea virginica* (*C. virginica*) larvae after a 4-day exposure to polystyrene microbeads. (A) larval size, (B) respiration rates, (C) algal ingestion rates, and (D) carbon assimilation rates were measured on day 4. No statistical differences (using one way ANOVA, $p > 0.05$) were observed between all three treatments in respiration, algal ingestion, and carbon assimilation rates or larval size. Error bars show standard error.

Figure 3.4 Physiological responses of *Crassostrea virginica* (*C. virginica*) larvae after a 6-day exposure to 100 and 1000 polystyrene microbeads mL^{-1} . (A) larval size and (B) respiration rates were measured on day 6 and (C) algal ingestion and (D) carbon assimilation rates were measured on days 3 and 6. ANOVAs and Tukey's post hoc tests show no significant differences in larval size or respiration, algal ingestion, and carbon assimilation rates ($p > 0.05$). Error bars show standard error.

Figure S3.1 Conceptual diagram for ^{14}C radio-labelled phytoplankton method steps.

Figure S3.2 Respiration (A) and carbon assimilation (B) rates for *Crassostrea virginica* (*C. virginica*) larvae (8 days post fertilization, 80 - 150 μm) exposed to 10 and 100 polystyrene microbeads mL^{-1} after 3 and 2 days respectively. ANOVAs ($p > 0.05$) show no significant differences between treatments. Error bars show standard error.

Figure 4.1 *Crassostrea virginica* (*C. virginica*) larval exposure to nylon 6, 6 (10 x 10 μm , 10 x 30 μm) or polyethylene terephthalate (PET, 14 x 14 μm , 14 x 28 μm) microfibers at 100 and 1000 fiber mL^{-1} . Larvae and all particles were kept in suspension by aeration with glass tubes.

Figure 4.2 Filter manifold used to separate and collect *Crassostrea virginica* (*C. virginica*) larvae and *Isochrysis galbana* (*I. galbana*) for analysis in the liquid scintillation analyzer. Samples are poured through the blue 40 μm sieves on top of the steel cylinders. Glass fiber filters (Whatman 0.7 μm pore size) catch ^{14}C labelled algal cells at the bottom of the steel cylinders.

Figure 4.3 *Crassostrea virginica* (*C. virginica*) larva with three Nile red stained, 14 x 28 μm polyethylene terephthalate (PET) microfibers in its gut after six days of exposure to 1000 fiber mL^{-1} . Larva was visualized and imaged using an Olympus IX73 inverted fluorescent microscope (Ex/Em 480/600nm) and cellSens Dimension software (v. 1.18).

Figure 4.4 *Crassostrea virginica* (*C. virginica*) larval growth after a 6-day exposure to 100 and 1000 polyethylene terephthalate (PET) microfibers mL^{-1} (14 x 14 μm , 14 x 28 μm). Box whisker plot shows median larval sizes and variation with inter-quartile range, min-max values, and outliers. Statistical differences in the mean larval sizes (two-way ANOVA and Tukey's post hoc tests, $p < 0.05$) are indicated by letters.

Figure 4.5 *Crassostrea virginica* (*C. virginica*) larval respiration rates after a 6-day exposure to 100 and 1000 polyethylene terephthalate (PET) microfibers mL^{-1} (14 x 14 μm , 14 x 28 μm). Box whisker plot shows median respiration rates and variation with inter-quartile range, and min-max values. Statistical differences in the mean rates (two-way ANOVA and Tukey's post hoc tests, $p < 0.05$) are indicated by letters.

Figure 4.6 *Crassostrea virginica* (*C. virginica*) larval algal ingestion rates after a 6-day exposure to 100 and 1000 polyethylene terephthalate (PET) microfibers mL^{-1} (14 x 14 μm , 14 x 28 μm). Bars are mean algal ingestion rates with standard error. Day 3 data were not suited for analysis. Statistical differences in the mean rates (two-way ANOVA and Tukey's post hoc tests, $p < 0.05$) are indicated by letters.

Figure 4.7 *Crassostrea virginica* (*C. virginica*) larval carbon assimilation rates after a 6-day exposure to 100 and 1000 polyethylene terephthalate (PET)

microfibers mL⁻¹ (14 x 14 μm, 14 x 28 μm). Bars show mean assimilation rates with standard error. Statistical differences in the mean rates (two-way ANOVA and Tukey's post hoc tests, p < 0.05) are indicated by letters.

Figure 4.8 *Crassostrea virginica* (*C. virginica*) larval growth after a 6-day exposure to 100 and 1000 nylon 6, 6 microfibers mL⁻¹ (10 x 10 μm, 10 x 30 μm). Box whisker plot shows median larval sizes and variation with inter-quartile range, min-max values, and outliers. Statistical differences in the mean larval sizes (two-way ANOVA and Tukey's post hoc tests, p < 0.05) are indicated by letters. Significant mortality and setting were seen after 6 days of exposure so day 6 data were excluded.

Figure 4.9 *Crassostrea virginica* (*C. virginica*) larval respiration rates after a 6-day exposure to 100 and 1000 nylon 6,6 microfibers mL⁻¹ (10 x 10 μm, 10 x 30 μm). Box whisker plot shows median respiration rates and variation with inter-quartile range, and min-max values. Statistical differences in the mean rates (two-way ANOVA and Tukey's post hoc tests, p < 0.05) are indicated by letters. Significant mortality and setting were seen after 6 days of exposure so day 6 data were excluded.

Figure 4.10 *Crassostrea virginica* (*C. virginica*) larval algal ingestion rates after a 6-day exposure to 100 and 1000 nylon 6, 6 microfibers mL⁻¹ (10 x 10 μm, 10 x 30 μm). Bars are mean respiration rates with standard error. Statistical differences in the mean rates (two-way ANOVA and Tukey's post hoc tests, p < 0.05) are indicated by letters. Significant mortality and setting were seen after 6 days of exposure so day 6 data were excluded.

Figure 4.11 *Crassostrea virginica* (*C. virginica*) larval carbon assimilation rates after a 6-day exposure to 100 and 1000 nylon 6, 6 microfibers mL⁻¹ (10 x 10 μm, 10 x 30 μm). Bars shows mean assimilation rates with standard error. Statistical differences in the mean rates (two-way ANOVA and Tukey's post hoc tests, p < 0.05) are indicated by letters. Significant mortality and setting were seen after 6 days of exposure so day 6 data were excluded.

Figure S4.1 Conceptual diagram for ¹⁴C radio-labelled phytoplankton method steps.

Figure 5.1 Creating paraffin-embedded parallel fibers for cutting with a microtome A) A 30 mm wide band of multifilament fiber precisely wound around the wooden spindle without overlap. B) Spindle with wound fibers immersed diagonally in a custom rectangular mold filled with molten paraffin wax. Maximum band width of multifilament fibers and mold dimensions constrained by microtome cassette dimensions. C) Central section of paraffin-embedded fibers excised from the wooden spindle creating a block about 65 mm long; black line also indicates orientation of fibers. D) Cutting the long 65 mm block into 10 to 11 mm blocks using the wooden mold as a miter box and a fine Japanese saw. E) A thin 10 mm block, with

diagonally embedded fibers, cut to fit the microtome cassette; Arrows indicate diagonal white lines, which are stacks of parallel fibers that lie perpendicular to the cutting plane of the microtome blade. F) A thin block of embedded fibers mounted on a microtomy cassette, with excess wax trimmed.

Figure 5.2 Nylon 6, 6 and polyethylene terephthalate (PET) manufactured microfibers imaged using a Nikon Eclipse E600 microscope with an AmScope MU800B digital camera. A) Nylon 10 x 10 μm ; B) Nylon 30 x 10 μm ; C) Nylon 100 x 10 μm ; D) PET 14 x 14 μm ; E) PET 28 x 14 μm ; F) PET 42 x 14 μm ; G) PET 42 x 14 μm microfibers stained with Nile red under fluorescent light (Ex/Em 480/600nm) using an Olympus IX73 inverted microscope.

Figure 5.3 The length distributions of cut nylon 6, 6 and polyethylene terephthalate (PET) microfibers for target lengths of 10 and 30 μm (nylon 6, 6, diameter 10 μm , pink boxes) and 14, 28, and 42 μm (PET, diameter 14 μm , blue boxes). Box whisker plots demonstrate variation in data with median, inter-quartile range, and min-max values. Letters signify statistical significance in mean microfiber length (Welch's ANOVA and Games-Howell post-hoc test $p < 0.01$).

Figure 5.4 Manufactured polyethylene terephthalate (PET) microfibers ingested by *Crassostrea virginica* larvae, indicated by white arrows. A) 14 x 14 μm PET fibers fluoresce yellow/orange in the guts of two larvae; B) 28 x 14 μm PET fiber fluoresces yellow/orange in the gut of one larva. *Chaetoceros muelleri* and *Tetraselmis chuii* cells fluoresce red and green respectively.

Figure S5.1 Semi-aerial view of the fiber winding instrument from the crank (right) side. The multifilament polymer fibers were precisely wound onto a wooden spindle (A) using a fiber spool dispenser (B) and fiber guide level-wind assembly (C). The spindle is attached to a crank wheel (D). The fiber guide level-wind assembly (C) consists of a fiber guide traveler (E) on a threaded drive shaft, attached to an operation wheel (F), and 2 guide rods.

Figure S5.2 Side views of the fiber winding instrument. A) Right side view. The crank wheel is attached to the wooden spindle and 1 full rotation adds 2 lengths of parallel fibers to the spindle. B) Left side view. The operation wheel advances the fiber guide traveler, which precisely winds the fibers onto the spindle. The operation wheel is sectioned into eights, so for each 1/8th advance of the wheel, the fiber guide traveler moves 63 μm along the threaded drive shaft rod. For each full rotation of the crank wheel (in A), the operation wheel is rotated 1/8th, until the desired amount of fiber lengths are wound on the spindle. The fiber spool dispenser is parallel to the fiber guide level-wind assembly so fibers are wound precisely. The

spool is free to move laterally with the fiber guide traveler and the fiber must be taught throughout the winding process.

Figure S5.3 A) Close up view of the fiber guide level-wind assembly. Spindle dimensions are constrained by microtome cassette dimensions. B) The fiber guide traveler (E) is made of 2 mm-thick plywood with a 45 mm sewing needle and a small nut to run along the threaded drive shaft (F). The 2 non-threaded rods keep the fiber guide traveler vertical to properly wind the fiber onto the spindle. Precise control of the horizontal movement of the traveler unit with its needle-eye fiber guide, is achieved by rotating the operation wheel which rotates the fine-threaded drive shaft rod (F). The threaded drive shaft passes through the small, threaded nut embedded in the traveler unit. Each 1/8th advance of the operation wheel in Figure S2 B moves the fiber guide traveler to the right by about 63 μm , ensuring the fibers are not overlapping and there is space between each length to securely embed the fibers. Alternate thread pitches or divisions of the operation wheel can be used to adjust the spacing between the precisely wound fiber lengths on the spindle.

Figure S5.4 A) Sectioning of the paraffin-embedded fiber block using a standard paraffin microtome (Microm HM-330). Sections cut from the trapezoidal block face curl into conical tubes. B) One section of embedded microfibers, arrows indicate the line of stacked embedded microfibers.

Figure S5.5 Post-cutting processing of microfibers. A) 75 - 150 microfiber-embedded sections of the same thickness were collected in polypropylene centrifuge tubes. B) Dissolving the paraffin wax in the centrifuge tubes using xylene. C) Tubes with > 100 sections were placed in 60°C water bath for 5-minute intervals to fully dissolve paraffin wax. D) Once most of the wax was dissolved, tubes were centrifuged to pellet the released microfibers. E) Pelleted microfibers after centrifugation and supernatant removal. Steps D and E were repeated 3 times with xylene. Xylene was solvent exchanged with 100% (v/v) ethanol and steps D and E were repeated 3 times with 100% ethanol. F) Microfibers of the same length were consolidated into 1 centrifuge tube and 100% ethanol was solvent exchanged for 70% (v/v) ethanol for long-term storage.

Figure S5.6 The length distributions of cut nylon 6, 6 and polyethylene terephthalate (PET) microfibers for target lengths of 10, 30, and 100 μm (nylon 6, 6, diameter 10 μm , pink boxes) and 14, 28, and 42 μm (PET, diameter 14 μm , blue boxes). Box whisker plots demonstrate variation in data with median, inter-quartile range, and min-max values. Letters signify statistical significance in mean microfiber length (Welch's ANOVA and Games-Howell post-hoc test $p < 0.01$). * Indicates estimated 100 μm nylon microfiber length mean and min-max values from Cole 2016 Figure 2 for comparison to our 100 μm lengths.

Chapter 1: Introduction and Overview

Plastic Pollution

Plastic is ubiquitous in society and has become an integral material for everyday life. It is used in a wide variety of markets including packaging, automotive, electrical, construction, agriculture, healthcare, leisure and sports, and many more. Plastic has been revolutionary for advances in technology and science. The benefits of plastic include fuel efficient cars, numerous advancements in medicine, and the manufacture of cell phones and advanced computing devices (R. C. Thompson et al., 2009). Additional benefits include increased access to fresh food, decreased food borne diseases, space exploration, and numerous other innovations over the last 70 years. Plastic is fittingly called a miracle material for many reasons; it is synthetic, cheap, easy to mass produce, sturdy, malleable, heat resistant, and can be colorful or clear. These same characteristics that plastic is lauded for also make it environmentally hazardous. Although the benefits of plastic have led to its widespread use, the image of plastic, more recently, has transformed from beneficial, society-changing inert materials to harmful persistent pollution.

After the end of World War II, plastic manufacturers turned their focus away from military applications and focused on consumer products. Improved manufacturing processes yielded more efficient mass production of plastics, making them cheaper to produce than other materials. Plastic production has boomed globally since the 1950s reaching 380 million tons (including fibers) in 2015 (Geyer et al., 2017; Plastics Europe, 2016) and production is expected to “double by 2025

and more than triple by 2050” (Lusher et al., 2017; World Economic Forum, 2016). China, the European Union, and North America are the largest plastic producers contributing 29.4%, 18.5%, and 17.7% to total production respectively (Plastics Europe, 2018). Polyethylene (PE), polypropylene (PP), polyvinyl chloride (PVC), polyethylene terephthalate (PET), polyurethane (PUR), and polystyrene (PS) represent the majority of polymers produced globally (Geyer et al., 2017).

Approximately 8 million metric tons of plastic pollution enter the ocean each year from mismanaged waste (Jambeck et al., 2015). Studies shows that plastic is the most abundant type of marine debris (Barnes et al., 2009; Moore, 2008) and can be found in every aquatic environment, such as oceans (Desforges et al., 2014), estuaries (Yonkos et al., 2014), freshwater lakes (Free et al., 2014), rivers (Eerkes-Medrano et al., 2015) and remote areas (Barnes et al., 2010; Tekman et al., 2017). Plastic pollution can also be found in all types of matrices, such as the water column, beaches, sediments, and the deep sea (Lusher et al., 2017; Tekman et al., 2017). One study estimated that more than 5 trillion pieces of plastic are floating in the oceans (Eriksen et al., 2014). Plastic particles disperse throughout the oceans because of wind, currents, polymer density, particle size, and biofouling (Barnes et al., 2009; Lusher, 2015).

Plastic particles are categorized by size to organize sources, fates, and environmental effects. Macroplastic consists of particles > 20 mm, mesoplastic is between 5 and 20 mm and microplastic is between 100 nm and 5 mm (Barnes et al., 2009; SAPEA, 2019). There are two sources of microplastic pollution: primary and secondary. Primary microplastics are intentionally manufactured to be small and are

in personal care products or used as preproduction beads (Ha & Yeo, 2018; Lusher et al., 2017). Secondary sources are from serial fragmentation of larger plastic debris and fibers from clothing, other textiles, fishing nets, and boating lines (Cole et al., 2011). Plastic does not directly degrade into simple compounds; over time it is broken down mechanically and photochemically, fragmenting into smaller microscopic pieces (microplastics) (Andrady, 2011). The different categories of microplastics include microbeads, pellets, fragments, films, and fibers (Cózar et al., 2017) with fragments and fibers representing the majority of particles found in the environment.

Estimates of plastic pollution vary between systems because of differences between site ecology, physics, water circulation, land use, and plastic input. Ocean gyre concentrations can range from 0 - 0.5 particles L⁻¹ while semi enclosed seas have higher ranges up to a maximum of 102 particles L⁻¹ (Lusher et al., 2017 and references therein p. 90-91). Coastal zones are particularly vulnerable to plastic pollution because of high coastal populations, shipping activities, aquaculture, and tourism (Lusher et al., 2017). Coastal microplastic concentrations vary widely between locations and have been reported from 0 – 40,000 particles L⁻¹ in water column samples (Lusher et al., 2017 and references therein p. 89-91; Brandon et al. 2020). The Chesapeake Bay showed a range of 0 - 297,927 ± 180,252 particles km⁻² (approx. 0 - 4.47 x 10⁻⁷ ± 0.27 x 10⁻⁷ particles L⁻¹ assuming 15 cm sampling depth) (Bikker et al., 2020; Yonkos et al., 2014) while Mosquito Lagoon, Florida had an average of 21.4 ± 13.1 (± SD) particles L⁻¹ (Waite et al., 2018), the Yangtze Estuary,

China had a range of 0.5 - 10.2 microplastic particles L⁻¹ (Zhao et al., 2014), and an estuary in Qatar had means between 0 and 0.01 particles L⁻¹ (Castillo et al., 2016).

Various sampling and identification methods can lead to differences in reported estimates of environmental samples. Common water sampling methods include surface trawls and vertical sampling with nets of different mesh sizes or whole water grabs (Cole et al., 2011; Lusher et al., 2017). Smaller mesh sizes in surface trawls resulted in collection of 100,000 times more particles than larger mesh sizes (Lozano & Mouat, 2009). Kooi et al. (2016) predicted an underestimation of particle abundance by a factor of 2.08-2.74 (manta trawl vs neuston net) when sampling the surface waters (15 – 25 cm) compared to a depth of 5 m. Common identification methods include microscopy (e.g., visual inspection, fluorescent staining), spectroscopy (FTIR and Raman), and thermal analyses (e.g. pyro-GC/MS) (Chialanza et al., 2018; Shim et al., 2017). Combining techniques can be reliable for identifying plastic polymers in environmental samples however, dyes and particle size and weathering, can confound results, and some methods require sample destruction (Shim et al., 2017). It is difficult to quickly and accurately identify microplastics in a nondestructive and cost-effective manner. Because of the challenges associated with sampling and identifying small microplastics (< 100 µm), very little is known about their environmental concentrations and fate (Cole et al., 2011; Lusher et al., 2017). It is likely that reported concentrations in the Chesapeake Bay underestimate particle concentrations because particles < 330 µm and > 15 cm below the water surface were omitted by the sampling techniques. Developing better detection and quantification methods for small microplastics in environmental

samples is required to accurately test realistic environmental risks of microplastics on organisms (Lusher et al., 2017).

Plastic is problematic because it impacts organisms in many ways. Effects on wildlife include ingestion (Cole et al., 2013), entanglement (Cole et al., 2011; Gall & Thompson, 2015), transportation of microorganisms leading to invasive species (NOAA, 2017), disruptions in food chains, and contamination of commercial fish and shellfish (Rochman et al., 2015). There are also possible human health risks because of exposure to contaminated food and water (Smith et al., 2018). Microplastics pollutes drinking waters (Kosuth et al., 2018; Mason et al., 2018) and other human consumables (Kosuth et al., 2018). The ingestion of microplastics can cause physical impacts to many organisms but also toxic effects from chemicals added during polymer manufacturing (e.g., polybrominated diphenyl ethers (PBDEs), bisphenol A (BPA)) and from the release of persistent organic pollutants (POPs) or metals adsorbed from the environment (Barboza et al., 2018; Browne et al., 2007; Hartmann et al., 2017; Hermabessiere et al., 2017). It is still unclear which effect (physical or chemical) impacts organisms more.

At the beginning of this research little was known about which organisms ingest plastic, how much they could ingest, and subsequent effects. Although in the last three years more studies have broadened our understanding of animal ingestion, very little has been done on larval organisms, some of which are the most sensitive life stage of the species. Table 1.1 summarizes microplastic studies examining bivalves of the *Crassostrea* spp. Only four studies have been conducted with any species of bivalve larvae (Bringer, Cachot, et al., 2020; Bringer, Thomas, et al., 2020;

Cole & Galloway, 2015; Tallec et al., 2018). With microplastic pollution increasing, understanding the impacts that such pollution has on aquaculture and oyster survival and sustainability is necessary. Some studies have been conducted at high concentrations in the laboratory, but fewer observations are available for environmentally relevant concentrations (Cole & Galloway, 2015; Sussarellu et al., 2016; Tallec et al., 2018). Also, standardized methods for testing environmentally relevant plastic particle types and concentrations are lacking.

Table 1.1 Previous microplastic studies using the bivalves *Crassostrea gigas* (*C. gigas*) and *Crassostrea virginica* (*C. virginica*).

Species	Life Stage	Type of Experiment	Finding	Reference
<i>C. gigas</i>	Adult	Field study (Half Moon Bay, CA, USA)	Avg 0.6 ± 0.9 microfibers ind ⁻¹	Rochman et al. 2015
<i>C. gigas</i>	Adult	Field study (Brittany, France)	0.47 ± 0.16 particles g ⁻¹ ww	van Cauwenberghe & Janssen 2014
<i>C. gigas</i>	Adult	Field study (Oregon coast, USA)	Avg 10.95 ± 0.77 micropalstics ind ⁻¹ , over 99% were fibers	Baechler et al. 2020
<i>C. gigas</i>	Adult	Field study (Seoul, Gwangju, Busan, South Korea)	Avg 0.77 ± 0.74 particles ind ⁻¹ , fragments were dominant shape	Cho et al. 2019
<i>C. gigas</i>	Adult & larval	Lab exposure	PS microbeads affected adult reproduction and their offspring's development	Sussarellu et al. 2016
<i>Bivalve (sp. undetermined)</i>	Larval	Lab exposure	Ingestion of 7.3 μm PS beads	Cole et al. 2013

<i>C. gigas</i>	Larval	Lab exposure	Ingestion of 0.16-20.3 μm PS beads, 1 μm beads reduced algal ingestion, no change in growth after 8 d.	Cole and Galloway 2015
<i>C. gigas</i>	Gamete & larval	Lab exposure	Nanoplastics decreased fertilization, embryogenesis, and larval development in dose-response	Tallec et al. 2018
<i>C. gigas</i>	Larval	Lab exposure	Proprietary polymer microbeads caused developmental malformations and arrest, reduced swimming speed, altered swimming trajectory	Bringer et al. 2020 a
<i>C. gigas</i>	Larval	Lab exposure	HDPE microbeads caused developmental malformations and arrest, reduced swimming speed, altered swimming trajectory	Bringer et al. 2020 b
<i>C. virginica</i>	Adult	Field study (Mosquito Bay, FL, USA)	Avg. $7.6 \pm 4.2 - 23.5 \pm 6.7$ microplastics ind^{-1}	Waite et al. 2018
<i>C. virginica</i>	Adult	Lab exposure	Individuals selectively ingested microplastics, selected microspheres by size	Ward et al. 2019
<i>C. virginica</i>	Adult	Lab exposure	No toxicity for short exposures with 3 μm PS microbeads	Gaspar et al. 2018
<i>C. virginica</i>	Larval	Lab exposure	Ingestion of microspheres 0.21-27.4 μm	Baldwin & Newell 1991

Avg - average; ww - wet weight; PS - polystyrene; d.- days; ind - individual; HDPE - high density polyethylene

Crassostrea virginica

Historically the Eastern Oyster, *Crassostrea virginica* (*C. virginica*), has been ecologically and economically vital to the Chesapeake Bay. Oysters are crucial filter feeders for the Bay, important ecosystem engineers, and also participate in nutrient

cycling and benthic-pelagic coupling (Wilberg et al., 2011). As a keystone species, oysters provide many ecosystem services to the Bay. Oysters filter nutrients and phytoplankton from the water column, provide habitat for many benthic organisms and fish, and provide shore line stabilization. In the 18th century, high oyster abundances presented navigational hazards for ships (Chesapeake Bay Foundation, n.d.). A single adult can filter up to 50 gallons of water a day and populations in the early 1800s could filter the equivalent of the entire volume of the Bay in 3 - 6 days (Newell, 1988). At its peak in the late 1800s, "Maryland was the greatest oyster-producing region of the world." (Kennedy & Breisch, 1983). It produced 39% of the total US oyster catch and 20% of Americans in the fishing industry were employed in Maryland. The pinnacle of the Maryland harvest in 1885 included landings of 15 million bushels (Kennedy & Breisch, 1983); wild harvest in 2018 was just under 180,000 bushels (Maryland Department of Natural Resources, 2018). Because of the economic opportunities provided by the thriving oyster fishery, being a waterman was lucrative over many generations. The trade was passed down within local families, making the waterman lifestyle integral in the local culture.

C. virginica have a complex life history and go through multiple stages of development before reaching the adult life stage. Oyster are broadcast spawners and oysters in a reef release their gametes into the water column in mass spawning events to maximize fertilization success (R. J. Thompson et al., 1996). Fertilization occurs within an hour and individuals hatch from their eggs into swimming trochophores within 5-9 hours (R. J. Thompson et al., 1996). Larvae remain trochophores for 24-48 hours, then they become veliger or D-stage larvae when they develop shells (R. J.

Thompson et al., 1996). The veliger stage lasts for about 2-3 weeks depending on environmental and individual factors (Tallec et al., 2018; R. J. Thompson et al., 1996). The final stage of the larval period, before settling and metamorphosis into a sessile spat, is the pediveliger stage (R. J. Thompson et al., 1996). This stage is characterized by a foot that larvae use to search for suitable substrate to settle (R. J. Thompson et al., 1996). Finally, spat or juvenile oysters develop into adults (Wallace, 2001). Multiple broods occur throughout the spring and summer spawning season and many factors, such as time of year, spawn number, parental genes, and parental conditioning, affect brood performances (R. J. Thompson et al., 1996).

Overfishing and diseases contributed to the decline of Maryland's oyster populations, while nutrient pollution and associated decreased dissolved oxygen and increased suspended sediments degraded oyster habitats. To combat population declines, Maryland has invested tens of millions of dollars in oyster restoration (U.S. Army Corps of Engineers, 2019) and research to restore the oyster population, with the goal being self-sustaining oyster bars.

The Chesapeake Bay is vulnerable to plastic pollution because of input from urban areas (Yonkos et al., 2014), input from agricultural runoff, especially on the Eastern Shore (Piehl et al., 2018), and aquaculture and fishing activities (Isensee & Valdes, 2015). Precipitation for the region is projected to increase up to 20%, likely increasing the number of plastic particles reaching the Bay (Easterling et al., 2017). It is unclear how microplastic pollution is affecting this restoration and the overall success and sustainability of oysters.

Dissertation overview

The larval life stage of oysters is vastly understudied, compared to the adult life stage, in the microplastic pollution field. Therefore, this dissertation was designed to examine microplastic interactions with oyster larvae in order to evaluate risks. While microplastic pollution is considered a contaminant suite, with a wide variety of sizes, shapes, surface functionalities, polymers, additives, and sorbed chemicals, model microplastics (non-functionalized, non-weathered, and standard microbeads and microfibers) were necessary as a starting point for this fundamental research.

In chapter 2, I examined the effects of food and microplastic availability on the uptake and egestion by oyster larvae. I also examined microplastic ingestion threshold concentrations and larval saturation of microplastics. Larvae were exposed to a range of phytoplankton and microplastic concentrations, in a factorial design, and microplastic ingestion was evaluated for different exposure parameters.

At the beginning of this research there was one published paper that examined microplastic effects from ingestion by oyster larvae (Cole & Galloway, 2015). Using ingestion threshold concentrations determined in chapter 2 to evaluate *C. virginica* physiological responses to PS microbead ingestion, Chapter 3 addressed larval physiological responses including growth, respiration rates, algal ingestion rates, and carbon assimilation rates. Because microbeads are not as environmentally abundant as other microplastic particle types, Chapter 4 examined larval exposures using manufactured PET and nylon microfibers. Finally, chapter 5 describes the novel

manufacturing method that I developed to create standard plastic microfibers for laboratory experiments.

In summation, this work will provide the basic information needed to evaluate risks of microplastics to the larval life stage of oysters.

Chapter 2: The effects of food availability and microplastic availability on the uptake of polystyrene microbeads in Eastern oyster larvae

Abstract

The Eastern Oyster (*Crassostrea virginica*, *C. virginica*) is an ecologically and economically important species for estuarine ecosystems and in the Chesapeake Bay there have been large public investments to restore oyster populations. Plastic pollution could pose a problem for current oyster populations and the success of restoration efforts if micrometer sized particles are available and ingested by *C. virginica* larvae. Little is known about how algae and microplastic abundance influence uptake, or the egestion abilities of larval oysters that have ingested microplastics. To determine the amount of microplastic ingestion under different food and microplastic concentrations, larvae that were 1- and 5-days post-fertilization were fed varying concentrations of the algae *Isochrysis galbana* (2,000-50,000 cells mL⁻¹) and 2 or 6 µm polystyrene microbeads (0-20,000 beads mL⁻¹) for 24 hours. Larvae were then placed into water without microbeads and allowed to egest microbeads with subsamples taken at 1, 6, and 24 hours. Microbead concentration was an important factor for larval uptake of both size beads but food concentration was not. The larval ingestion threshold concentration for 2 µm beads was 20 beads mL⁻¹ for 1 day-post-fertilization larvae and the threshold concentration for 6 µm beads was 50 beads mL⁻¹ for 5 days-post-fertilization larvae. Microbead ingestion saturation for *C. virginica* larvae were calculated to occur at exposure concentrations

of 5,295 and 65,297 beads mL⁻¹ for 2 and 6 µm bead sizes respectively. Finally, larvae egested microbeads but not all after 24 hours in clean water. As microplastic contamination in the environment increases, it is likely that oyster larvae will ingest more plastic particles and potentially be more at risk.

Introduction

Ingestion is one of the major concerns of plastic pollution for many organisms. With plastic production reaching 322 million tons in 2015 and projections estimating 1.1 billion tons yr⁻¹ by 2050 (Geyer, 2020), plastic pollution, and therefore the probability of plastic ingestion will increase (Plastics Europe, 2016). Plastic particles in the environment occur in a wide variety of shapes, sizes, and materials; many particles are very similar to food and prey items of most feeding organisms (Cole et al., 2011 and references therein; Lusher et al., 2017). The vast amount of plastic pollution in global waters suggests that understanding how plastic ingestion affects organisms is important. Plastic ingestion is a concern for two main reasons: plastic particles can cause physical effects and particle-associated contaminants can expose organisms to harmful chemicals. For example, ingested plastic can induce excess energy expenditures to egest plastic particles (Cole et al., 2019), disrupt or block digestion resulting in starvation (Pierce et al., 2004), or induce other physiological changes (Liu et al., 2019). Plastic also contains added chemicals within the polymer and adsorbs organic chemicals, which can be persistent, bioaccumulative, and toxic, in the water column. Both leaching and desorption of these chemicals may harm organisms (Hermabessiere et al., 2017; Lusher et al., 2017).

Oyster larvae are susceptible to microplastic ingestion because their distributions often overlap. *Crassostrea virginica* (*C. virginica*) larvae in the Chesapeake Bay move vertically through the water column and aggregate at different depths based on larval size, swimming and sinking speeds, water column stratification, temperature, salinity, and physical processes such as upwelling/downwelling (Deksheniaks et al., 1996). Microplastics are observed throughout the water column and are in a constant state of flux because of wind-driven and tidal water motion, particle aggregation, and biofouling processes (Barnes et al., 2009; Woodall et al., 2014). Small microplastics (25 – 1000 μm) are estimated to be 300-7000 times more abundant than large microplastics ($> 1000 \mu\text{m}$) and small microplastics were more susceptible to vertical transport (Poulain et al., 2019). Over the full larval time period (about 2 - 3 weeks; Bahr & Lanier, 1981), individuals will spend time at different depths from the surface to the bottom, thus interacting with all possible pools of suspended microplastic particles.

Oysters are important to the health of the Chesapeake Bay and similar ecosystems (Chapter 1) and understanding the effects of microplastics is important to sustain the populations, to continue improving the water quality, and to develop a more robust and sustainable fishery. Two studies examining microplastics in the Chesapeake Bay reported a range of $0 - 297,927 \pm 180,252$ particles km^{-2} ($\sim 0 - 4.47 \times 10^{-7} \pm 0.27 \times 10^{-7}$ particles L^{-1} assuming 15 cm sampling depth) in four tributaries and the main stem, using a 330 μm mesh size (Bikker et al., 2020; Yonkos et al., 2014). Although these are extremely small concentrations, sampling with finer mesh nets, collected up to 10 fold greater concentrations in coastal waters (Lindeque et al.,

2020). Cole et al. (2013) noted that sampling of small microplastics is difficult and there are insufficient data to determine realistic environmental concentrations of these particles. Lusher et al. (2017) suggest that new detection and identification methods and subsequent exposure experiments should focus on particles < 150 μm .

Microplastics are distributed throughout the water column so surface trawls will miss a large proportion of particles (Kooi et al., 2016). Therefore, the reported concentrations likely underestimate microplastics in the Chesapeake Bay, including size ranges bioavailable to Eastern oyster larvae.

Most studies examining microplastic ingestion and associated effects have provided data on adult oysters. Waite et al. (2018) found that *C. virginica* adults from Mosquito Bay, Florida, USA had an average of 16.5 particles ind^{-1} among three sites, with 67% of the particles consisting of fibers; 74% of these were dark blue (Waite et al., 2018). *Crassostrea gigas* (*C. gigas*) adults from the coast of Brittany, France had an average of $0.47 \pm 0.16 \text{ g}^{-1}$ wet weight (ww) (Van Cauwenberghe & Janssen, 2014). Sussarellu et al. (2016) exposed adult *C. gigas* to polystyrene (PS) microbeads for a two-month reproductive cycle. The adults showed a significant decrease in oocyte number and diameter, and decreased sperm velocity (Sussarellu et al., 2016). Their dynamic energy budget model suggested a reallocation of energy from reproduction to structural growth (Sussarellu et al., 2016). Microplastic ingestion by adults occurs in the environment and clear effects have been shown in laboratory studies however, little is known about factors affecting microplastic ingestion and associated effects in the larval stage.

The few studies that have examined larval ingestion and effects of microplastics in *C. gigas* and *C. virginica* have used microbeads. Microbeads are useful tools in laboratory exposure studies because they are commercially available in a variety of standard sizes, surface functionalities, and fluorescent wavelengths (Ward, Rosa, et al., 2019). According to Cole et al. (2013), 13 of the 15 species (including copepods and bivalve and decapod larvae) of zooplankton exposed to PS microbeads (7.3 - 30.6 μm) were able to ingest microplastics when exposed to 1000 particles mL^{-1} . *C. gigas* larvae from PS bead exposed adults ($1,816 \pm 76$ and 21 ± 6 beads per mL^{-1} for 2- and 6- μm PS particles respectively) showed a decrease in survival to the D-stage and impaired larval development (Sussarellu et al., 2016). Tallec et al. (2018) exposed *C. gigas* embryos and larvae to microplastics and nanoplastics at similar concentrations to Sussarellu et al. (2016). After short exposures, nanoplastics reduced fertilization success and effected embryo-larval development (Tallec et al., 2018). *C. virginica* larvae ingested microspheres (Polysciences) ≤ 4.80 to $27.4 \mu\text{m}$ diameters and larvae, up to $300 \mu\text{m}$, could ingest particles as small as $0.21 \mu\text{m}$ (Baldwin & Newell, 1991). Finally, *C. gigas* larvae exposed to microbeads had higher rates of malformations and developmental arrest and they also had reduced swimming speed and altered swimming trajectories (Bringer, Cachot, et al., 2020; Bringer, Thomas, et al., 2020).

Two studies have examined the effects of food availability or microplastic availability on the adult life stage of mussels. In a freshwater mussel (*Dreissena polymorpha*), higher food abundance caused a significant dose-dependent decrease in PS microbead ingestion and higher microbead exposure concentrations showed

increased non-linear ingestion (Weber et al., 2021). *Mytilus edulis* adults ingested more microfibers as exposure concentrations increased and showed a Holling's Type II functional response, with a maximum uptake rate of 5227 fiber hr⁻¹ when exposed to 13 fiber mL⁻¹ (Woods et al., 2018). Microplastic concentration effects on the uptake of 3 µm PS microbeads by *Mytilus galloprovincialis* larvae were determined by Capolupo et al. 2018. Their study suggested that higher microplastic exposure concentrations led to higher numbers of microbeads ingested and 80% of ingested microbeads were egested after 24 hours, with 8 days for complete egestion. Studies that include microplastic ingestion with food and microplastic availability are absent from the literature.

The goal of this chapter was to examine how food and microplastic availability influences microplastic uptake in *C. virginica* larvae. The questions that guided this research were: 1) what are the threshold concentrations for *C. virginica* larvae to ingest PS microbeads, 2) is microbead uptake influenced by algal concentrations or microbead concentrations in the seawater 3) do larvae reach an ingestion saturation of microplastics, and 4) can larvae rapidly egest ingested microbeads.

Methods

To determine the amount of microplastic ingested by *C. virginica* larvae under different food concentrations, laboratory feeding experiments with different concentrations of *Isochrysis galbana* (*I. galbana*) and PS microbeads were conducted. Two sets of full factorial experiments were created (Method 1 and 2) and conducted in a similar manner. The first (Method 1) consisted of five microbead and four algal

concentrations (Table 2.2). Multiple runs using separate broods of larvae were used to observe natural variations in feeding and provide replicates. A wide range of microbead concentrations was used to examine larval microbead ingestion capacity. The lowest concentration (0.02×10^3 beads mL^{-1}) is three orders of magnitude greater than reported estimates in estuaries (Waite et al., 2018; Zhao et al., 2014) but in the same order of magnitude for microplastics ($< 333 \mu\text{m}$) in coastal, near shore samples (Brandon et al., 2020). Experiments were conducted with 1 day-post-fertilization (dpf) larvae to prevent any prior plastic ingestion.

Table 2.2 Design parameters used in Method 1 feeding experiments of *Crassostrea virginica* larvae. Larvae were exposed to a full-factorial design of different polystyrene (PS) microbeads and *Isochrysis galbana* (*I. galbana*).

Component	Description	Concentrations	Units
<i>I. galbana</i>	cells in exponential growth	0, 2, 10, 20	10^3 cells mL^{-1}
PS microbeads	$2\mu\text{m}$ and $6\mu\text{m}$ diameter	0, 0.02, 2, 10, 20	10^3 beads mL^{-1}

The second set of experiments (Method 2) consisted of three microbead and three algal concentrations with treatments in triplicate. Experiments were conducted with 1 and 5 dpf larvae. Microbead concentrations were chosen to better represent environmental concentrations (Gonçalves et al., 2019; Lenz et al., 2016). *I. galbana* concentrations were determined by the number of days post-fertilization of the larvae (Helm & Bourne, 2004). The cell concentration for an optimum diet, 50% optimum, and no algae correlate to the three concentrations used for each age of larvae (Table

2.3). Microbead concentrations were 0%, 0.1%, or 10% of algal concentrations for an optimal larval diet.

Table 2.3 Design parameters used in Method 2 feeding experiments. *Isochrysis galbana* (*I. galbana*) and polystyrene (PS) microbead concentrations used for each days-post-fertilization (dpf) of *Crassostrea virginica* larvae. *I. galbana* concentrations represent either 0%, 50%, or 100% of optimal larval diet (based on dpf) and microbead concentrations represent 0%, 0.1%, or 10% of optimum algal cell concentration.

Days post fertilization	Algal concentrations (10 ³ cells mL ⁻¹)			PS microbead concentrations (10 ³ beads mL ⁻¹)			
	% of optimum algae	0%	50%	100%	0%	0.1%	10%
1		0	10	20	0	0.02	2
5		0	25	50	0	0.05	5

Both sets of experiments were conducted with larval concentrations of 10 ind mL⁻¹ in 250mL round glass jars in artificial seawater (ASW, 1 µm filtered, 15 salinity). Larvae can tolerate salinity changes from their initial rearing salinity and perform well in a range of salinities from 11-30 (Priester, 2016). ASW was made using 1µm filtered deionized water and was 1 µm filtered immediately prior to use, minimizing plastic contamination (Table S2.1). *C. virginica* and *I. galbana* were obtained from the Horn Point Lab Oyster Hatchery, Cambridge, Maryland, USA. Larvae were collected on a 40 µm sieve and rinsed with ASW before being concentrated in a stock solution of ASW.

Fluoresbrite® PS microbeads (2µm diameter, CAT #18338-5 and 6µm diameter, CAT #17156-2, density: 1.05g mL⁻¹; Polysciences) were chosen because *C.*

gigas larvae ingest a range (0.16 - 20.3 μm) of microplastic PS beads (Cole & Galloway, 2015). Larvae from *C. gigas* adults that were exposed to 2 and 6 μm sizes, showed a settlement delay of 6 days compared to the control (Sussarellu et al., 2016). Two different diameter PS microbeads were chosen because larvae select larger food items as they get bigger (Baldwin, 1995). Stock solutions were made for microbeads of each diameter individually and used for all subsequent experiments. Diluted samples of the stock solutions were saved for verification of exposure concentrations using a coulter counter (Beckman Multisizer 4).

After addition of larvae, PS microbeads, *I. galbana*, and ASW, the glass jars were capped and attached to a slowly spinning plankton wheel (1 rotation per min.) to keep larvae, algae, and beads suspended. Larvae were allowed to feed for 24 hours to assure ample time for exposure and subsamples were fixed with formaldehyde for analysis. The remaining samples were then washed onto 40 μm sieves and cleaned with ASW. Larvae were then moved to clean, microbead free, 250 mL glass jars for the egestion period and placed on the plankton wheel. *I. galbana* was added to the jars at the same concentrations from the first 24 hours, maintaining the treatment conditions throughout the entire experiment. Subsamples of larvae were taken at 1, 6, and 24 hours after placement into clean jars and they were placed in 20 mL vials and fixed for analysis.

A fluorescent microscope (Olympus IX73 Research Inverted Microscope with reflected fluorescence system and ET-ECFP filter cube, Ex. 436/20x, Em. 480/40m) was used for analysis to count the number of beads in 50-150 larvae from each sample. The average numbers of microbeads ingested were calculated and compared

across algal concentrations and microbead concentrations. Ingestion threshold concentrations were determined by observing the lowest exposure concentration leading to microplastic uptake, generally characterized by observing few microbeads in a very small number of individuals.

Statistical analysis

Data were tested for normality and homogeneity of variance by visualizing histograms and by using the Shapiro-Wilk and Levene's tests. When data violated the assumptions for an ANOVA, data were \log_{10} transformed (method 2 ingestion: 2 μm , 1 dpf; method 2 egestion: 2 μm , 1 dpf, 2 10^3 beads mL^{-1}) or square root transformed (method 2 ingestion: 2 μm , 5 dpf and 6 μm 1 dpf). Then a two-way ANOVAs and Tukey's post hoc tests were used to compare the average number of beads ingested ind^{-1} and to determine significance across algal and microbead treatments. Egestion data were analyzed in the same manner; comparing the average number of beads remaining ind^{-1} at each time point.

To analyze microbead ingestion saturation, a model was fit to the data from the large range of microbead exposures for 2 and 6 μm microbeads using a Holling's Type II functional response equation:

$$y = y_{max} \frac{[x]}{[x] + x_{half}}$$

where y is the average number of microbeads ingested ind^{-1} , y_{max} is the ingestion saturation, x is the microbead exposure concentration, and x_{half} is the half saturation constant. Then the y_{max} and half saturation constant were calculated and an analysis

of fit was performed. All statistical analyses were performed in R Studio version 1.4.1103 and significance reported at $p < 0.05$.

Results

C. virginica larvae were able to ingest both PS microbead sizes but ingested higher amounts of 2 μm versus 6 μm (Figures 2.1, 2.2). The uptake of PS microbeads by larvae was influenced significantly by microbead concentration in the solution for both sizes of microbeads and all microbead treatments tested (Figures 2.2, 2.3, 2.4, 2.6, 2.8, 2.10). In contrast, the number of algal cells available did not significantly affect the uptake of PS microbeads of either size by larvae (Figures 2.2, 2.3, 2.4, 2.6, 2.8, 2.10). *C. virginica* reached an ingestion saturation at high microbead exposures and larvae were able to egest some, but not all, microbeads after 24 hours. Finally, the ingestion threshold for 2 μm PS microbeads was $0.02 \cdot 10^3 \text{ mL}^{-1}$ for 1 dpf larvae. The ingestion threshold for 6 μm PS microbeads was between 0.02 and $2 \cdot 10^3 \text{ mL}^{-1}$ for 1 dpf larvae and was $0.05 \cdot 10^3 \text{ mL}^{-1}$ for 5 dpf larvae. NOTE: Units in figures use full notation instead of scientific notation (e.g. $0.02 \cdot 10^3 \rightarrow 20$).

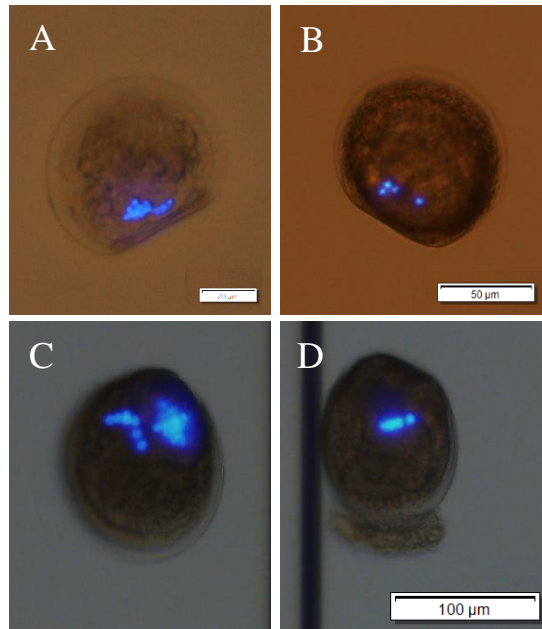


Figure 2.1 Polystyrene microbeads in *Crassostrea virginica* larvae after a 24-hour exposure to 2 µm microbeads at 2×10^3 beads mL^{-1} treatment (A, B, 1 day-post-fertilization) and 6 µm microbeads at 5×10^3 beads mL^{-1} treatment (C, D, 5 day-post-fertilization).

Method 1

For 1 dpf larvae, the greatest number of PS microbeads ingested ind^{-1} occurred at the highest 2 µm diameter bead concentration (20×10^3 cells mL^{-1}), with the highest value equaling 9.88 ind^{-1} (Figure 2.2). *C. virginica* ingested more 2 µm beads than 6 µm beads by 1-2 orders of magnitude. The highest number of ingested 6 µm was 0.24 ind^{-1} and occurred at the highest microbead concentration and lowest algal concentration (Figure 2.2). Minimal ingestion of 2 µm beads and no ingestion of 6 µm beads occurred at the lowest microbead concentration (0.02×10^3 cells mL^{-1}).

Ingestion saturation for 2 μm beads was calculated by fitting a Holling's Type II functional response equation, where the R^2 value was 0.885 (Figure 2.3). Saturation was calculated to be 10.145 beads ingested ind^{-1} and the half saturation constant was 5,295 beads mL^{-1} . Ingestion saturation for 6 μm PS microbeads was 0.765 beads ingested ind^{-1} and the half saturation constant was 65,297 beads mL^{-1} for 1 dpf larvae (Figure S2.1).

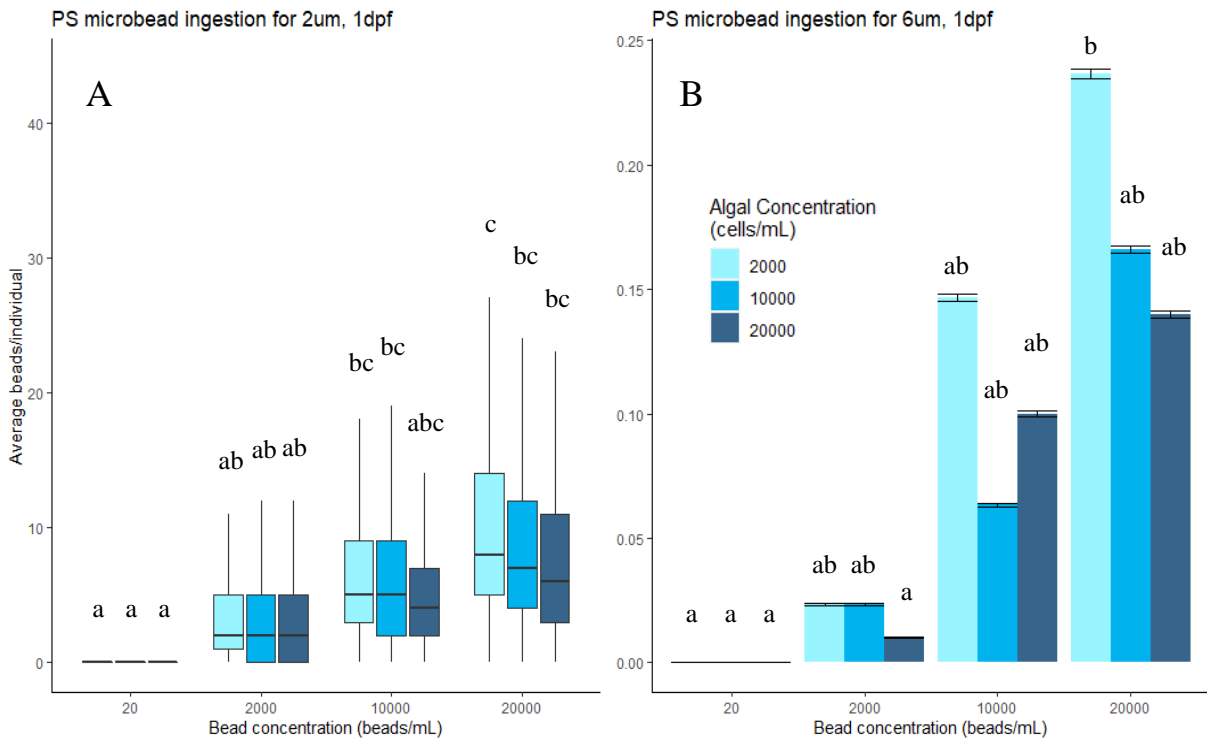


Figure 2.2 Average number of polystyrene (PS) microbeads in *Crassostrea virginica* larvae after ingestion for each microbead solution. A) 2 μm microbeads B) 6 μm microbeads. The experiment consisted of a full factorial design of four concentrations of *Isochrysis galbana* algal cells and five concentrations of PS microbeads (0, 10, 20 $\times 10^3$ cells mL^{-1} ; 0, 0.02, 2, 10, 20 $\times 10^3$ beads mL^{-1}). Larvae were exposed to the solutions for 24 hours. Each combination of feeding conditions was replicated across three broods for 2 μm (n=450) and two broods for 6 μm (n=300). A box plot for 6 μm data was not used because microbead ingestion was so low that the interquartile range was too small to show boxes. Statistical differences in the average number of beads ingested ind^{-1} are indicated by letters (two-way ANOVAs and Tukey's post hoc tests, $p < 0.05$). Note the differences in y-axis scales between A and B.

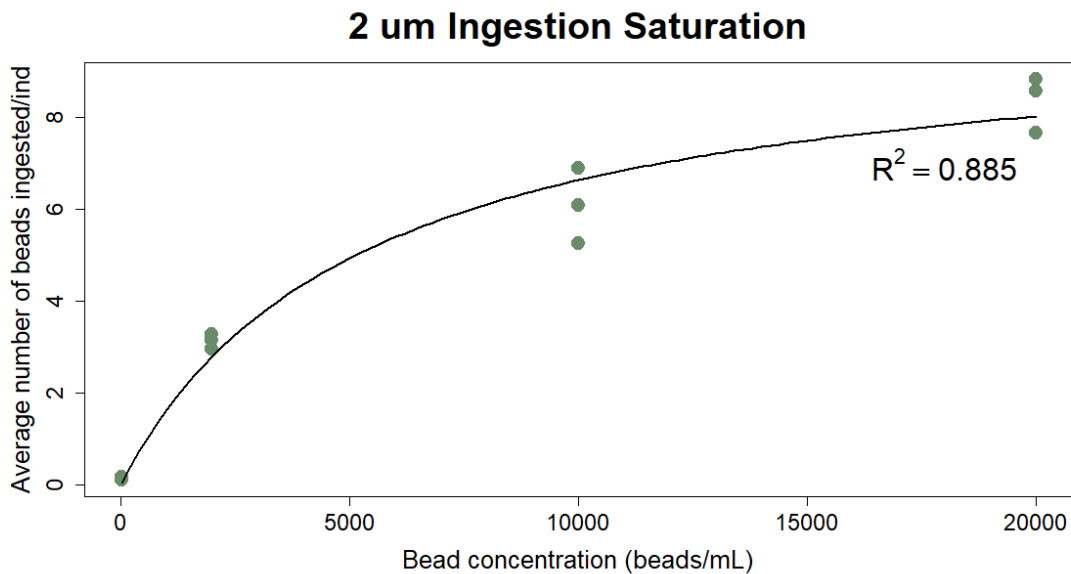


Figure 2.3 Polystyrene (PS) microbead ingestion saturation in *Crassostrea virginica* larvae (1-day-post-fertilization) for exposures to 2 μm PS beads and all algal concentrations. Trendline represents the model fit of the Holling's Type II functional response equation: $y = y_{max} \frac{[x]}{[x] + x_{half}}$ with $R^2 = 0.885$, $y_{max} = 10.145$ beads ingested ind^{-1} , and $x_{half} = 5,295$ beads mL^{-1} .

Method 2

C. virginica larvae ingested more PS microbeads at 5 dpf, compared to 1 dpf., for both bead sizes and all microbead concentrations. Larvae preferentially ingested 2μm microbeads versus 6 μm at both dpf. Finally, larvae egested both size microbeads but were not able to egest all of them after 24 hours. For 2μm beads, 1dpf larvae egested some of the ingested microbeads, with the lowest algal treatment retaining the highest number of beads (Figure 2.5). 5 dpf larvae did not significantly reduce their microbead burdens especially at the high microbead concentration, retaining 10-15 microbeads ind^{-1} (Figure 2.6). For the 6 μm beads, 1 dpf larvae did

not ingest microbeads at the low concentration so egestion was not assessed (Figure 2.8, 2.9). *C. virginica* (1 dpf) exposed to 2×10^3 beads mL^{-1} egested $6 \mu\text{m}$ microbeads but ingestion was so low that not a significant amount of microbeads were egested after 24 hours (Figure 2.9). Histograms of larval microbead burden over the egestion period are found in the Supporting Information (Figures S2.2-S2.8). *C. virginica* (5 dpf) ingested a maximum of 4.63 beads ind^{-1} at the highest microbead concentration (5×10^3 beads mL^{-1}) and significantly reduced their microbead burden after 24 hours but did not egest all microbeads (Figure 2.10, 2.11).

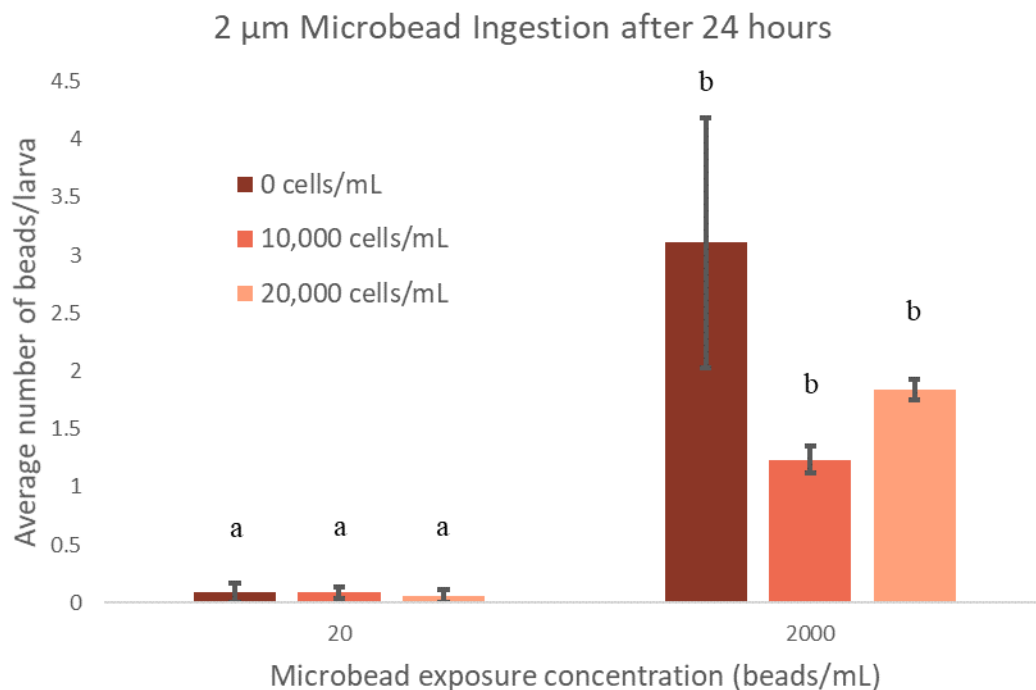


Figure 2.4 *Crassostrea virginica* larval (1-day post-fertilization) average polystyrene (PS) microbead ingestion after 24-hour exposure. Statistical differences in the average number of beads ingested ind^{-1} are indicated by letters (two-way ANOVA and Tukey's post hoc tests, $p < 0.05$). Error bars represent standard deviation.

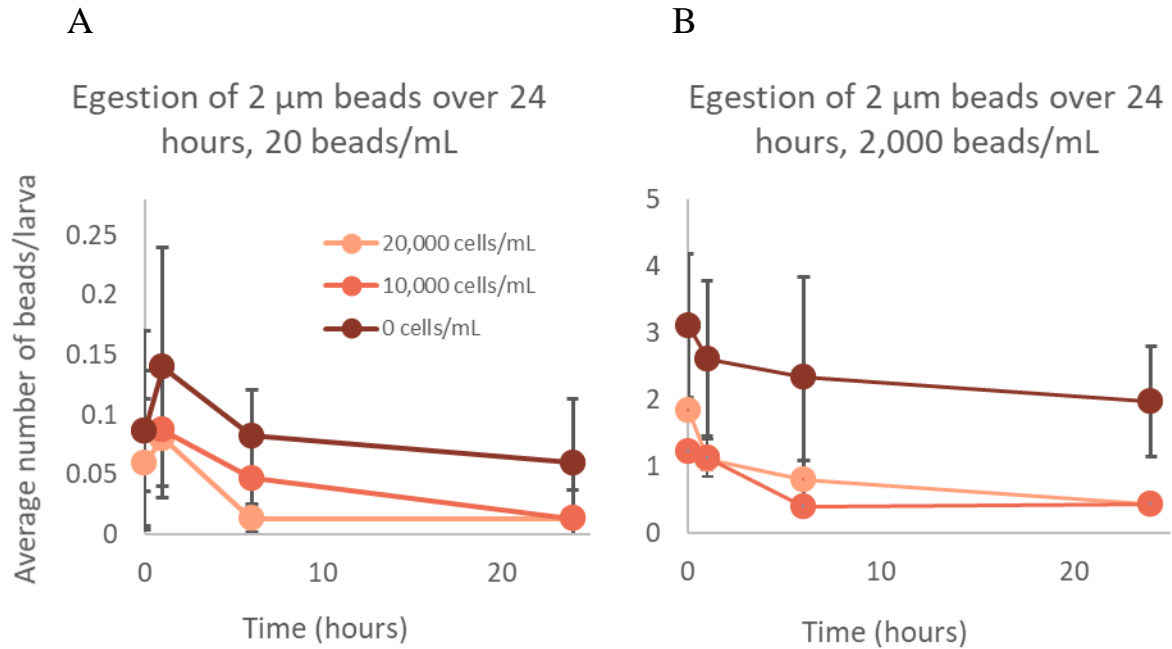


Figure 2.5 *Crassostrea virginica* larval (1-day post-fertilization) egestion of 2 μm polystyrene (PS) microbeads for A) 20 beads mL^{-1} and B) 2,000 beads mL^{-1} . Note the differences in y-axis scales between A and B. Error bars represent standard deviation. Larvae exposed to 2,000 beads mL^{-1} and 0 cells mL^{-1} had significantly more microbeads ind^{-1} than the other two algal treatments at 6- and 24-hour time points (two-way ANOVAs with Tukey's post hoc tests, $p < 0.05$). Statistical significance of average beads ingested ind^{-1} within algal treatments over time were excluded for clarity.

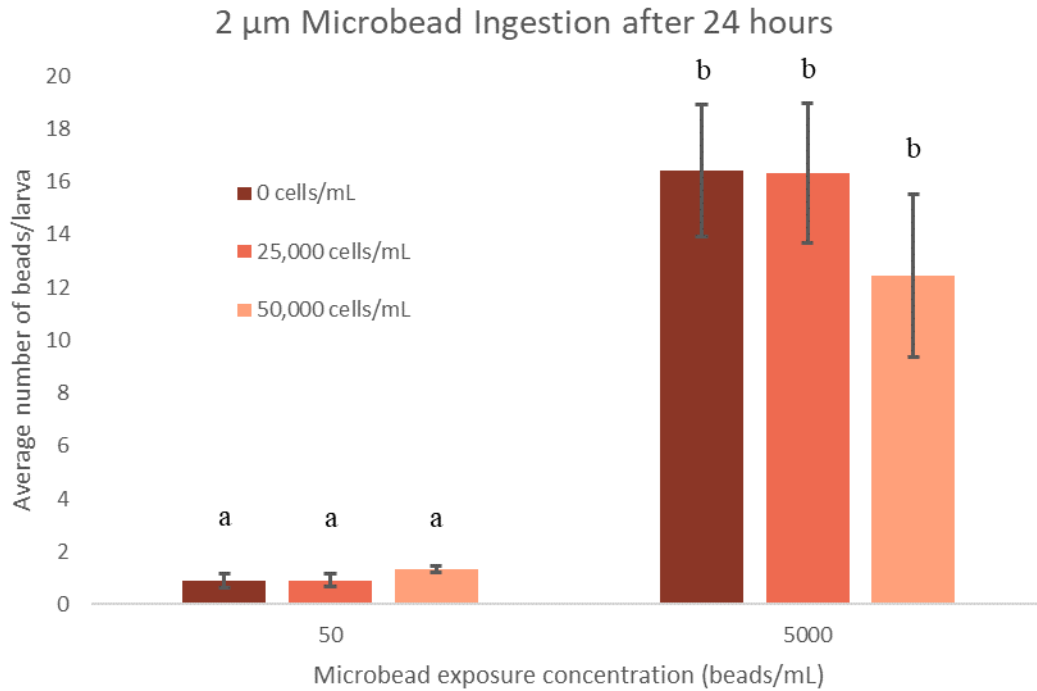


Figure 2.6 *Crassostrea virginica* larval (5-days-post-fertilization) average polystyrene (PS) microbead ingestion after 24-hour exposure. Statistical differences in the average number of beads ingested ind⁻¹ are indicated by letters (two-way ANOVA and Tukey’s post hoc tests, $p < 0.05$). Error bars represent standard deviation.

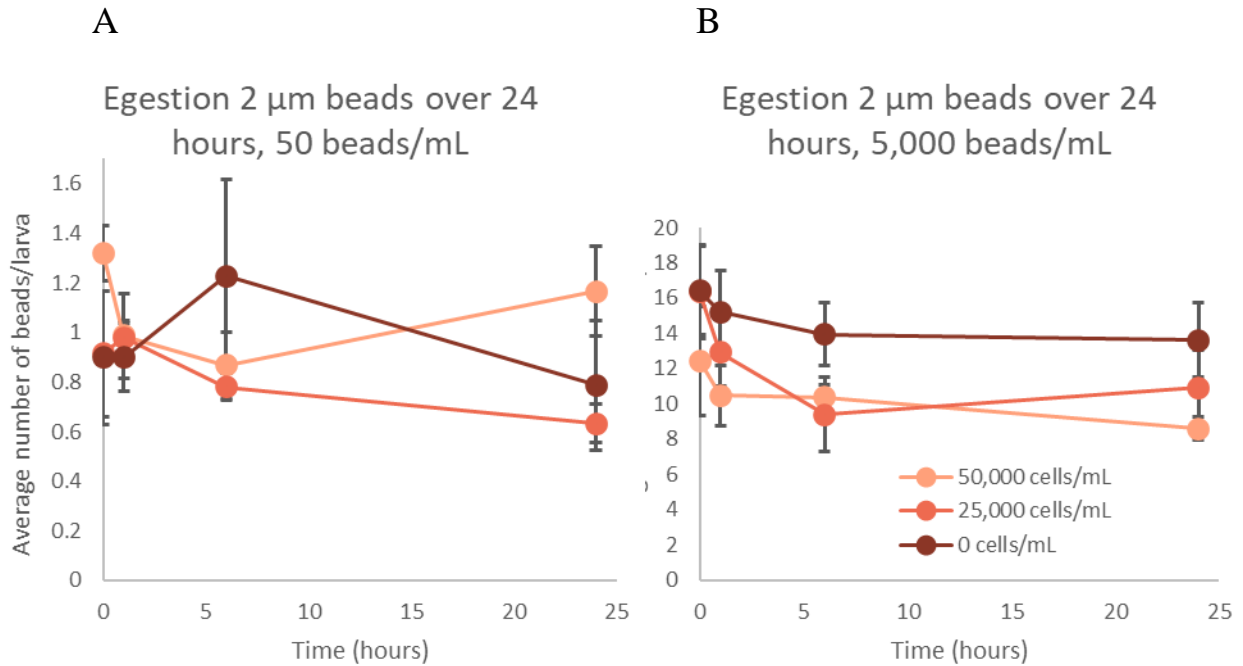


Figure 2.7 *Crassostrea virginica* larval (5-days-post-fertilization) egestion of 2 μm polystyrene (PS) microbeads for A) 50 beads mL^{-1} and B) 5,000 beads mL^{-1} . Note the differences in y-axis scales between A and B. Error bars represent standard deviation. No statistical significance was observed between the average number of beads ingested ind^{-1} for each time point (two-way ANOVAs with Tukey's post hoc tests, $p < 0.05$).

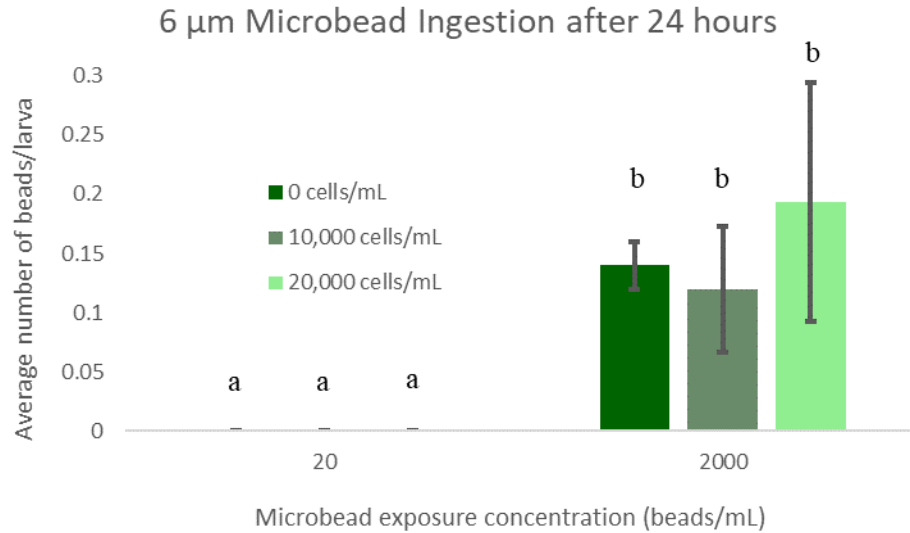


Figure 2.8 *Crassostrea virginica* larval (1-day-post-fertilization) average polystyrene (PS) microbead ingestion after 24-hour exposure. Statistical differences in the average number of beads ingested ind^{-1} are indicated by letters (two-way ANOVA and Tukey's post hoc tests, $p < 0.05$). Error bars represent standard deviation.

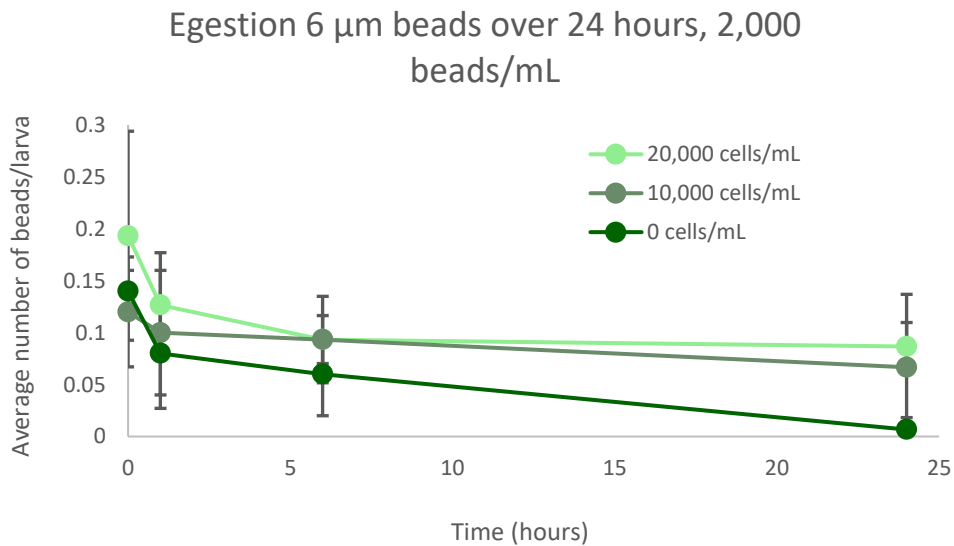


Figure 2.9 *Crassostrea virginica* larval (1-day-post-fertilization) egestion of 6 μm polystyrene (PS) microbeads for 2,000 beads mL^{-1} . Error bars represent standard deviation. No statistical significance was observed between the average number of beads ingested ind^{-1} for each time point (two-way ANOVA with Tukey's post hoc tests, $p < 0.05$).

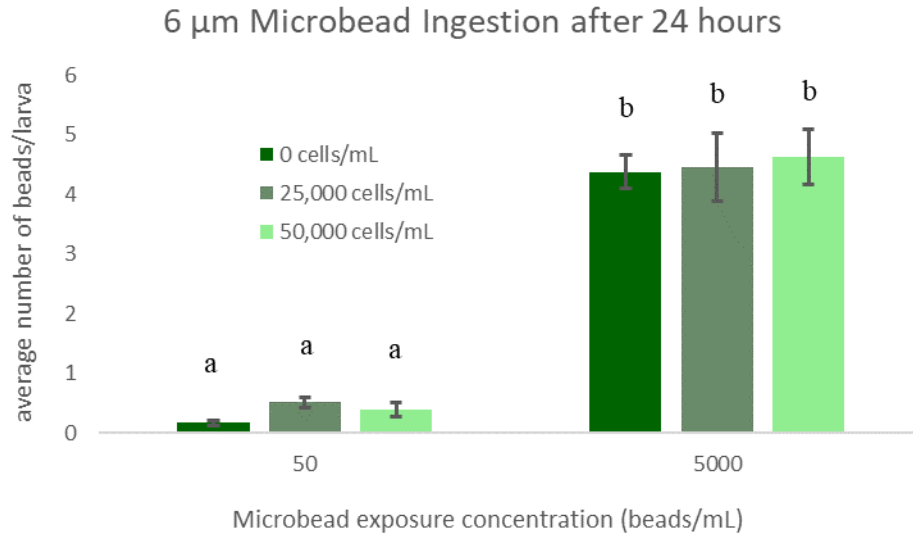


Figure 2.10 *Crassostrea virginica* larval (5-days-post-fertilization) average polystyrene (PS) microbead ingestion after 24-hour exposure. Statistical differences in the average number of beads ingested ind^{-1} are indicated by letters (two-way ANOVA and Tukey's post hoc tests, $p < 0.05$). Error bars represent standard deviation.

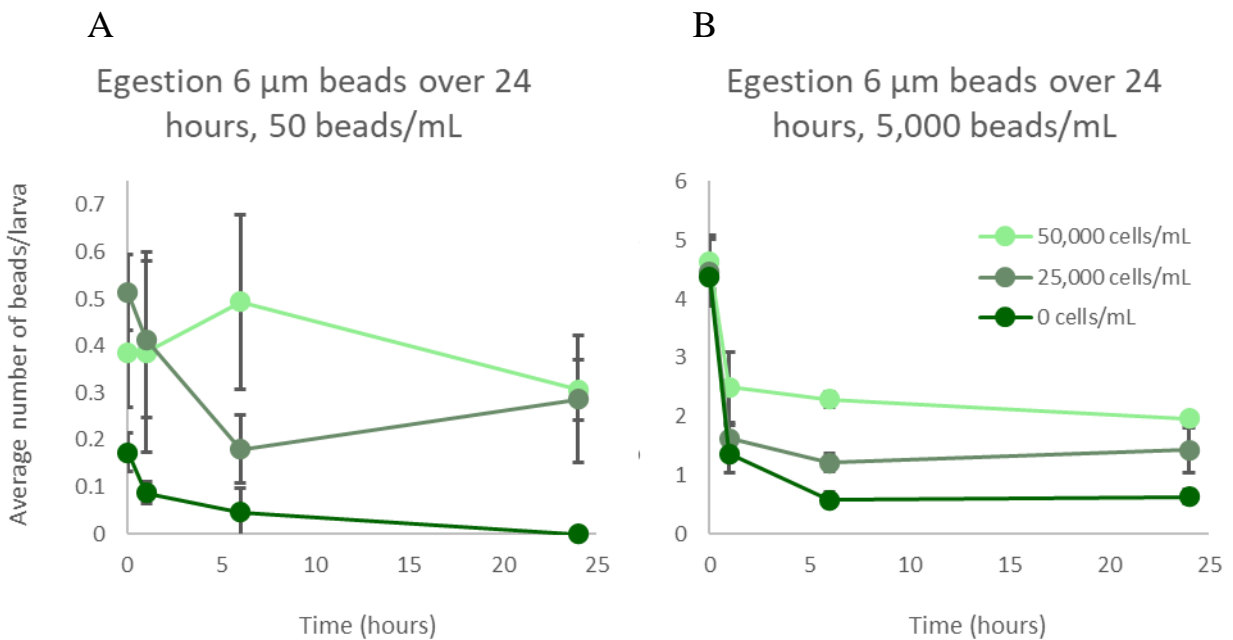


Figure 2.11 *Crassostrea virginica* larval (5-days-post-fertilization) egestion of 6 μm polystyrene (PS) microbeads for A) 50 beads mL^{-1} and B) 5,000 beads mL^{-1} . Note the

differences in y-axis scales between A and B. Error bars represent standard deviation. Larvae exposed to 50 beads mL⁻¹ and 50,000 cells mL⁻¹ had a significantly higher average number of beads ingested ind⁻¹ compared to the 0 cells mL⁻¹ treatment at 6 hours (two-way ANOVAs with Tukey's post hoc tests, $p < 0.05$). Larvae exposed to 5,000 beads mL⁻¹ and 50,000 cells mL⁻¹ had significantly higher average numbers of beads ingested ind⁻¹ compared to 0 and 25,000 cells mL⁻¹ treatments at 6 hours and the 0 cells mL⁻¹ treatment at 1 and 24 hours (two-way ANOVAs with Tukey's post hoc tests, $p < 0.05$). Statistical significance of average beads ingested ind⁻¹ within algal treatments over time were excluded for clarity.

Discussion

C. virginica ingested microbeads when in treatments of environmentally relevant concentrations of microplastics (0.02 and 0.05 10³ beads mL⁻¹) (Brandon et al., 2020) and larvae had different ingestion threshold concentrations for the different diameter microbeads. For 1 dpf larvae, ingestion threshold concentrations were 0.02 10³ beads mL⁻¹ and between 0.02 and 2 10³ beads mL⁻¹ for 2 and 6 µm microbeads respectively. For 5 dpf larvae, the threshold of ingestion for 6 µm microbeads was much lower at 0.05 10³ beads mL⁻¹. Larvae also preferred 2 µm beads over 6 µm beads, ingesting on average about 4 - 10 times more 2 µm beads for all exposure concentrations and larval ages (Figures 2.4, 2.6, 2.8, 2.10). This is likely due to larval selectivity of particles and is consistent with larval selectivity of algal cells. As individuals grow, their preferences of algal cell size shifts toward larger particles (Baldwin, 1995).

Microbead exposure concentration significantly influenced microbead ingestion in *C. virginica* larvae for both diameters and dpf larvae. This is consistent with the study using larvae of the Mediterranean mussel (Capolupo et al., 2018) and the adult life stages of blue mussels (Woods et al., 2018) and fresh water mussels

(Weber et al., 2021). As microplastics increase in the environment, it is likely that ingestion of microplastics by filter feeding bivalves will also increase.

Food availability was a not a factor affecting microbead ingestion for any microbead concentration or larval age. Although not statistically significant, 1 dpf larvae exposed to 2 μm microbeads and low algal concentrations had more ingestion of microbeads consistently across high microbead concentrations. This result may indicate that larvae ingested more beads in these treatments to gain nutrition from the biofilm that develops during the experiment the particles. Aggregates of bacteria and microplastics increased ingestion of both particles in adult *C. virginica* (Kach & Ward, 2008). Findings from the current study imply that no matter how much food is available in the water column, microplastics will be ingested if they are available above microplastic threshold concentrations. In contrast, adult fresh water mussels decreased microplastic ingestion in a dose-dependent manner in the presence of high food abundance (Weber et al., 2021).

While the microbeads used in this study were virgin microplastics, environmental microplastics typically contain chemical additives and sorb organic pollutants from the environment (Lusher et al., 2017; Rochman et al., 2013). Retention of a small amount of microplastics, at times scales up to 8 days, could allow sorption or desorption/leaching of these contaminants, thus increasing or decreasing chemical exposures to larvae (Koelmans et al., 2016). Sorption and desorption are dependent on microplastic contaminant load, organismal contaminant load, gut residence time, and gut chemistry (Koelmans et al., 2016).

An important finding from this research was that larvae reach microplastic saturation at very high concentrations (Figures 2.3, S2.1). Data for 1 dpf larvae were fit to a Holling's Type II functional response, where ingestion half saturation maxima were 5,295 beads mL⁻¹ and 65,297 beads mL⁻¹ for 2 and 6 µm particles respectively. These concentrations far exceed the current environmental microplastic concentrations (0.1 - 40 particles mL⁻¹) (Brandon et al., 2020; Desforges et al., 2014). The increased amount of microbeads ingested from 1 to 5 dpf larvae, suggests that half saturation maxima concentrations are different based on larval age. *M. edulis* adults showed a Holling's Type II functional response with ingestion of microfibers (PET, average length 459 ± SE 2.25 µm) (Woods et al., 2018). The freshwater mussel, *D. polymorpha*, also showed non-linear increased ingestion when exposed to a variety of sizes of PS microbeads at 0.3 or 3 beads mL⁻¹ (Weber et al., 2021). However, Mediterranean mussel larvae showed a linear increase of PS microbead ingestion, with concentrations ranging from 50 to 10,000 beads mL⁻¹ (Capolupo et al., 2018).

C. virginica larvae were able to egest microbeads but were unable to egest all microbeads after 24 hours and there is no clear influence of food abundance on egestion. Egestion figures (2.5, 2.7, 2.9, 2.11) show average microbead body burdens for pooled larval subsamples, creating continuous quantitative data, summarizing the overall egestion and retention trends for each exposure treatment. These figures indicate an overall trend of a certain level of microbead retention after 24 hours but there is large variability within and between treatments. It is unlikely that whole microbeads, retained after the 24-hour egestion period, translocated across the gut

epithelia. While this process has been observed in adult mussels for similar sized microbeads (Browne et al., 2008), it has not been observed in bivalve larvae (Cole & Galloway, 2015). Histograms (Figures S2.2-S2.8) indicate many larvae, especially in low exposure concentrations, do not ingest microbeads. They also show shifts toward lower microbead body burdens over the egestion period.

Egestion of microplastics by other bivalves and life stages have been observed. *M. galloprovincialis* larvae rapidly egested 3 μm PS microbeads but it took 8 days for all individuals to egest all particles (Capolupo et al., 2018). Adult *M. edulis* with high body burdens of microfibers egested microfibers rapidly after 1 hour but did not egest all particles (Woods et al., 2018). Adults with low body burdens of microfibers did not egest microfibers after 1 hour (Woods et al., 2018). Finally, *C. virginica* and *M. edulis* adults egested higher proportions of large microbeads compared to small microbeads after a 3 hour egestion period and microfibers were egested at high proportions except for 1075 μm length microfibers in the mussels (Ward, Zhao, et al., 2019).

This work assumed that larval digestion processes do not fragment ingested microbeads and egestion occurred in a quantized manner (i.e., in whole numbers of microbeads). However, Antarctic krill fragmented microplastics during digestion, reducing mean particle size by an average of 78% and significantly shifting size distributions toward smaller particles (Dawson et al., 2018), indicating more complex interactions than currently understood in the literature. This phenomenon has yet to be examined in oysters but, with a crystalline style, aiding digestive enzymes by

grinding particles in the gut (Langdon & Newell, 1996), it is plausible that weathered, more fragile microplastics could fragment into smaller particles during digestion.

Conclusion

Microbeads were utilized in this study, recognizing that recent advances in characterization of the composition of microplastic pollution in the environment has provided more a detailed view of the issue. Nevertheless, the information gleaned from this study describes a general capacity for microplastic uptake and provides data for future, more complex, exposure experiments. These experiments illustrate that while food availability does not affect microplastic ingestion, microplastic exposure concentration is an important factor. Saturation is reached at concentrations that far exceed current environmental concentrations but microplastic concentrations are expected to increase in the environment as plastic production and mismanagement continues to increase (Lusher et al., 2017). This work suggests that oyster larvae in the environment will show increased ingestion of microplastics because environmental concentrations are much less than larval ingestion saturation.

The observations in this study provide valuable data on threshold ingestion concentrations and ingestion saturation; however, microplastics are a complex contaminant suite and results from one type of exposure should be extrapolated cautiously to particles with different characteristics. Further studies examining ingestion thresholds and factors influencing microplastic uptake are necessary and should use other particle types (fragments, fibers), sizes, polymer types, and surface functionalities.

Supporting Information

Table S2.1: Modified Artificial Seawater

To dH₂O add the following per 200 L for 15 ± PSU:

Salts	Amount
400 mM NaCl	2.3375 kg
20 mM MgSO ₄ •7H ₂ O	492.5 g
10 mM CaCl ₂	111 g
1.7 mM KBr	20.25 g
10 mM KCl	74.5 g
20 mM MgCl ₂ •6H ₂ O	406.3 g
0.404 mM H ₃ BO ₃	2.5 g

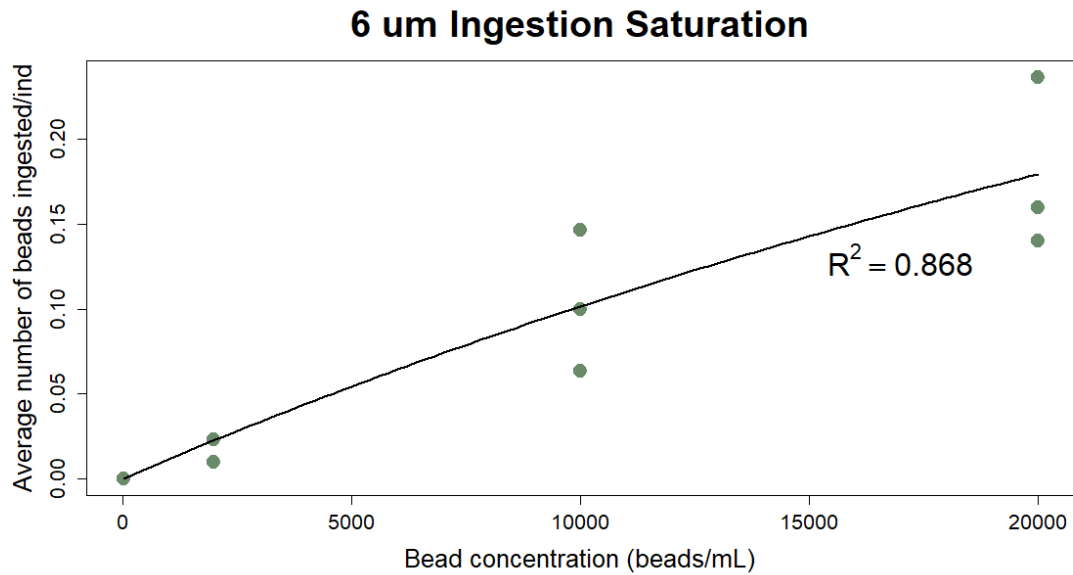


Figure S2.1 Polystyrene (PS) microbead ingestion saturation in *Crassostrea virginica* larvae (1-day-post-fertilization) for exposures to 6 μm PS beads and all algal concentrations. Trendline represents the model fit of the Holling's Type II functional response equation: $y = y_{\text{max}} \frac{[x]}{[x] + x_{\text{half}}}$ with $R^2 = 0.868$, $y_{\text{max}} = 0.765$ beads ingested ind^{-1} , and $x_{\text{half}} = 65,297$ beads mL^{-1} .

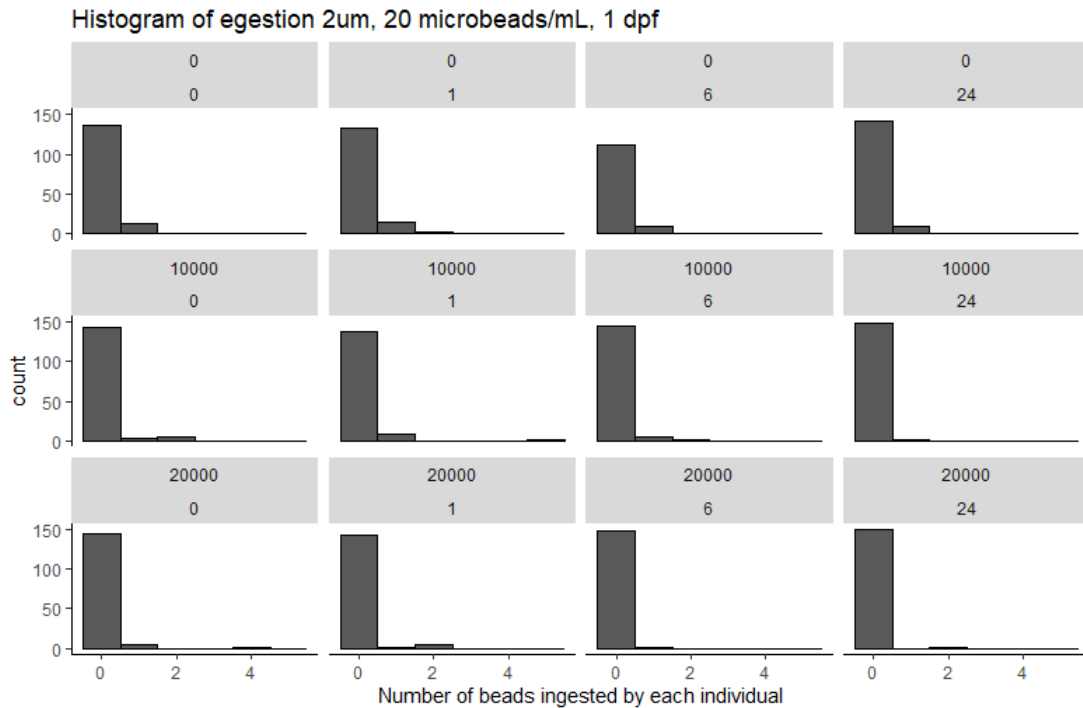


Figure S2.2 Histogram depicting 2 μm polystyrene microbead burden for each larva (1 day-post-fertilization) for three algal concentrations used in Method 2 (0, 10, 20 10^3 cells mL^{-1}) over the egestion period. Time zero is after a 24-hour ingestion exposure to 20 microbeads mL^{-1} and egestion subsamples were taken 1, 6, and 24 hours after placement in microbead free water. Microbead burden was assessed by observing the number of microbeads in each individual.

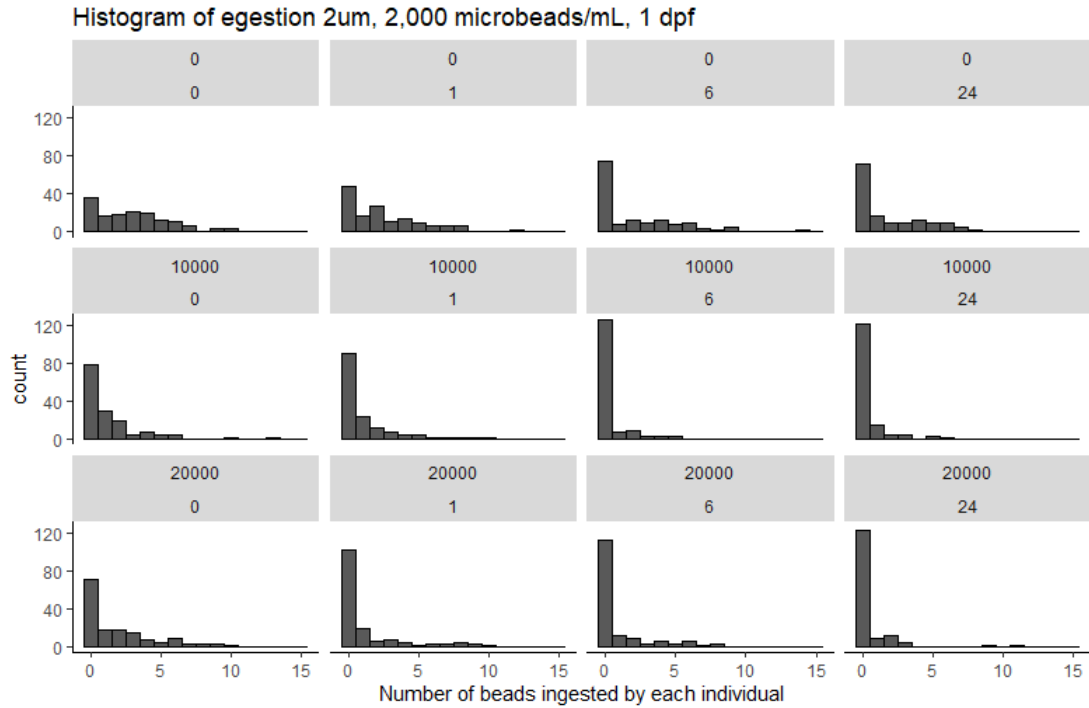


Figure S2.3 Histogram depicting 2 μ m polystyrene microbead burden for each larva (1 day-post-fertilization) for three algal concentrations used in Method 2 (0, 10, 20 10^3 cells mL^{-1}) over the egestion period. Time zero is after a 24-hour ingestion exposure to 2,000 microbeads mL^{-1} and egestion subsamples were taken 1, 6, and 24 hours after placement in microbead free water. Microbead burden was assessed by observing the number of microbeads in each individual.

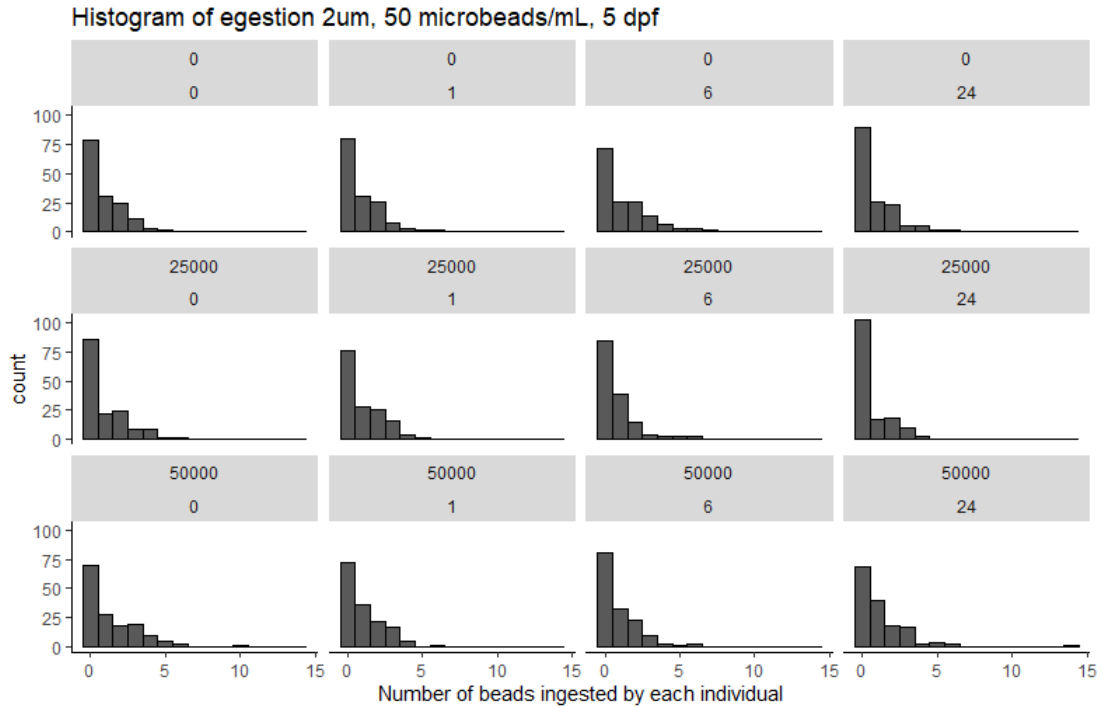


Figure S2.4 Histogram depicting 2 μ m polystyrene microbead burden for each larva (5 days-post-fertilization) for three algal concentrations used in Method 2 (0, 25, 50 10^3 cells mL⁻¹) over the egestion period. Time zero is after a 24-hour ingestion exposure to 50 microbeads mL⁻¹ and egestion subsamples were taken 1, 6, and 24 hours after placement in microbead free water. Microbead burden was assessed by observing the number of microbeads in each individual.

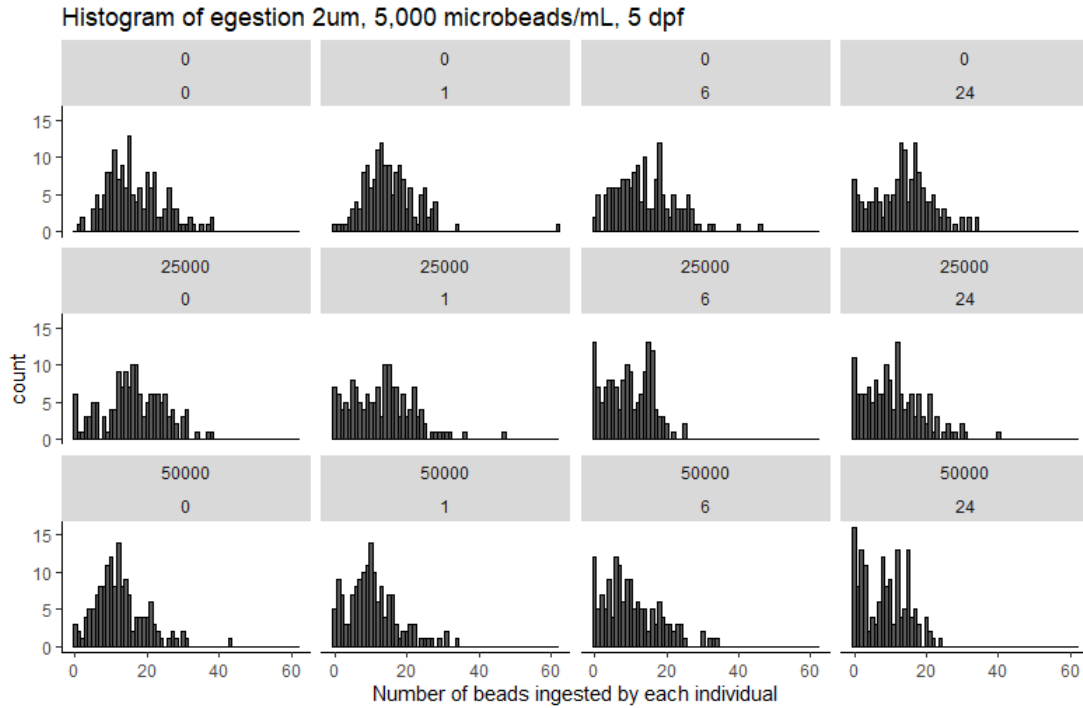


Figure S2.5 Histogram depicting 2 μ m polystyrene microbead burden for each larva (5 days-post-fertilization) for three algal concentrations used in Method 2 (0, 25, 50 10^3 cells mL^{-1}) over the egestion period. Time zero is after a 24-hour ingestion exposure to 5,000 microbeads mL^{-1} and egestion subsamples were taken 1, 6, and 24 hours after placement in microbead free water. Microbead burden was assessed by observing the number of microbeads in each individual.

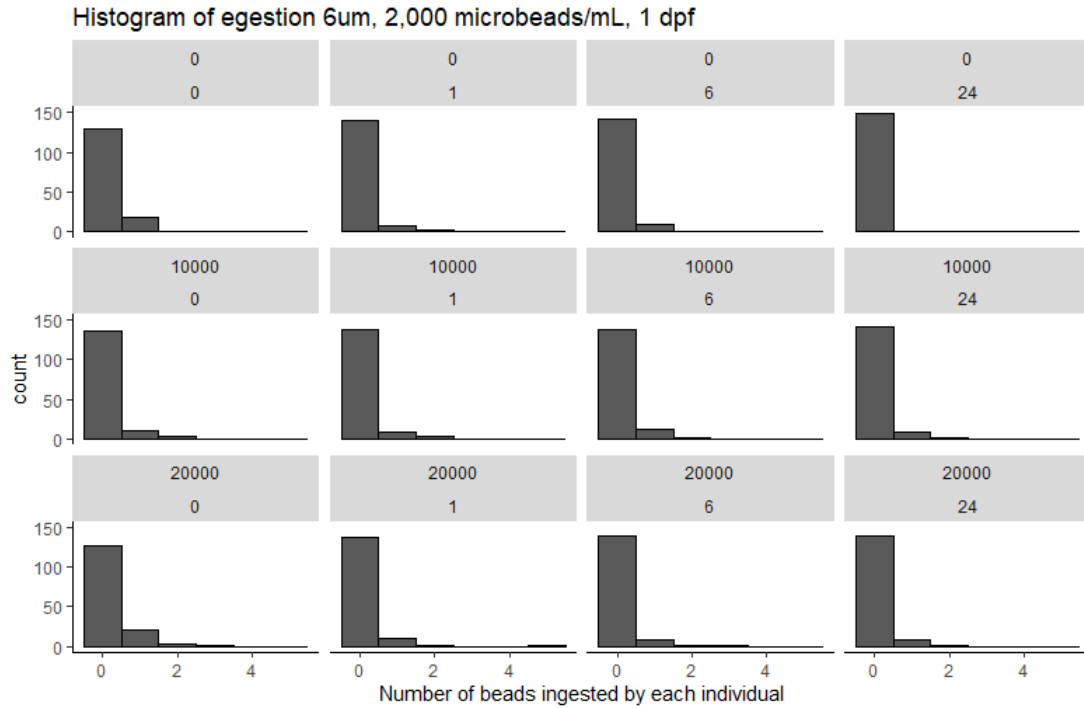


Figure S2.6 Histogram depicting 6 µm polystyrene microbead burden for each larva (1 day-post-fertilization) for three algal concentrations used in Method 2 (0, 10, 20 10³ cells mL⁻¹) over the egestion period. Time zero is after a 24-hour ingestion exposure to 2,000 microbeads mL⁻¹ and egestion subsamples were taken 1, 6, and 24 hours after placement in microbead free water. Microbead burden was assessed by observing the number of microbeads in each individual.

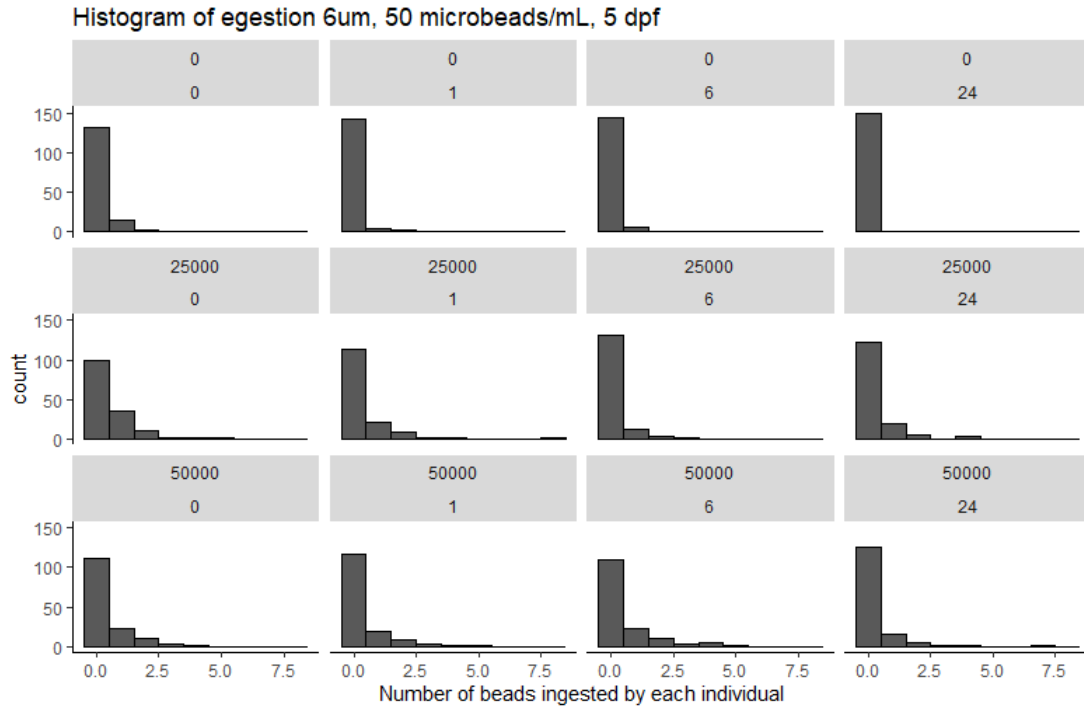


Figure S2.7 Histogram depicting 6 µm polystyrene microbead burden for each larva (5 days-post-fertilization) for three algal concentrations used in Method 2 (0, 25, 50 10³ cells mL⁻¹) over the egestion period. Time zero is after a 24-hour ingestion exposure to 50 microbeads mL⁻¹ and egestion subsamples were taken 1, 6, and 24 hours after placement in microbead free water. Microbead burden was assessed by observing the number of microbeads in each individual.

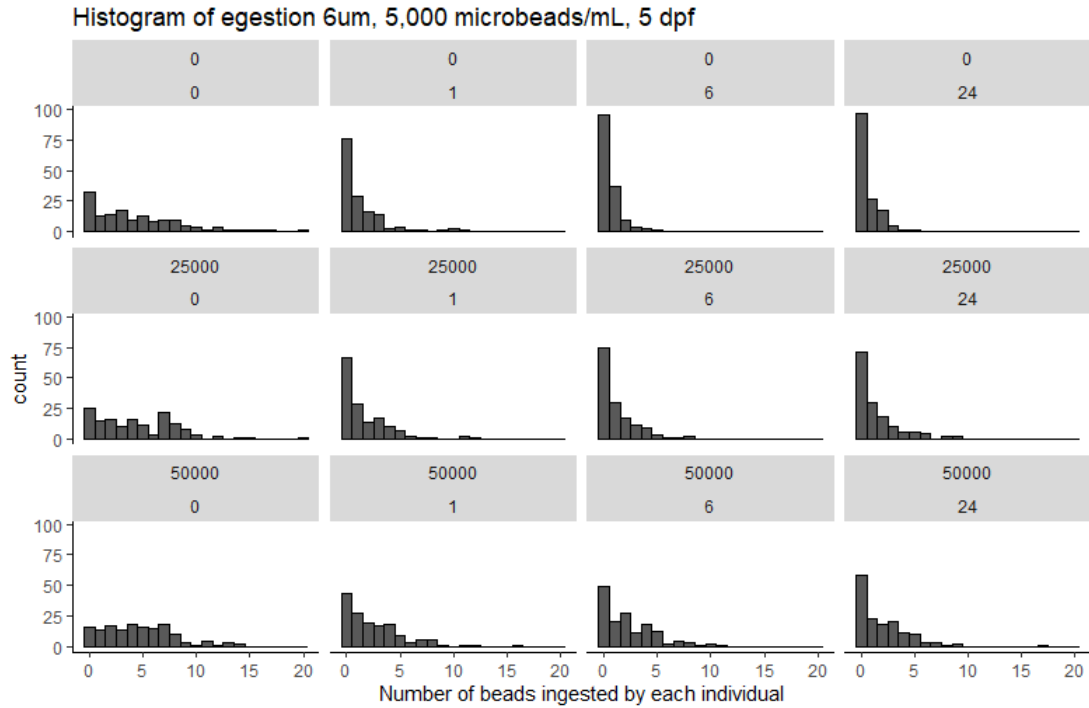


Figure S2.8 Histogram depicting 6 μ m polystyrene microbead burden for each larva (5 days-post-fertilization) for three algal concentrations used in Method 2 (0, 25, 50 10^3 cells mL^{-1}) over the egestion period. Time zero is after a 24-hour ingestion exposure to 5,000 microbeads mL^{-1} and egestion subsamples were taken 1, 6, and 24 hours after placement in microbead free water. Microbead burden was assessed by observing the number of microbeads in each individual.

Chapter 3: Physiological Effects of Microbeads on *Crassostrea virginica* Larvae

Abstract

Ecologically and economically important filter-feeding bivalves process large volumes of water and readily ingest microplastics. As plastic production and plastic pollution in coastal ecosystems increase, oysters and other bivalves will be exposed to higher concentrations of microplastics. Although, the effects of microplastic ingestion by adult bivalves has been assessed, little is known about the effects of microplastic ingestion on the larval life stage, the most sensitive life stage. In this study, *Crassostrea virginica* larvae were exposed to microplastic particles in a series of experiments to examine physiological effects from ingestion. Larvae (8-15 days-post-fertilization) were exposed to two sizes of virgin polystyrene (PS) microbeads (2 and 6 μm diameter, Polysciences) for various lengths of time (2-6 days) at multiple microbead concentrations (10, 100, 1000 beads mL^{-1}). Physiological rates (growth, respiration, algal ingestion and carbon assimilation) were measured over the exposure time and compared to controls. Results showed that microbead ingestion did not significantly affect larval growth or respiration, algal ingestion, or carbon assimilation rates for any microbead concentration or exposure time. Microbead concentrations used for this study were at and above the larval threshold for ingestion but orders of magnitude greater than estimated environmental concentrations. Ingestion of small spherical microplastics in the environment likely pose minimal risks to oyster larvae, however, extrapolation of these results to the particle types more abundant in coastal

ecosystems, such as fragments and fibers, and to chemical contamination (inherent and adsorbed) associated with plastic, remain to be addressed.

Introduction

Microplastics are a complex suite of contaminants that are pervasive and persistent in the environment. They exist in all environmental compartments and are consistently found in estuaries and coastal ecosystems (Lusher et al., 2017; Piehl et al., 2018; Waite et al., 2018; Wright et al., 2020; Yonkos et al., 2014). Global plastic production is expected to reach 1.1 billion tons yr⁻¹ by 2050 in business-as-usual scenarios (Geyer, 2020) and plastic pollution is expected to double from about 40 to 80 million metric tons yr⁻¹ by 2040 (Lau et al., 2020). For micron-sized particles, large scale clean ups are not feasible because microplastics are similar in size to phytoplankton, zooplankton, and other organic particles. Therefore, it is crucial to understand the dynamics between, and impacts of, microplastics on organisms.

Plastic concentrations in coastal ecosystems vary by plastic disposal, population density, land use, water circulation, and site ecology. Coastal concentrations of microplastics have been reported from 0-359 particles L⁻¹ (Lusher et al., 2017 and references therein p. 89-91). The Mosquito Lagoon estuary, Florida, USA had an average of 21.4 ± 13.1 (mean \pm SD) particles L⁻¹ between three sites (Waite et al., 2018) and a range of 0.5-10.2 microplastic particles L⁻¹ was reported for the Yangtze Estuary, China (Zhao et al., 2014). Two studies examined microplastic concentrations in the Chesapeake Bay with ranges in concentrations from 0 - 297,927 \pm 180,252 particles km⁻² (approximately 0 - $4.47 \times 10^{-7} \pm 0.27 \times 10^{-7}$ particles L⁻¹ assuming 15 cm sampling depth) in four tributaries (Yonkos et al., 2014) and 1366-

248,946 particles km⁻² (7×10^{-6} - 0.00125 particles L⁻¹) in the main stem of the Bay, with fragments, films, and fibers comprising 32%, 26%, and 18% of the particles respectively (Bikker et al., 2020). However, the majority of microplastic sampling occurs at the surface, while microplastics exist throughout the water column, and most sampling uses mesh nets > 330 µm, missing smaller microplastics available in the ingestible size range for oysters. Few studies have been able to sample for particles < 100 µm, limiting a more complete assessment of environmental concentrations. This is a critical data gap because small microplastics are more abundant than larger microplastics (Lindeque et al., 2020).

Filter feeding organisms are particularly at risk to microplastic pollution because they process large volumes of water, and therefore, have been a focus for microplastic exposures. It is important to understand the interactions and risks from microplastic pollution to bivalves, like oysters, because they live in shallow coastal waters, are keystone species, provide vital ecological services, and are an important global shellfishery (Wilberg et al., 2011). Microplastics have been found in many species of bivalves around the globe, including species sold for human consumption (Cho et al., 2019; Van Cauwenberghe & Janssen, 2014). For example, *Crassostrea gigas* (*C. gigas*) purchased in markets in South Korea had an average of 0.77 ± 0.74 particles ind⁻¹, ranging in size from 100-200 µm, with fragments being the dominant shape (Cho et al., 2019). Adult *Crassostrea virginica* (*C. virginica*) collected from Mosquito Bay, Florida, USA had an average of 16.5 microplastics ind⁻¹, with the majority being dark blue fibers (Waite et al., 2018). Finally, adult *C. gigas* collected from the Oregon coast averaged 10.33 ± 1.92 to 17.50 ± 3.85 (mean \pm SE)

microplastics ind⁻¹ in the spring and 5.20 ± 1.54 to 11.00 ± 3.03 particles ind⁻¹ in the summer (Baechler et al., 2020).

Microbeads were originally thought to be inert particles and were used frequently in laboratory experiments with filter feeding organisms to assess particle selection processes, to determine baseline clearance and ingestion rates, and to examine gut residence time (Ward, Rosa, et al., 2019). For example, previous studies determined that oyster larvae of all ages readily ingested microbeads with diameters between 0.16 μm -27.4 μm , with 27.4 μm as the maximum particle diameter tested, and saw ingestion within 10 minutes for particles $\leq 4.80 \mu\text{m}$ in diameter (Baldwin & Newell, 1991; Bringer, Cachot, et al., 2020; Bringer, Thomas, et al., 2020; Cole & Galloway, 2015). Microbeads are useful tools in research because they have standardized sizes, a variety of surface functionalities, availability in different fluorescent wavelengths for visualization, resistance to organismal digestive degradation, and are commercially available in the ingestion size range of organisms (Ward, Rosa, et al., 2019). With the diameter, density or polymer type, and concentration, conversions of units between studies can be made.

Over the last decade, it has become clear that microplastic particles are not inert and they interact with chemicals, metals, other organic particles, and organisms. Evidence from the literature suggests mixed effects of microplastic ingestion on adult and juvenile oysters. Adult *C. gigas* exposed to 2 and 6 μm polystyrene (PS) microbeads for two months, during a reproductive cycle, had increased algal consumption and absorption efficiency, decreased oocyte number and diameter, and decreased sperm velocity (Sussarellu et al., 2016). Also, D-stage larval yield was

reduced and metamorphosis was delayed by 6 days in larvae with microbead exposed parents (Sussarellu et al., 2016). Juvenile *C. gigas* exposed to 6µm PS microbeads for 80 days showed increased mortality and decreased lysosomal membrane stability and Condition Index (Thomas et al., 2020). In contrast, *C. gigas* adults exposed to polyethylene and polypropylene fragments (< 400 µm) at environmentally relevant concentrations for 10 days showed no significant changes in clearance rate, oxidative stress, tissue integrity, immune parameters, and DNA damage (Revel et al., 2020). While many laboratory exposure concentrations are consistently higher than what is reported in the environment, reliable techniques and methods to collect, identify, and quantify microplastics < 100 µm are lacking so concentrations for these small microplastics are not well understood (Covernton et al., 2019).

Only four studies have examined effects of microplastic ingestion on the larval life stage of oysters. Exposures with *C. gigas* showed that, after 24 hours, 1 µm PS microbeads significantly reduced algal ingestion at 1000 particles mL⁻¹ but minimal effects were observed for exposures at lower concentrations (1, 10, 100 microbeads mL⁻¹) (Cole & Galloway, 2015). The same study found that 8 day exposures to 1 or 10 µm PS microbeads (100 beads mL⁻¹) did not affect *C. gigas* larval growth (Cole & Galloway, 2015). Another study determined that 2 µm PS microbeads, with non-functionalized surfaces, did not affect *C. gigas* fertilization yield, embryo-larval development, or metamorphosis (Tallec et al., 2018). *C. gigas* exposed to high density polyethylene (HDPE) microbeads caused higher rates of malformation and developmental arrest, caused dose-dependent decreases in swimming speed and altered swimming trajectories (Bringer, Thomas, et al., 2020).

Finally, *C. gigas* exposed to microbeads (1 - 5 μm , proprietary polymer, Cospheric, California, USA) also showed increased malformations and developmental arrest, decreased maximum swimming speed, and altered swimming behavior (Bringer, Cachot, et al., 2020).

Previous work (Chapter 2) showed that *C. virginica* larvae ingested microbeads in higher numbers as microbead exposure concentrations increased. As microplastic concentrations in the environment continue to increase, it is important to understand how microplastic ingestion affects the most vulnerable life stage of oysters. However, the effects of ingestion by the larval life stage are limited and no study has examined microplastic ingestion effects on the species *C. virginica*. Therefore, this study exposed *C. virginica* larvae to microplastics to examine physiological responses. *C. virginica* larvae were exposed to polystyrene (PS) microbead concentrations at and above their threshold of ingestion, determined from the previous chapter, for various lengths of time, up to about half of the larval period. Larval physiological response was then evaluated by measuring growth, algal ingestion, carbon assimilation, and respiration.

Methods

To examine physiological effects of microplastic ingestion, *C. virginica* larvae were exposed to various PS microbead concentrations for different lengths of time. An initial experiment exposed larvae to low PS microbead concentrations (10, 100 beads mL^{-1}) on a short timescale (2 - 3 days). Based on results from the initial experiment (Figure S3.2), two additional experiments with higher PS bead

concentrations (100, 1000 beads mL⁻¹) and longer exposure times (4 and 6 days) were conducted, examining concentration thresholds for physiological responses.

Experimental design

Larvae from the Horn Point Oyster Hatchery (Cambridge, Maryland, USA) (8, 13, 15 days-post-fertilization, dpf) were placed in 250 mL glass jars at a concentration of 10 larvae mL⁻¹ (total 2500 larvae per jar) with optimum concentrations of *Isochrysis galbana* (*I. galbana*) based on standard hatchery protocol (Helm & Bourne, 2004) and 0, 10, 100, or 1000 PS microbeads mL⁻¹ (Table 1). *I. galbana* provides high quality nutrition for bivalve larvae and provides cells with a similar size and shape as the PS microbeads (Helm & Bourne, 2004). Microbeads (Polysciences Fluoresbrite 2 µm, CAT #18338-5 and 6 µm, CAT #17156-2, density: 1.05 g mL⁻¹) were used because of their commercial availability, uniform and appropriate sizes, and standard application in plastic pollution studies. Two different diameter PS microbeads were chosen because larvae select larger food items as they grow (Baldwin 1995). With growth, larvae consistently have PS microbeads within their desired prey size. Microplastic concentrations were based on the ingestion threshold concentration determined in the previous chapter. All treatments were in triplicate.

Treatment jars were placed on a slowly rotating plankton wheel (one rotation per minute) for the allotted treatment duration. For the initial experiment, larvae (8 dpf) were exposed for 2-3 days. For the higher dose experiments, larvae (13 and 15 dpf) from the same brood were exposed for 4 and 6 days. Larvae were then subsampled for physiological measurements: growth/larval size and respiration, algal

ingestion, and carbon assimilation rates. For the 6-day treatment, subsamples of 200 larvae were collected on day 3 for analysis of algal ingestion and carbon assimilation (Figure 3.1), resulting in three sample time points. Larvae in the 4-day exposure were only sampled for algal ingestion and carbon assimilation before and after exposure. Larval treatments were too dilute (10 larvae mL⁻¹) to use subsamples directly with the instruments used to measure respiration and larval size. Concentrating subsamples was challenging with small numbers of larvae (250) and a maximum volume of 2 mL required for respiration analysis. Therefore, these measurements were only collected at the beginning and end for 4- and 6-day exposures.

Table 3.1 Design parameters used for *Crassostrea virginica* (*C. virginica*) larval exposures to polystyrene (PS) microbeads and fed with *Isochrysis galbana* (*I. galbana*).

Component	Description	Concentrations	Units
<i>C. virginica</i>	8-, 13- and 15-days post fertilization	10	Larvae mL ⁻¹
<i>I. galbana</i>	cells in exponential growth	80-100	10 ³ cells mL ⁻¹
PS microbeads	50/50 mix, 2 and 6 μm diameter	0, 10, 100, 1000	Beads mL ⁻¹

Subsampling and larval growth measurements

At the end of the allotted treatment time, three larval subsamples from each treatment were analyzed for four different physiological measurements: algal ingestion, carbon assimilation, respiration, and larval size. The first subsample of 200

larvae from each jar were analyzed for algal ingestion and carbon assimilation rates. The remaining larvae from each jar were washed onto a 40 μm sieve, rinsed with 15 salinity artificial sea water (ASW) (see Table S3.1), and concentrated in a 20 mL glass scintillation vial. Three measurements using 1 mL of concentrated larvae were taken from each treatment triplicate to determine larval size and concentration using a Beckman Coulter Multisizer 4. These concentrations were then used to take subsamples of 250 larvae to measure oxygen consumption, a proxy for respiration.

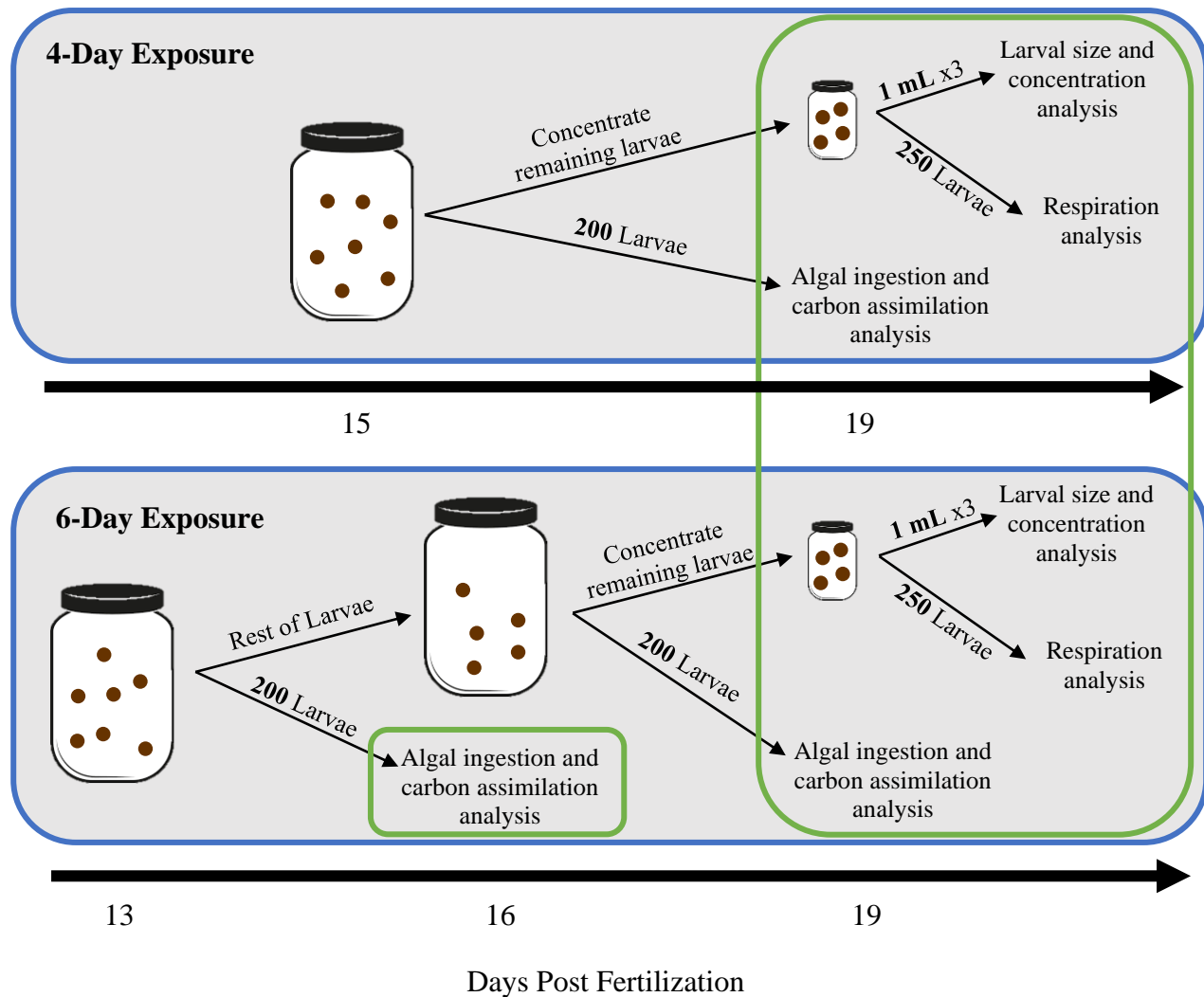


Figure 3.1 Conceptual diagram of treatment sampling for the 4- and 6-day exposures. The 6-day exposure began 13 days post fertilization (dpf), while the 4-day exposure began 15 dpf. On day 19, both experiments were terminated and larvae were concentrated and subsampled for physiological measurements. Green boxes indicate all time points where larvae were subsampled for analysis.

Respiration rate measurements

Respiration was measured using a Presens SDR multiwell instrument using fiber optic oxygen analysis (Presens, Denmark). The larval subsamples (250 larvae) were rinsed with 1 μm filtered ASW and placed in 2 mL vials with an attached

oxygen sensor “spot”, with vials placed randomly on the instrument. Measurements were taken at 3-minute intervals over 5 hours, under dark conditions. ASW controls were run simultaneously to determine background oxygen consumption. Respiration rates were determined using the Presens SDR software version 4.0.0. The slope of the linear region was used as the depletion of oxygen over time.

Algal ingestion and carbon assimilation rate measurements

Algal ingestion and carbon assimilation rates were measured using a ^{14}C radio-labelled phytoplankton method ((method adapted from Baldwin & Newell, 1991; Gallagher et al., 1994; Pace et al., 2006) by Dr. Katie McFarland, see Figure S3.1 for detailed steps). Small volumes of *I. galbana* stock solutions were made and spiked with 0.012 mCi of ^{14}C from a concentrated stock solution. *I. galbana* were allowed to grow in the ^{14}C spiked solution for 5 days before the start of the experiment so all cells would be ^{14}C labelled. The day before sampling, ^{14}C spiked algal cells were filtered using a 0.2 μm Nuclepore filter (Whatman 25 mm diam.) to remove any unincorporated ^{14}C . Algal cells were resuspended in ASW (1 μm filtered, 15 salinity) and transferred to a 15 mL tube. On the day of sampling, 200 larvae in 10 mL (15 salinity ASW) were placed into 20 mL scintillation vials with 30×10^3 cells mL^{-1} ^{14}C labelled *I. galbana*. Larvae were allowed to feed on the ^{14}C labelled algae for one hour. After one hour, larvae were separated from the ^{14}C labelled algae using a filtration manifold (Figure 3.2). Larvae were caught on 40 μm sieves (Corning cell strainer) placed on top of the steel filter cylinders. The ^{14}C spiked

I. galbana were caught on 0.7 μm glass microfiber filters (Whatman 25 mm diam.) at the bottom of the filter cylinders.

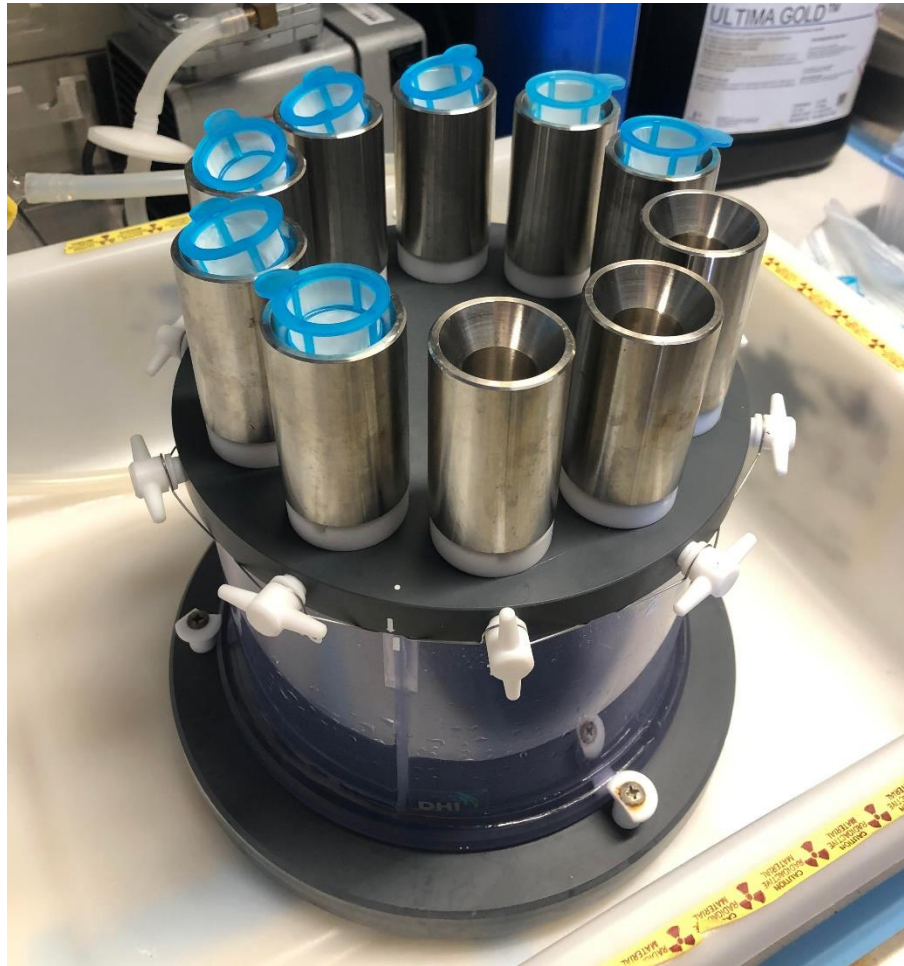


Figure 3.2 Filter manifold used to separate and collect *Crassostrea virginica* (*C. virginica*) larvae and *Isochrysis galbana* (*I. galbana*) for analysis in the liquid scintillation analyzer. Samples are poured through the blue 40 μm sieves on top of the steel cylinders. Glass fiber filters (Whatman 0.7 μm pore size) catch ^{14}C labelled algal cells at the bottom of the steel cylinders.

Larvae were immediately washed into clean 20 mL scintillation vials.

Unlabeled *I. galbana* (30×10^3 cells mL^{-1}) were added to the vials and larvae were allowed to feed for one hour. Filters with ^{14}C labelled *I. galbana* were transferred into 7 mL scintillation vials for counting. After the second feeding step, larval

samples were rinsed onto 0.7 µm glass microfiber filters (Whatman 25 mm diam.) using the filter manifold. Filters were placed in 7 mL scintillation vials for counting.

After collection on filters and placement in 7 mL scintillation vials, 0.5 N HCl was added to each sample to volatilize unassimilated ¹⁴C. Samples were left uncapped overnight. The next day, a tissue solubilizer (PerkinElmer Solvable™) was added to all scintillation vials to solubilize cells and vials were incubated for two hours. Finally, a liquid scintillation cocktail (Ultima Gold™) was added to each vial before placing the samples in a liquid scintillation analyzer (Packard Tri-carb 3100TR) using standard ¹⁴C settings.

Clearance rates were calculated following Coughlan (1969) and Pace et al. (2006):

$$Clearance\ rate = \frac{\ln(C_{initial}/C_{final})}{N \times T} \times V$$

where clearance rate is in mL min⁻¹ larva⁻¹, C_{initial} is DPM of the algal only control, C_{final} is the DPM of remaining *I. galbana* after 60 minutes of larval feeding, N is the number of larvae per vial, T is time (60 min), and V is the volume of solution (10 mL). Rates were converted to hourly rates. Clearance rate is transformed into ingestion rate using the equation:

$$Ingestion\ rate = Clearance\ rate \times \left(\frac{\#\ algal\ cells}{mL} \right)$$

Therefore, ingestion rate units are number of cells hour⁻¹ larva⁻¹. Carbon assimilation rate was calculated using the following equation:

$$Carbon\ assimilation\ rate = \left(\frac{DPM_{larval}}{N} \right) \left(\frac{1}{\frac{DPM_{algal\ control}}{P} \times T} \right)$$

where carbon assimilation rate units are the number of cells $\text{hour}^{-1} \text{larva}^{-1}$, N is the number of larvae, P is the number of algal cells fed to the larvae, and T is larval feeding time.

Statistical analysis

Data were tested for normality and homogeneity of variance using the Shapiro-Wilk and Levene's tests respectively. All data were normally distributed and showed homoscedasticity so ANOVAs and Tukey's post hoc tests were used to determine significant differences in means of larval size and respiration, algal ingestion, and carbon assimilation rates. Data reported are means with standard error. All statistical analyses were performed in R Studio version 1.4.1103 and significance reported at $p < 0.05$.

Results

Concentrations of 10 and 100 PS microbeads mL^{-1} in the initial experiment did not affect carbon assimilation rates or respiration rates of oyster larvae after they were exposed for 2 and 3 days respectively (Figure S3.2). Algal ingestion rates and larval growth were not determined. After 4- and 6-day exposures, no significant effects on the growth or respiration, algal ingestion, and carbon assimilation rates of larvae were observed for 100 and 1000 PS microbeads mL^{-1} treatments (Figures 3.3 and 3.4). After 4 days of exposure, increases in larval respiration rates were not significant ($p > 0.05$), but showed a dose dependent response with the 1000 beads mL^{-1} treatment having the highest rate (Figure 3.3B). The 6-day exposure did not replicate this pattern in respiration rates but did have a similar pattern for algal

ingestion rates after 3 and 6 days of exposure and carbon assimilation rates after 6 days of exposure (Figure 3.4B, C, D). Figure 3.4C shows overall decreased algal ingestion rates from day 3 to day 6 in all treatment groups. Larval growth over the 4- and 6-day exposures was minimal even in the control treatments (Table 3.2). Average rate measurements for respiration, algal clearance, algal ingestion, and carbon assimilation are provided in the supporting information (Table S3.2).

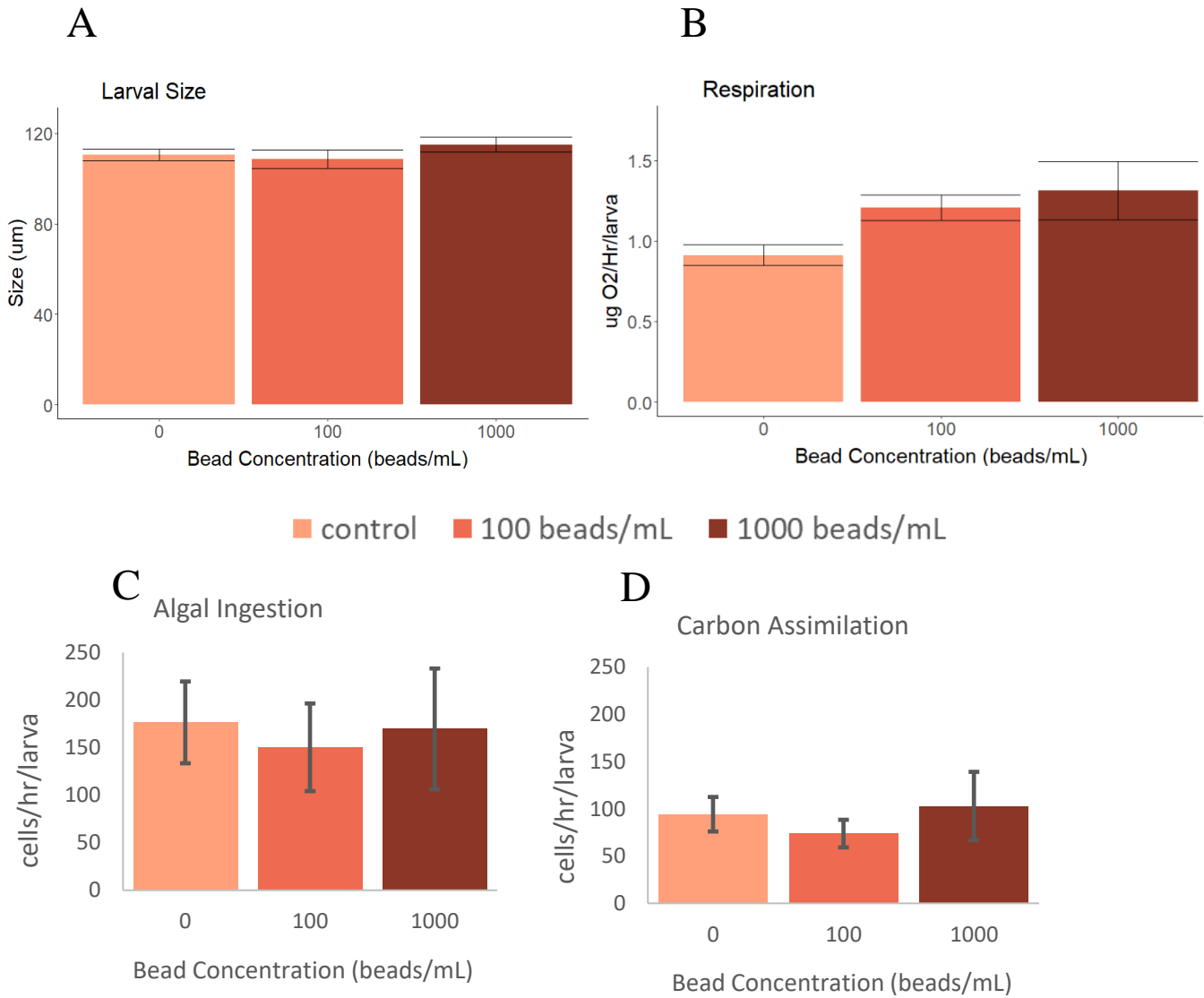


Figure 3.3 Physiological responses of *Crassostrea virginica* (*C. virginica*) larvae after a 4-day exposure to polystyrene microbeads. (A) larval size, (B) respiration rates, (C) algal ingestion rates, and (D) carbon assimilation rates were measured on day 4. No statistical differences (using one way ANOVA, $p > 0.05$) were observed between all three treatments in respiration, algal ingestion, and carbon assimilation rates or larval size. Error bars show standard error.

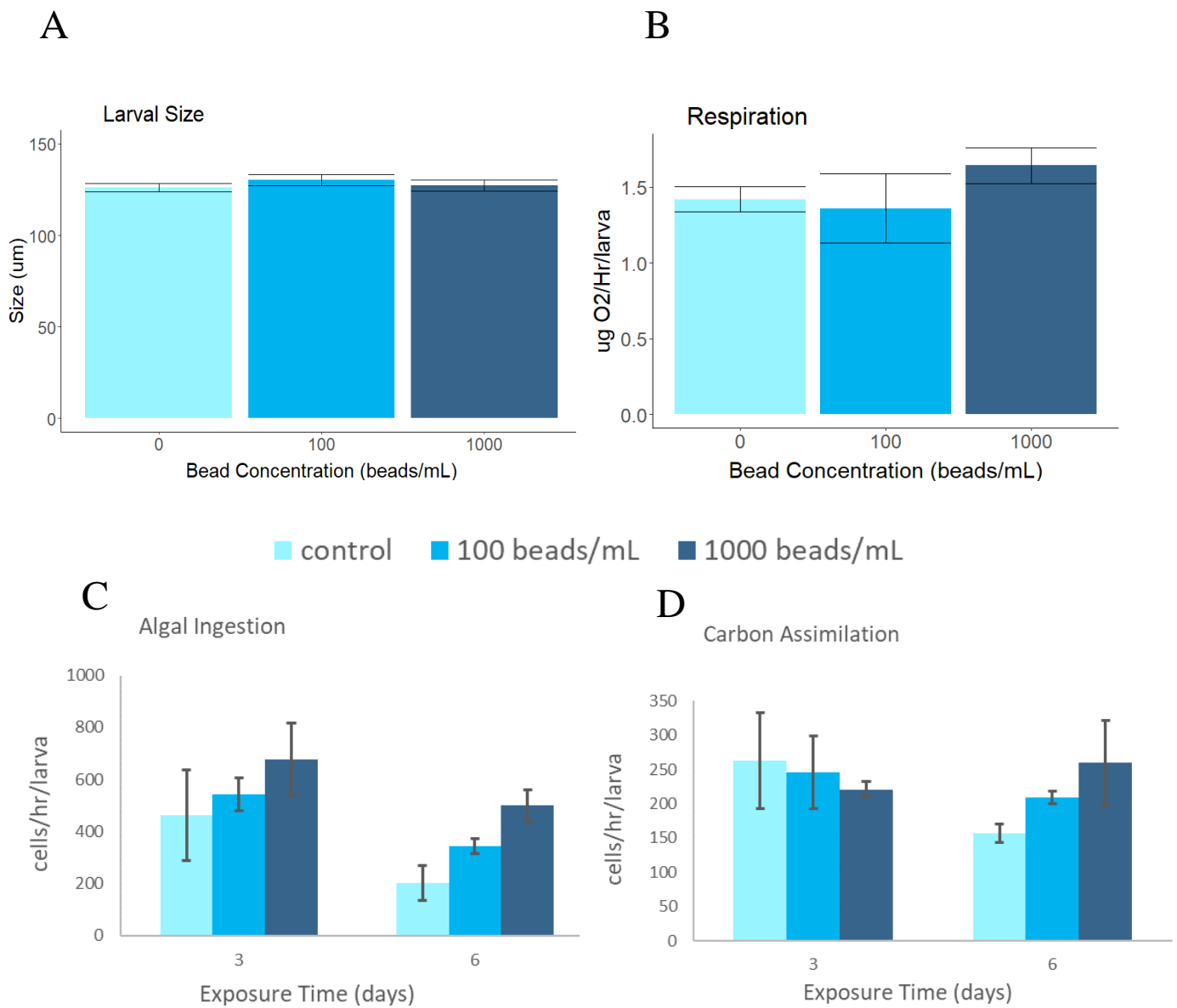


Figure 3.4 Physiological responses of *Crassostrea virginica* (*C. virginica*) larvae after a 6-day exposure to 100 and 1000 polystyrene microbeads mL⁻¹. (A) larval size and (B) respiration rates were measured on day 6 and (C) algal ingestion and (D) carbon assimilation rates were measured on days 3 and 6. ANOVAs and Tukey's post hoc tests show no significant differences in larval size or respiration, algal ingestion, and carbon assimilation rates ($p > 0.05$). Error bars show standard error.

Table 3.2 *Crassostrea virginica* (*C. virginica*) larval lengths ($\mu\text{m} \pm \text{SD}$) before and after 4- and 6- day polystyrene (PS) microbead exposures.

Day 0		Day 4	
Control	$107.47 \pm 1.89 \mu\text{m}$	Control	$110.42 \pm 4.90 \mu\text{m}$
		100 beads mL^{-1}	$108.59 \pm 9.23 \mu\text{m}$
		1000 beads mL^{-1}	$115.59 \pm 3.99 \mu\text{m}$

Day 0		Day 6	
Control	$109.77 \pm 2.89 \mu\text{m}$	Control	$125.80 \pm 2.67 \mu\text{m}$
		100 beads mL^{-1}	$130.30 \pm 6.63 \mu\text{m}$
		1000 beads mL^{-1}	$127.32 \pm 8.47 \mu\text{m}$

Discussion

The data presented here are the first to examine microplastic effects on *C. virginica* larvae. Results showed that PS microbeads have minimal physiological impacts on *C. virginica* larvae, even at high concentrations. In the initial experiment, concentrations of 10 and 100 beads mL^{-1} showed no effects on the respiration rate or carbon assimilation rate of larval oysters after 2 and 3 days. In the subsequent experiments, the microbead concentrations and length of exposure were increased to 100 and 1000 beads mL^{-1} and 3–6-day exposures. Dose-dependent increases were seen in algal ingestion rates after 3 and 6 days of exposure and carbon assimilation rates after 6 days of exposure but they were not significant ($p > 0.05$). The higher concentrations of microbeads and longer exposure times did not significantly affect oyster larval physiology in any of the parameters measured.

Findings from this study align with the limited number of other studies examining the effects of microplastic ingestion by filter-feeding bivalve larvae. After an 8-day exposure of 1 and 10 μm PS microbeads $< 100 \text{ beads mL}^{-1}$, *C. gigas* larval growth and feeding was unaffected (Cole & Galloway, 2015). Also, 2 μm PS microbeads did not affect fertilization yield, larval development, or metamorphosis of *C. gigas* (Tallec et al., 2018). An 80-day exposure of 6 μm PS microbeads, at the same concentrations to this study (10, 100, 1000 beads mL^{-1}), reduced lysosomal stability and increased mortality in juvenile *C. gigas* only at the highest concentration (Thomas et al., 2020).

Clearance and respiration rates from these experiments are similar to values found in the literature. Baldwin and Newell (1991) found clearance rates for *C. virginica* larvae with shell lengths of 179 μm to be 0.0017-0.0825 $\text{mL hr}^{-1} \text{larva}^{-1}$, while mean clearance rates in my experiments ranged from 0.0050 - 0.0226 $\text{mL hr}^{-1} \text{larva}^{-1}$ (Table S3.2). Mean respiration rates of control larvae (17 dpf, $\sim 200 - 260 \mu\text{m}$) ranged from about 0.8 to 1.25 $\mu\text{g O}_2 \text{Hr}^{-1} \text{larva}^{-1}$ while mean rates in my experiments ranged from 0.65 to 1.64 $\mu\text{g O}_2 \text{Hr}^{-1} \text{larva}^{-1}$ (Table S3.2) (McFarland et al., 2020).

Larval growth was not consistent with the literature. Table 3.2 showed minimal growth in the control treatment for the experiments over 4 and 6 days. Larvae typically grow tens of microns a day so they should have been much larger after 4 and 6 days (Helm & Bourne, 2004; Kennedy, 1996; McFarland et al., 2020). Stunted growth could have been caused by either the use of *I. galbana* as a monoculture food source or a tank effect from the sealed bottles. Stunted growth has

been observed when using *I. galbana* as the sole food source, with larvae > 110 μm (Helm & Bourne, 2004). This species was chosen because it is widely used in oyster aquaculture and is similar in size and shape to the PS microbeads used, reducing confounding factors in particle selection. Another explanation for stunted growth could be a tank effect. Bottles were opened and oxygen exchanged in the head space daily but it is possible that the sealed small bottles could have caused some type of negative effect on the larvae resulting in limited growth and reduced algal ingestion for all treatments from day 3 to day 6. One study determined that using a plankton wheel was the best for maintaining microplastic suspensions, but static bottles with aeration was not tested (Salaberria et al., 2020). In future studies, using an aeration system might reduce a tank effect.

Microplastic concentrations used in this study were higher than what is estimated to be in coastal ecosystems for these particle sizes. Microplastic concentrations were chosen based on ingestion thresholds (about 20 beads mL^{-1} for 2 dpf larvae) determined from the results of chapter 2. Effects of microplastics were assumed to occur only when ingested and not from other physical interactions; physical interactions between 2 μm PS beads and *C. gigas* larvae showed no effects (Tallec et al., 2018). The concentrations used (10, 100, 1000 beads mL^{-1}) were higher than what has been found in the Chesapeake Bay (highest concentration recorded $\sim 4.47 \times 10^{-7} \pm 0.27 \times 10^{-7}$ particles L^{-1} assuming 15 cm sampling depth) (Bikker et al., 2020; Yonkos et al., 2014), however, the vast majority of environmental sampling misses the size class of microplastics that are in the ingestible range for oyster larvae ($\leq 30 \mu\text{m}$) (Baldwin & Newell, 1991; Cole & Galloway, 2015). The only two studies

examining microplastics in the Chesapeake Bay used surface trawls and mesh nets; these data excluded microplastics < 330 μm and particles below the top 20 cm in the water column (Bikker et al., 2020; Yonkos et al., 2014). There are currently no reliable methods to accurately collect, identify, and quantify microplastics < 100 μm so environmental concentrations in this size range are unknown. However, when using a 100 μm mesh net vs. 333 or 500 μm mesh nets for surface manta trawls, microplastics were collected in 2.5- and 10-fold greater concentrations respectively (Lindeque et al., 2020).

Conclusion

As keystone species, oysters provide vital ecological functions for coastal regions and estuaries, like the Chesapeake Bay. Their filter feeding ability, a crucial characteristic of their ecological importance, also makes them particularly susceptible to microplastic contamination. Even though *C. virginica* larvae readily ingest microplastic beads, this was the first experiment examining the effects of microbead ingestion. Microbead ingestion did not affect larval physiology, even concentrations well above estimated environmental concentrations and with long exposures up to half of the larval period. Microbeads likely present minimal risks to oyster larvae based on these results and microbead environmental concentrations. Further studies using particles with characteristics (physical and chemical) more representative of microplastics in the environment are needed. Additionally, more microplastic studies using the larval stage of organisms are necessary to understand the interactions, effects, and risks microplastics have on the full life history of organisms. Finally, technical and methodological advancements to be able to collect, identify, and

quantify microplastics < 100 μm from the environment will help align laboratory exposure experiments with environmental microplastic risks.

Supporting Information

Table S3.1 Modified Artificial Seawater

To dH₂O add the following per 200 L for 15 ± PSU:

Salts	Amount
400 mM NaCl	2.3375 kg
20 mM MgSO ₄ •7H ₂ O	492.5 g
10 mM CaCl ₂	111 g
1.7 mM KBr	20.25 g
10 mM KCl	74.5 g
20 mM MgCl ₂ •6H ₂ O	406.3 g
0.404 mM H ₃ BO ₃	2.5 g

Table S3.2 Data means (± SE) for physiological measurements of *Crassostrea virginica* (*C. virginica*) larvae after exposure to polystyrene (PS) microbeads.

Experiment	Day	Measurement type	Treatment (beads mL ⁻¹)	Mean ± SE
Initial	2	Carbon assimilation (cells Hr ⁻¹ larva ⁻¹)	Control	249.25 ± 59.08
			10	282.03 ± 83.23
			100	220.27 ± 32.94
	3	Respiration (µg O ₂ Hr ⁻¹ larva ⁻¹)	Control	0.81 ± 0.10
			10	0.65 ± 0.16
			100	0.80 ± 0.24

4-day exposure	4	Respiration ($\mu\text{g O}_2 \text{ Hr}^{-1} \text{ larva}^{-1}$)	Control	0.91 ± 0.07
			100	1.21 ± 0.08
			1000	1.31 ± 0.18
	4	Algal clearance ($\mu\text{L Hr}^{-1} \text{ larva}^{-1}$)	Control	5.89 ± 1.43
			100	5.01 ± 1.54
			1000	5.66 ± 2.12
	4	Algal ingestion (cells $\text{Hr}^{-1} \text{ larva}^{-1}$)	Control	176.57 ± 43.02
			100	150.38 ± 46.08
			1000	169.68 ± 63.57
	4	Carbon assimilation (cells $\text{Hr}^{-1} \text{ larva}^{-1}$)	Control	94.26 ± 18.26
			100	73.80 ± 14.59
			1000	102.91 ± 36.19
6-day exposure	3	Respiration ($\mu\text{g O}_2 \text{ Hr}^{-1} \text{ larva}^{-1}$)	Control	X
			100	X
			1000	X
		Algal clearance ($\mu\text{L Hr}^{-1} \text{ larva}^{-1}$)	Control	15.43 ± 5.84
			100	18.08 ± 2.13
			1000	22.59 ± 4.67
		Algal ingestion (cells $\text{Hr}^{-1} \text{ larva}^{-1}$)	Control	462.95 ± 175.26
			100	542.40 ± 63.77
			1000	677.73 ± 140.10
	Carbon assimilation (cells $\text{Hr}^{-1} \text{ larva}^{-1}$)	Control	262.50 ± 70.27	
		100	245.54 ± 53.04	
		1000	220.73 ± 11.15	
	6	Respiration ($\mu\text{g O}_2 \text{ Hr}^{-1} \text{ larva}^{-1}$)	Control	1.42 ± 0.08
			100	1.36 ± 0.23
			1000	1.64 ± 0.12
		Algal clearance ($\mu\text{L Hr}^{-1} \text{ larva}^{-1}$)	Control	6.78 ± 2.22
			100	11.45 ± 0.91
			1000	16.65 ± 2.08
Algal ingestion (cells $\text{Hr}^{-1} \text{ larva}^{-1}$)		Control	203.43 ± 66.73	
		100	343.46 ± 27.17	
		1000	499.38 ± 62.48	
Carbon assimilation (cells $\text{Hr}^{-1} \text{ larva}^{-1}$)	Control	156.26 ± 13.32		
	100	209.27 ± 8.78		
	1000	259.60 ± 62.05		

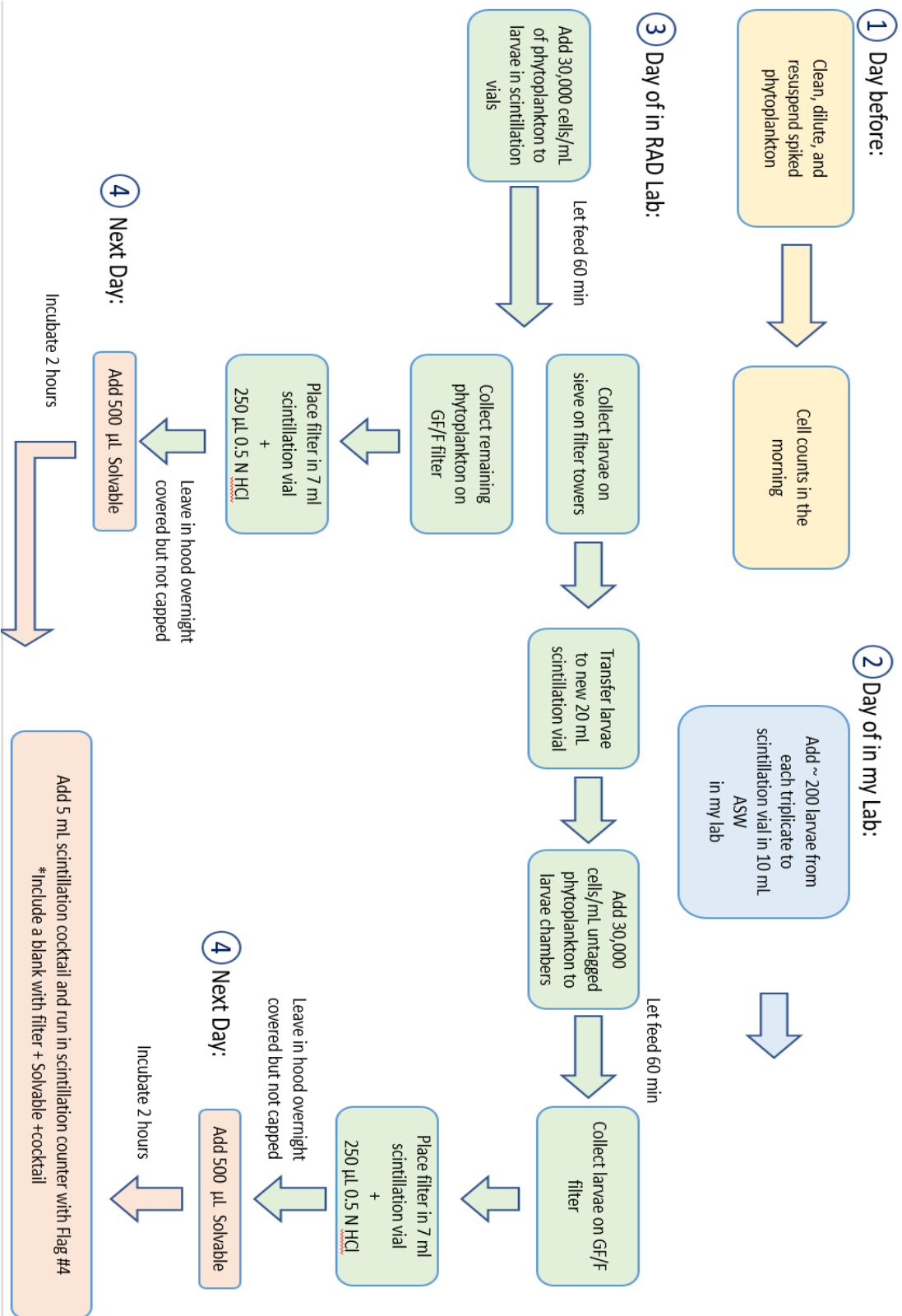


Figure S3.1 Conceptual diagram for ^{14}C radio-labelled phytoplankton method steps.

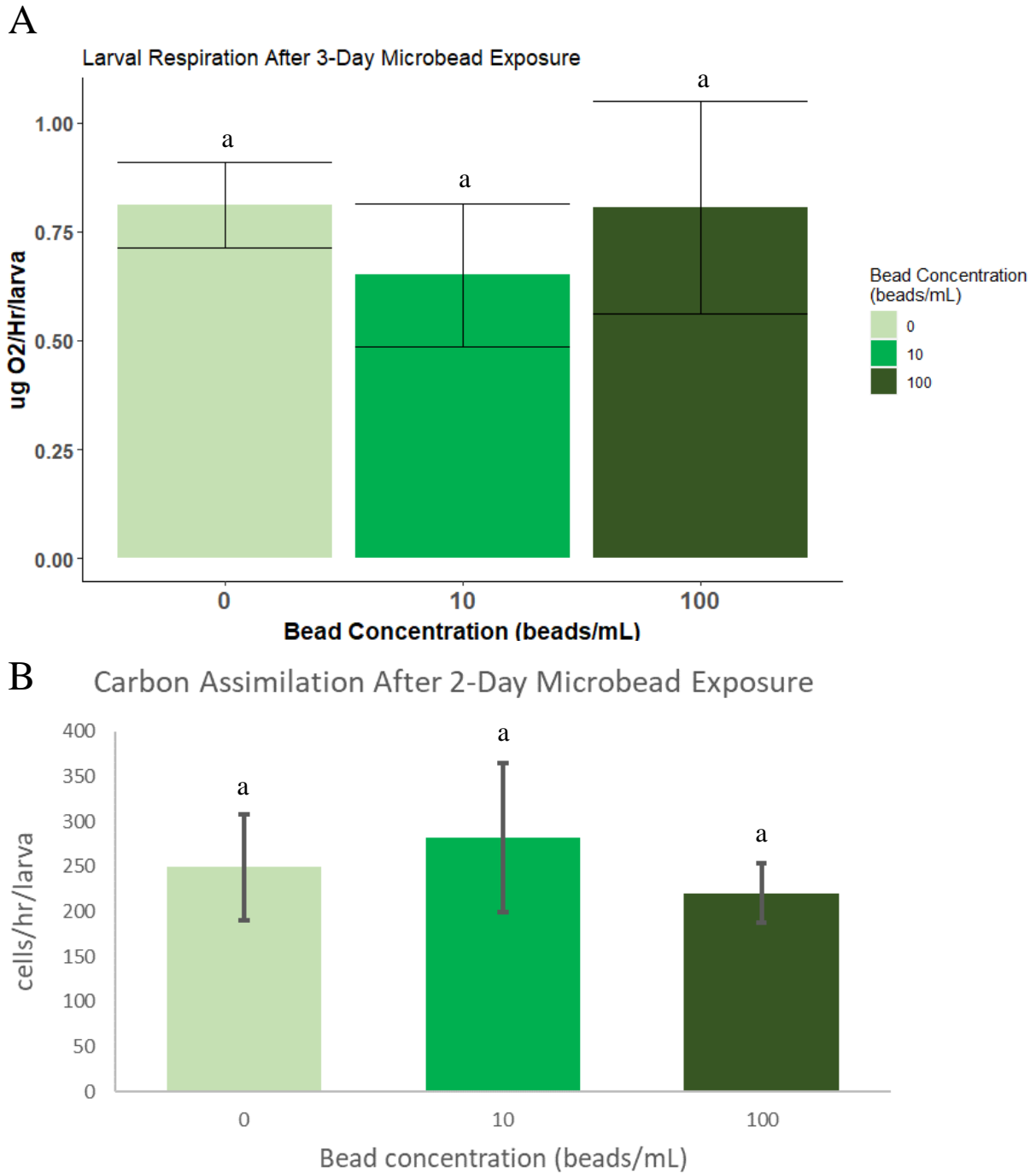


Figure S3.2 Respiration (A) and carbon assimilation (B) rates for *Crassostrea virginica* (*C. virginica*) larvae (8 days post fertilization, 80 - 150 μ m) exposed to 10 and 100 polystyrene microbeads mL^{-1} after 3 and 2 days respectively. ANOVAs ($p > 0.05$) show no significant differences between treatments. Error bars show standard error.

Chapter 4: Physiological Effects of Microfibers on *Crassostrea virginica* Larvae

Abstract

Microfibers are one of the most abundant particle types in the environment and are ingested by a variety of marine organisms including bivalves, but little is understood regarding early life stage exposure, when most vulnerable to contaminants. The Eastern oyster (*Crassostrea virginica*) is a valuable ecological and economic resource along the east coast of the United States, with the dynamics between microplastics and oysters of concern. Larvae (> 100 μm diameter) were exposed to virgin microfibers made from polymers commonly found in the coastal environment: polyethylene terephthalate (PET) (14 x 14 and 14 x 28 μm) and nylon 6,6 (10 x 10 and 10 x 30 μm). Exposure concentrations of 100 and 1000 microfibers mL^{-1} were compared to controls for six days, during which physiological rates (respiration, algal ingestion, carbon assimilation, and growth) were measured. PET microfiber exposure showed no significant differences in algal ingestion and carbon assimilation rates compared to controls; however, it showed reduced respiration rates. A significant growth penalty was observed in larvae exposed to 1000 microfibers mL^{-1} after 6 days. Larvae exposed to nylon microfibers showed reduced, but not significant, algal ingestion and carbon assimilation rates, with the lowest rates at the highest microfiber concentration after 3 days. There were no significant differences in larval growth or respiration when exposed to nylon microfibers. The microfiber concentrations used in this study were at and above the larval threshold of ingestion

but greater than environmental concentrations. Microfibers at current environmental concentrations are unlikely to pose significant risks to oyster larval physiology, however, further studies are needed to understand the effects of prolonged exposure to microplastics and multi-stressor interactions.

Introduction

Plastic production and pollution have increased drastically since the 1950s to the point that plastic pollution is now a major global issue (Geyer, 2020). Currently, about 40 million metric tons of plastic enter the environment each year (Lau et al., 2020). Microplastics are particles (< 5 mm) that come from the fragmentation of larger plastics or are manufactured to be micron-sized (Browne, 2015). They are well documented in a variety of environments (Lusher, 2015 and sources therein) and are integrated into the global atmospheric and water systems (Brahney et al., 2020; Lusher, 2015). Microplastic fibers are one of the most abundant particle types of microplastic pollution found in the environment (Barrows et al., 2018; Desforges et al., 2014).

Microfibers are typically defined as particles with an aspect ratio $\geq 3:1$ (length : diameter) (Cole, 2016) and they are used widely in a variety of applications, such as textiles and fishing gear (Andrady, 2011; Rochman et al., 2019). Synthetic fibers constituted about 63% of the global fiber market in 2019, with polyester and polyamide (e.g. nylon) accounting for 52% and 5% of all fibers produced respectively (Textile Exchange, 2020). Items made from synthetic fibers shed particles during typical use, with many ending up in the environment through laundering of synthetic fabrics and subsequent release of fibers through waste water, using microfiber

contaminated biosolids as fertilizer, and from normal wear and improper disposal of fishing gear (Andrady, 2011; Browne et al., 2011; Crossman et al., 2020; Rochman et al., 2019).

Microfibers are one of the dominant microplastic morphologies found in many estuaries and coastal regions (Desforges et al., 2014; Waite et al., 2018; Zhao et al., 2014). For example, an estuary in Florida, USA, had average microplastic concentrations (\pm SD) ranging from 15.6 ± 8.4 particles L^{-1} to 33.9 ± 11.6 particles L^{-1} , with microfibers being the dominant particle type (Waite et al., 2018). Near Vancouver Island, Canada, microfibers accounted for ~75% of microplastic particles across all samples, and nearshore samples had higher proportions of microfibers compared to offshore samples (Desforges et al., 2014). In the Yangtze estuary, China, microfibers made up 79.1% of all particles collected (Zhao et al., 2014).

Microplastics have been found in oysters from locations around the world, with microfibers being a common particle type ingested (Rochman et al., 2015; Van Cauwenberghe & Janssen, 2014; Waite et al., 2018). *Crassostrea gigas* (*C. gigas*) adults, from the Atlantic Ocean off the coast of Brittany, France, contained 0.47 ± 0.16 particles g^{-1} wet weight (ww) (Van Cauwenberghe & Janssen, 2014). *C. gigas* adults from the coast of Oregon, USA had average microplastic burdens (\pm SE) ranging from 0.10 ± 0.02 particles g^{-1} ww to 0.85 ± 0.41 particles g^{-1} ww, with microfibers representing over 99% of microplastics extracted (Baechler et al., 2020). *Crassostrea virginica* (*C. virginica*) adults from an estuary in Florida, USA, ingested 16.5 microplastics ind^{-1} , of which 67% were fibers (Waite et al., 2018).

The number of studies that use non-spherical particles in laboratory exposure experiments is increasing, but still limited (Bucci et al., 2020). Microfibers have shown a variety of effects in zooplankton and filter feeding bivalves. Adult female copepods (*Calanus helgolandicus*) exposed to nylon microfibers (10 x 40 μm , 100 fibers mL^{-1}), had reduced overall clearance rates and shifted algal preferences away from cells most similarly shaped to microfibers (Coppock et al., 2019). Adult mussels (*Mytilus* spp.) ingested nylon microfibers and initially showed an oxidative stress response but returned to normal after 7 days (Cole et al., 2020). Polyethylene terephthalate (PET) microfibers caused DNA damage and increased acetylcholine hydrolysis activity in Mediterranean mussels (*Mytilus galloprovincialis*) at low concentrations (Choi et al., 2021). Additionally, high fiber concentrations affected necrosis, DNA damage, acetylcholine hydrolysis activity, and reactive oxygen species (ROS) and nitric oxide production (Choi et al., 2021). *Daphnia magna* (*D. magna*) exposed to PET microfibers had higher mortality when not pre-fed before a 48 hour exposure (Jemec et al., 2016). Only one study performed a laboratory exposure using microfibers with adult oysters: *C. virginica* ingested and egested nylon 6,6 microfibers of different lengths (75, 587, 1075 μm) (Ward, Zhao, et al., 2019). The maximum average number of fibers ingested (\pm SD) was 241.3 ± 193.6 for the 75- μm length (Ward, Zhao, et al., 2019).

Five studies have examined the effects of microplastics on the larval life stage of oysters and all used virgin microbeads. *C. virginica* larvae exposed to polystyrene (PS) microbeads (10, 100, 1000 mL^{-1}) for up to 6 days showed no effects on physiology (Chapter 3). *C. gigas* larvae exposed to PS microbeads had reduced algal

ingestion at high concentrations (1000 mL^{-1}) but low concentrations did not affect growth, fertilization yield, embryo-larval development, or metamorphosis (Cole & Galloway, 2015; Tallec et al., 2018). Finally, *C. gigas* exposed to high density polyethylene (HDPE) or proprietary polymer (Cospheric, California, USA) microbeads, had increased larval malformations and altered swimming speed and trajectories (Bringer, Cachot, et al., 2020; Bringer, Thomas, et al., 2020).

Only one study exposed oyster larvae to particles other than microbeads (Chapter 5): *C. virginica* larvae ingested two sizes (14×14 and $14 \times 28 \mu\text{m}$) of manufactured standard polyethylene terephthalate (PET) microfibers. To date, no studies have examined the effects of microfiber ingestion on oyster larvae. Therefore, this study exposed *C. virginica* larvae to microfibers of two polymer types most abundant in coastal environments; PET and nylon 6, 6. The question that motivated this research was: do microfiber exposure times, exposure concentrations, or polymer types affect larval physiological responses? Physiological effects of microfiber ingestion were examined by measuring larval growth, respiration, algal ingestion, and carbon assimilation. Larvae were exposed at their ingestion threshold concentration and higher but these concentrations represent concentrations that are higher than what is estimated to be in the environment for this size class.

Methods

To determine physiological effects of microfibers on *C. virginica*, larvae were exposed to virgin nylon 6, 6 or PET microfibers at the ingestion threshold concentration and one higher concentration for 6 days. Growth, respiration rates,

algal ingestion rates, and carbon assimilations rates were measured to determine physiological responses.

Microfiber preparation

Microfibers were manufactured following the paraffin microtomy method described in Chapter 5. Polyethylene terephthalate and nylon are common polymers used to make textiles and fishing gear, and they comprise a majority of the microfiber polymers found in the environment (Andrady, 2011; Browne et al., 2011; Textile Exchange, 2020). In short, spools of multifilament thread (nylon 6, 6, 10 μm diameter or PET, 14 μm diameter, Goodfellow) were wound precisely onto a small wooden spindle using a custom instrument. The spindle with the wound plastic thread was then placed diagonally into liquid paraffin and allowed to harden. The solid block of paraffin and fibers was excised from the spindle, creating a long block of paraffin embedded stacks of parallel fibers. The long block was cut into smaller sections to fit a standard microtome cassette. The small blocks were mounted on microtome cassettes and sections were cut to desired lengths (Table 4.1) using a standard microtome (Microm HM-330). While not all of the manufactured particle dimensions conform to the definition of a “fiber”, with an aspect ratio $\geq 3:1$ (length : diameter) (Cole, 2016), for simplicity, all exposure particles are referred to as fibers. Cut sections were collected in polypropylene tubes and paraffin wax was dissolved using xylene. Then the tubes were centrifuged for 5 minutes, the supernatant was aspirated with a glass pipet, and these steps were repeated three times to ensure full removal of paraffin. Xylene was solvent exchanged with 100% ethanol and the fibers were washed three times as described with 100% ethanol. Finally, 100% ethanol was

solvent exchanged with 70% ethanol and the fibers in 70% ethanol were stored at 4°C in the dark.

Once manufactured and processed, stock solutions of individual fiber lengths were vortexed for 30 seconds and then aliquots of each length were taken immediately and placed into 15 mL polypropylene tubes. Both sizes of each polymer were combined to create a 50/50 mix of fiber lengths (Table 4.1). Two fiber lengths were included in each treatment to accommodate larval growth and particle size preference (Baldwin, 1995). Polymer types were kept separate. Fibers were centrifuged and ethanol was solvent exchanged with acetone because Nile red-stained fibers fluoresce more brightly in acetone. Fibers were stained for 24-48 hours using 800 μL of Nile red (500 $\mu\text{g mL}^{-1}$ acetone) in 3.25 mL of acetone. The day before the start of each experiment, fibers were washed with acetone to remove excess Nile red by centrifugation and aspiration of the supernatant. About 12 mL of acetone were added back to the tube and the tube was shaken vigorously for 1 min. This process was repeated three times. Finally, acetone was solvent exchanged with artificial seawater (ASW, 1 μm filtered, 15 psu, Table S4.1) and fibers were washed three times as described, with 0.1% (v/v) Tween 20 added in the first wash to keep the fibers in solution.

Experimental design

C. virginica larvae were obtained from the Ward Oyster Co. (Gloucester, VA, 8 days post fertilization, dpf) and the Horn Point Oyster Hatchery (Cambridge, MD, 17 dpf) for the PET and nylon experiments respectively. Larvae were washed through a series of stacked sieves (100 and 200 μm). Larvae from the 100 μm sieve

were collected and placed in 1 L glass bottles, with 800 mL of ASW, at a concentration of 10 mL⁻¹.

Previous observations (Chapter 5) determined that a range of sizes of laboratory manufactured standardized nylon (10 x 10 µm, 10 x 30 µm) and PET (14 x 14 µm, 14 x 28 µm) microfibers were ingested by *C. virginica* larvae. Preliminary experiments determined the ingestion threshold concentration of these manufactured microfibers (Chapter 5). Larvae (> 100 µm) were exposed to concentrations of 10-100 fibers mL⁻¹ with optimum food concentrations (Table 4.1) for 3 days (Helm & Bourne, 2004). Subsamples of larvae were taken after 1 and 3 days and visualized under fluorescent light using an Olympus IX73 inverted fluorescent microscope and cellSens Dimension software (v. 1.18). A very small number of Nile red stained microfibers were observed in a handful larval guts at 100 fibers mL⁻¹. Consequently, 100 and 1000 fibers mL⁻¹ exposure concentrations were chosen. Concentrations of environmental microplastics in this size range are not well understood but data suggest that concentrations increase as particle size decreases (Lenz et al., 2016).

Larvae were fed an optimum phytoplankton diet for individuals > 120 µm (Table 4.1) (Helm & Bourne, 2004). *Chaetoceros muelleri* (CHGRA) and *Tetraselmis chuii* (PLY429) provide quality nutrition, with cells similar in size to the microfibers, reducing confounding factors from selective particle feeding (Arora et al., 2013; Baldwin, 1995; Burge & Edlund, 2017; Helm & Bourne, 2004). Larvae were fed CHGRA (60%) and PLY492 (40%) twice a day for a total of 120,000 cells mL⁻¹ (Table 4.1). Phytoplankton were grown in covered flasks with 1µm filtered water and 0.22 µm filtered F/2 medium to minimize particle contamination.

Table 4.1 Design parameters used for *Crassostrea virginica* (*C. virginica*) larval exposures to nylon 6, 6 and polyethylene terephthalate (PET) microfibers and fed with *Chaetoceros muelleri* (CHGRA) and *Tetraselmis chuii* (PLY429).

Component	Description	Concentrations	Units
<i>C. virginica</i>	100 μm < X > 200 μm	10	Larvae mL^{-1}
CHGRA	cells in exponential growth	72	10^3 cells mL^{-1}
PLY429	cells in exponential growth	48	10^3 cells mL^{-1}
Nylon 6,6	50/50 mix of 10x10 μm , 10x30 μm	0, 100, 1000	fibers mL^{-1}
PET	50/50 mix of 14x14 μm , 14x28 μm	0, 100, 1000	fibers mL^{-1}

Treatments were conducted in triplicate (9 bottles total for each polymer exposure) and once all components were placed in the bottles, lids with small glass tubes for aeration were placed on top and tightened (Figure 4.1). Larvae were gently aerated to keep all particles suspended. Larvae were exposed for 6 days, with a water change and subsampling on the third day of exposure. Lids were only removed for short periods of time during feeding and subsampling to minimize particle contamination.



Figure 4.1 *Crassostrea virginica* (*C. virginica*) larval exposure to nylon 6, 6 (10 x 10 μm , 10 x 30 μm) or polyethylene terephthalate (PET, 14 x 14 μm , 14 x 28 μm) microfibers at 100 and 1000 fiber mL^{-1} . Larvae and all particles were kept in suspension by aeration with glass tubes.

Subsampling and larval growth measurements

After 3 days of exposure, each treatment triplicate was concentrated by sieving the entire sample with a 40 μm sieve and washing the larvae into a 100 mL beaker. Larval concentrations were obtained by subsampling 250 μL , in triplicate, from each of the 9 concentrated treatments and counting the number of larvae on a Sedgewick-Rafter slide using an Olympus IX73 inverted fluorescent microscope and cellSens Dimension software (v. 1.18). Images were taken during the concentration analysis to obtain growth measurements and cellSens Dimension software was used to measure at least 50 individuals from each treatment triplicate. Mean larval concentrations were used to subsample 200 larvae from each treatment triplicate for respiration analysis and algal ingestion and carbon assimilation analysis.

Once subsamples were collected for further analysis, the remaining larvae were washed into clean 1 L glass bottles. Total volume was adjusted to 10 larvae mL⁻¹. Phytoplankton and microfibers were restocked according to Table 4.1 and the exposure continued for an additional 3 days. After 6 days of exposure, larvae were concentrated and subsampled as described above.

Respiration measurements

Respiration was measured via oxygen consumption using a Presens SDR multiwell instrument (Presens, Denmark) (Chapter 3). The larval subsamples (200 larvae) were rinsed with 1 µm filter ASW and placed in 2 mL vials with an oxygen sensor “spot”, with vials placed randomly on the plate. Vials were filled to the top using ASW, making sure all visible air bubbles were removed. ASW controls were run simultaneously to determine background oxygen consumption and all samples were run under dark conditions. Measurements were taken at 3-minute intervals over 5 hours using the Presens SDR software (version 4.0.0). Respiration rates were reported as the slope of the linear regression of oxygen consumption over time and corrected for background respiration.

Algal ingestion and carbon assimilation measurements

Algal ingestion and carbon assimilation were measured using a ¹⁴C radio-labelled phytoplankton method ((method adapted from Baldwin and Newell 1991; Gallagher et al., 1994; Pace et al., 2006), by Dr. Katie McFarland, see Figure S4.1 for detailed steps). Small volumes of *Isochrysis galbana* (*I. galbana*) stock solutions were spiked with 0.012 mCi of ¹⁴C from a concentrated stock solution. For

experiments, *I. galbana* was grown in the ^{14}C spiked solution for 5 days before the start of the experiment so all cells would be ^{14}C labelled. The day before sampling, ^{14}C spiked algal cells were filtered using a $0.2\ \mu\text{m}$ Nuclepore filter (Whatman 25 mm diam.) to remove any unincorporated ^{14}C . Algal cells were resuspended in ASW and transferred to a 15 mL tube. On the day of sampling, 200 larvae in 10 mL of ASW were placed into 20 mL scintillation vials with $30 \times 10^3\ \text{cells mL}^{-1}$ ^{14}C labelled *I. galbana*. Larvae were allowed to feed on the ^{14}C labelled algae for two hours. After two hours, larvae were separated from the ^{14}C labelled algae using a filtration manifold (Figure 4.2). Larvae were collected on $40\ \mu\text{m}$ sieves (Corning cell strainer) placed on top of the steel filter cylinders. The ^{14}C spiked *I. galbana* were caught on $0.7\ \mu\text{m}$ glass microfiber filters (Whatman 25 mm diam.) at the bottom of the filter cylinders.

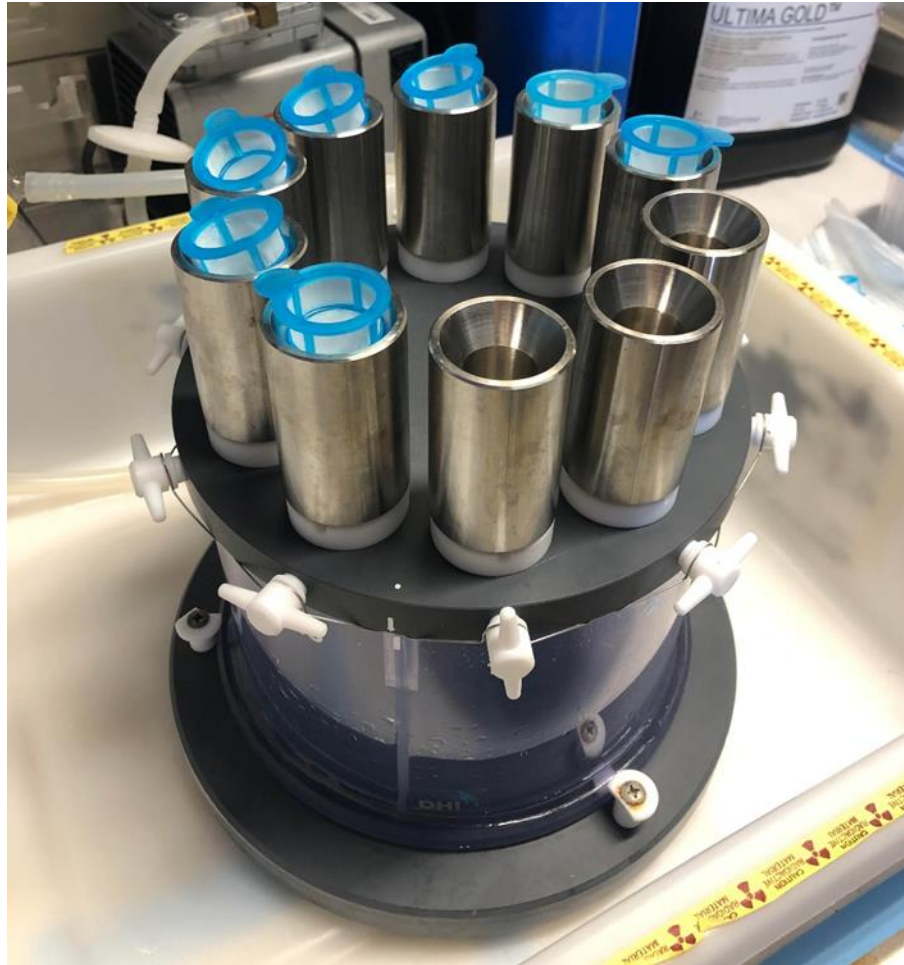


Figure 4.2 Filter manifold used to separate and collect *Crassostrea virginica* (*C. virginica*) larvae and *Isochrysis galbana* (*I. galbana*) for analysis in the liquid scintillation analyzer. Samples are poured through the blue 40 μm sieves on top of the steel cylinders. Glass fiber filters (Whatman 0.7 μm pore size) catch ^{14}C labelled algal cells at the bottom of the steel cylinders.

Larvae were immediately washed into clean 20 mL scintillation vials.

Unlabeled *I. galbana* (30×10^3 cells mL^{-1}) were added to the vials and larvae were allowed to feed for two hours. Filters with ^{14}C labelled *I. galbana* were transferred into 7mL scintillation vials for counting. After the second feeding, larval samples

were rinsed onto 0.7 µm glass microfiber filters (Whatman 25 mm diam.) using the filter manifold. Filters were placed in 7 mL scintillation vials for counting.

After collection on filters and placement in 7 mL scintillation vials, 0.5 N HCl was added to each sample to volatilize unassimilated ¹⁴C. Samples were left uncapped overnight. The next day, a tissue solubilizer (PerkinElmer Solvable™) was added to all scintillation vials to solubilize cells and vials were incubated for two hours. Finally, a liquid scintillation cocktail (Ultima Gold™) was added to each vial before placing the samples in a liquid scintillation analyzer (Packard Tri-carb 3100TR) using standard ¹⁴C settings.

Clearance rates were calculated following Coughlan (1969) and Pace et al. (2006):

$$Clearance\ rate = \frac{\ln(C_{initial}/C_{final})}{N \times T} \times V$$

where clearance rate is in mL min⁻¹ larva⁻¹, C_{initial} is DPM of the algal only control, C_{final} is the DPM of remaining *I. galbana* after 120 minutes of larval feeding, N is the number of larvae per vial, T is time (120 min), and V is the volume of solution (10 mL). Rates were converted to hourly rates. Clearance rate is transformed into ingestion rate using the equation:

$$Ingestion\ rate = Clearance\ rate \times \left(\frac{\# \text{ algal cells}}{mL} \right)$$

Therefore, ingestion rate units are number of cells hour⁻¹ larva⁻¹. Carbon assimilation rate was calculated using the following equation:

$$Carbon\ assimilation\ rate = \left(\frac{DPM_{larval}}{N} \right) \left(\frac{1}{\frac{DPM_{algal\ control}}{P} \times T} \right)$$

where carbon assimilation rate units are the number of cells $\text{hour}^{-1} \text{larva}^{-1}$, N is the number of larvae, P is the number of algal cells fed to the larvae, and T is larval feeding time.

Statistical analysis

Data were tested for normality using the Shapiro-Wilk test and by visualizing histogram and density plots. Data were tested for homogeneity of variance using Levene's test. When assumptions were met, two-way ANOVAs and Tukey's post hoc tests were conducted to determine differences in physiological measurements with microfiber concentrations and exposure time as the independent variables. Growth data from both experiments did not satisfy the assumptions necessary for ANOVAs, however, the central limit theorem states that data means are approximately normal for large sample sizes (> 40) and parametric tests can be used (Elliott & Woodward, 2007). Sample sizes for each treatment were 125 in the nylon experiment and 217 in the PET experiment so two-way ANOVAs followed by Tukey's post hoc tests were utilized for their statistical power. All statistical analyses were performed in R Studio version 1.4.1103 and significance reported at $p < 0.05$.

Results

Very few larvae exposed to either polymer type at $100 \text{ fiber mL}^{-1}$ treatments had microfibers in their guts when examined for larval concentration and growth analysis after 3 and 6 days. At $1000 \text{ fiber mL}^{-1}$ treatments, more larvae had ingested microfibers but the majority did not have fibers in their guts when examined after both time points. Larvae ingested both sizes of each polymer type and the highest

number of fibers observed in one individual was 4 fibers from a 1000 fiber mL⁻¹ treatment. Figure 4.3 is one example of a live individual that had three 14 x 28 µm PET microfibers in its gut. All data means (± SE) are reported in Table S4.2.

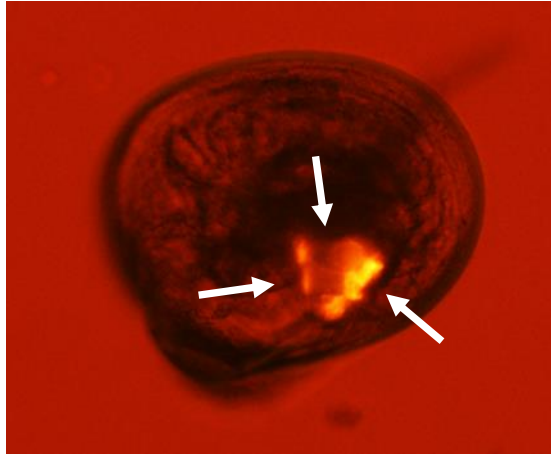


Figure 4.3 *Crassostrea virginica* (*C. virginica*) larva with three Nile red stained, 14 x 28 µm polyethylene terephthalate (PET) microfibers in its gut after six days of exposure to 1000 fiber mL⁻¹. Larva was visualized and imaged using an Olympus IX73 inverted fluorescent microscope (Ex/Em 480/600nm) and cellSens Dimension software (v. 1.18).

PET fiber exposure

Growth. There was significant growth in all treatments from day 0 to day 3 ($p < 0.05$) (Figure 4.4). After 3 days of exposure, the 100-fiber mL⁻¹ treatment had significantly larger mean growth than the control treatment but after 6 days, mean larval size between these two treatments were not significantly different. The high fiber treatment (1000 fiber mL⁻¹) did not grow significantly from day 3 to 6 and these larvae were significantly smaller than the other two treatments on day 6.

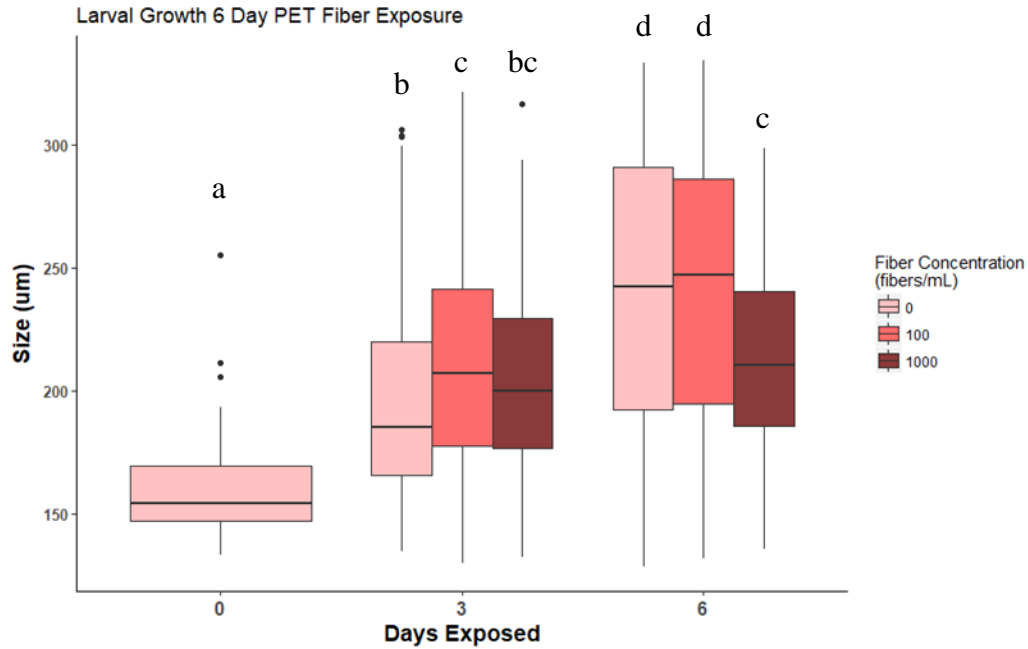


Figure 4.4 *Crassostrea virginica* (*C. virginica*) larval growth after a 6-day exposure to 100 and 1000 polyethylene terephthalate (PET) microfibers mL⁻¹ (14 x 14 µm, 14 x 28 µm). Box whisker plot shows median larval sizes and variation with inter-quartile range, min-max values, and outliers. Statistical differences in the mean larval sizes (two-way ANOVA and Tukey's post hoc tests, $p < 0.05$) are indicated by letters.

Respiration. After 3 days, *C. virginica* larvae unexposed to microfibers showed no significant increase in mean respiration rate from day 0 but larvae exposed to both microfiber treatment concentrations showed significantly increased respiration rates from the day 0 control treatment ($p < 0.05$) (Figure 4.5). Mean respiration rates for microfiber exposed larvae were not different from each other on day 3. From day 3 to day 6, respiration rate for the control treatment increased significantly but microfiber exposed larvae showed smaller increases.

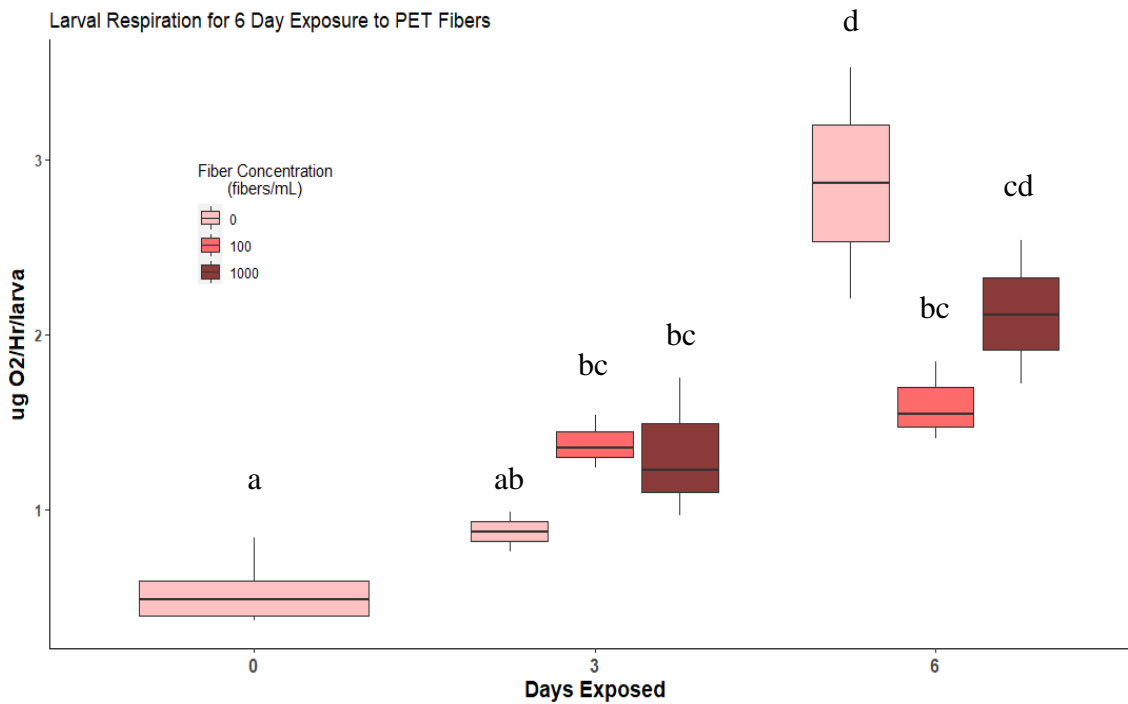


Figure 4.5 *Crassostrea virginica* (*C. virginica*) larval respiration rates after a 6-day exposure to 100 and 1000 polyethylene terephthalate (PET) microfibers mL⁻¹ (14 x 14 μ m, 14 x 28 μ m). Box whisker plot shows median respiration rates and variation with inter-quartile range, and min-max values. Statistical differences in the mean rates (two-way ANOVA and Tukey's post hoc tests, $p < 0.05$) are indicated by letters.

Algal ingestion and carbon assimilation. Issues with the number of algal cells removed on day 3 made the data unreliable so algal ingestion data for this day were not reported. The amount of ¹⁴C was directly measured for assimilation so data for both days were included for this measurement. Ingestion rate means showed a dose-dependent decrease as microfiber concentration increased, however, the differences in means were not significant ($p < 0.05$) (Figure 4.6). There were no significant differences in carbon assimilation after 3 or 6 days of PET microfiber exposure for either treatment ($p < 0.05$) (Figure 4.7).

Algal Ingestion Rate for PET Exposure

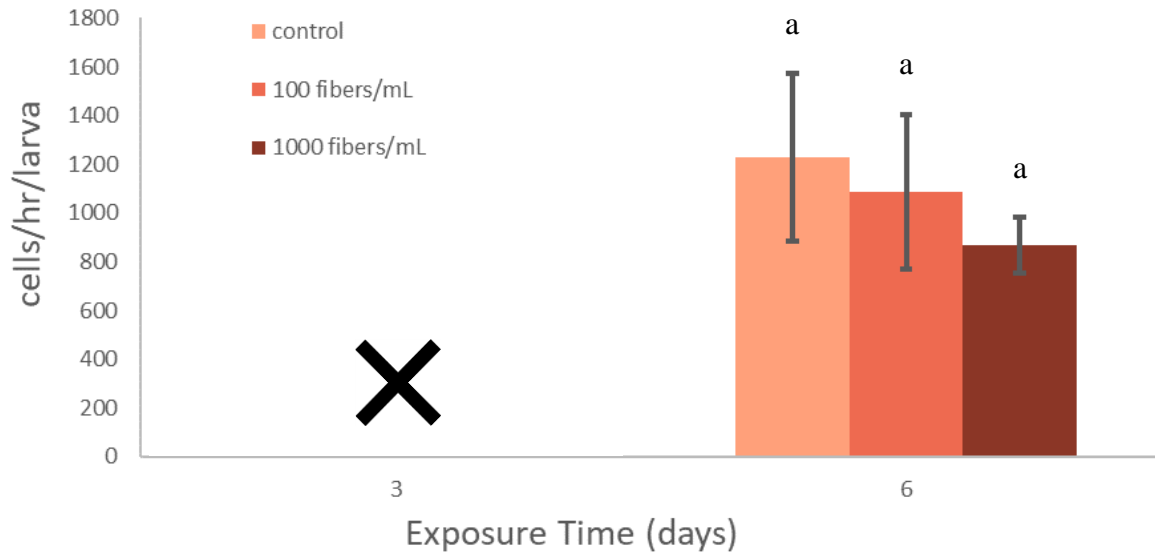


Figure 4.6 *Crassostrea virginica* (*C. virginica*) larval algal ingestion rates after a 6-day exposure to 100 and 1000 polyethylene terephthalate (PET) microfibers mL^{-1} (14 x 14 μm , 14 x 28 μm). Bars are mean algal ingestion rates with standard error. Day 3 data were not suited for analysis. Statistical differences in the mean rates (two-way ANOVA and Tukey's post hoc tests, $p < 0.05$) are indicated by letters.

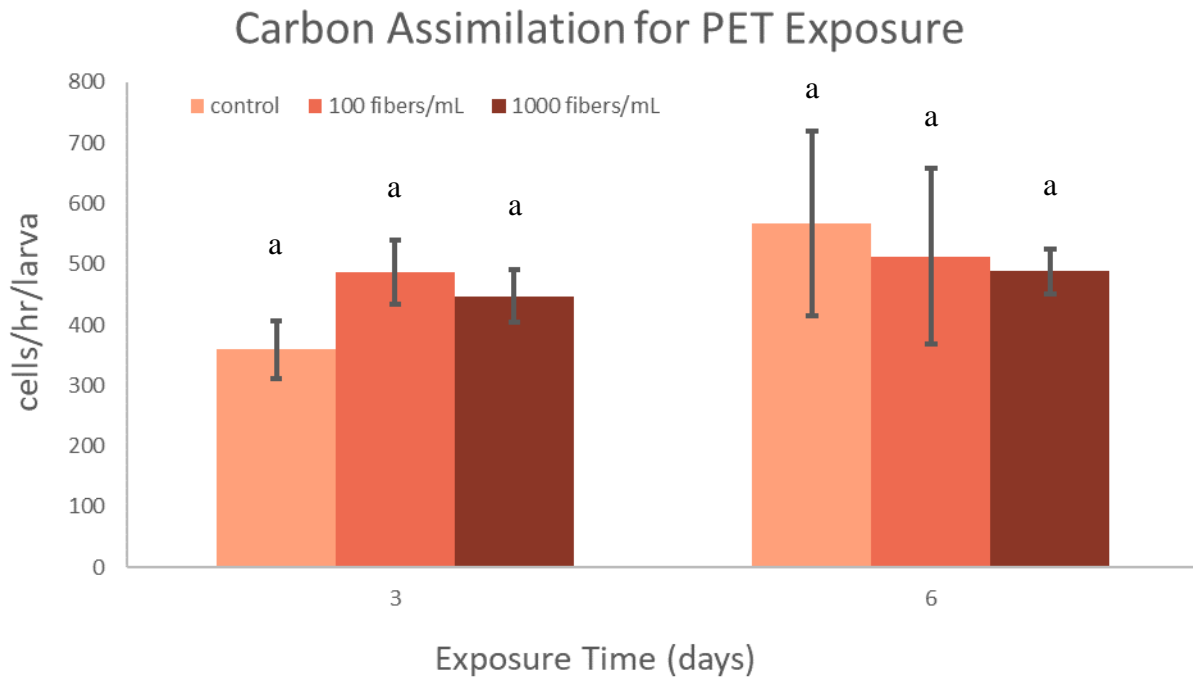


Figure 4.7 *Crassostrea virginica* (*C. virginica*) larval carbon assimilation rates after a 6-day exposure to 100 and 1000 polyethylene terephthalate (PET) microfibers mL⁻¹ (14 x 14 μm, 14 x 28 μm). Bars show mean assimilation rates with standard error. Statistical differences in the mean rates (two-way ANOVA and Tukey’s post hoc tests, p < 0.05) are indicated by letters.

Nylon fiber exposure

Significant mortality and setting were seen after 6 days of nylon 6,6 fiber exposure so all data for this day were excluded.

Growth. There were no significant differences in mean larval size after 3 days of exposure for all treatments (p < 0.05) (Figure 4.8). There was also no growth in the control treatment after 3 days and the mean larval size was significantly smaller than at the beginning of the experiment.

Respiration. There were no significant differences in mean respiration rates after 3 days for any treatment (p < 0.05) (Figure 4.9).

Algal ingestion and carbon assimilation. Larvae showed a dose-dependent response in mean algal ingestion and mean carbon assimilation rates, with the highest treatment having the lowest rates. However, the rates were not significantly lower for either treatment or measurement ($p < 0.05$) (Figure 4.10, 4.11).

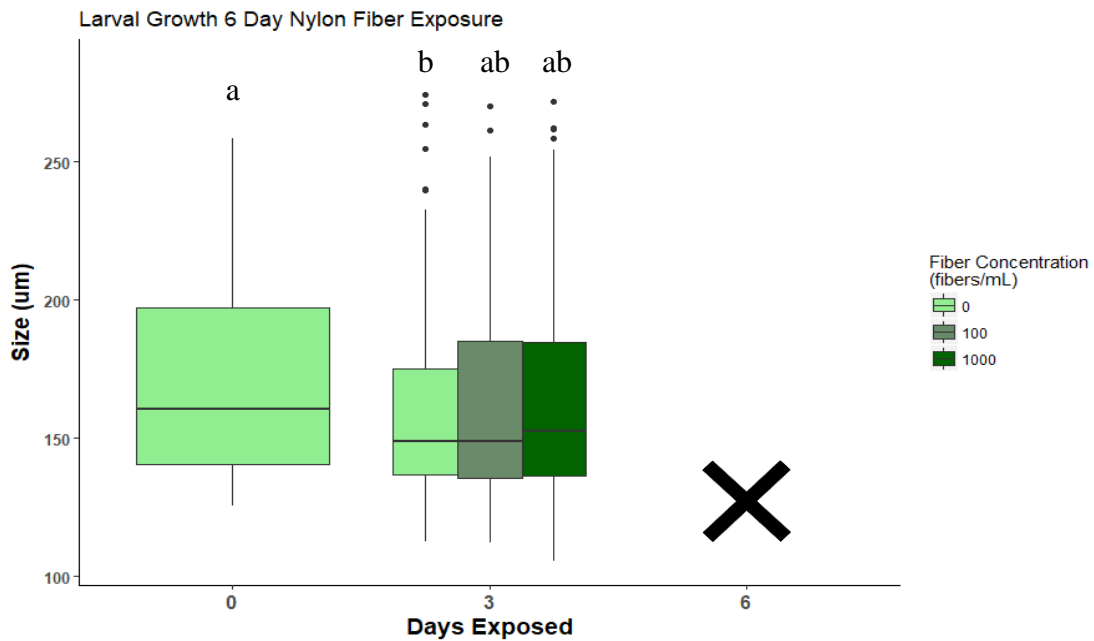


Figure 4.8 *Crassostrea virginica* (*C. virginica*) larval growth after a 6-day exposure to 100 and 1000 nylon 6, 6 microfibers mL^{-1} ($10 \times 10 \mu\text{m}$, $10 \times 30 \mu\text{m}$). Box whisker plot shows median larval sizes and variation with inter-quartile range, min-max values, and outliers. Statistical differences in the mean larval sizes (two-way ANOVA and Tukey's post hoc tests, $p < 0.05$) are indicated by letters. Significant mortality and setting were seen after 6 days of exposure so day 6 data were excluded.

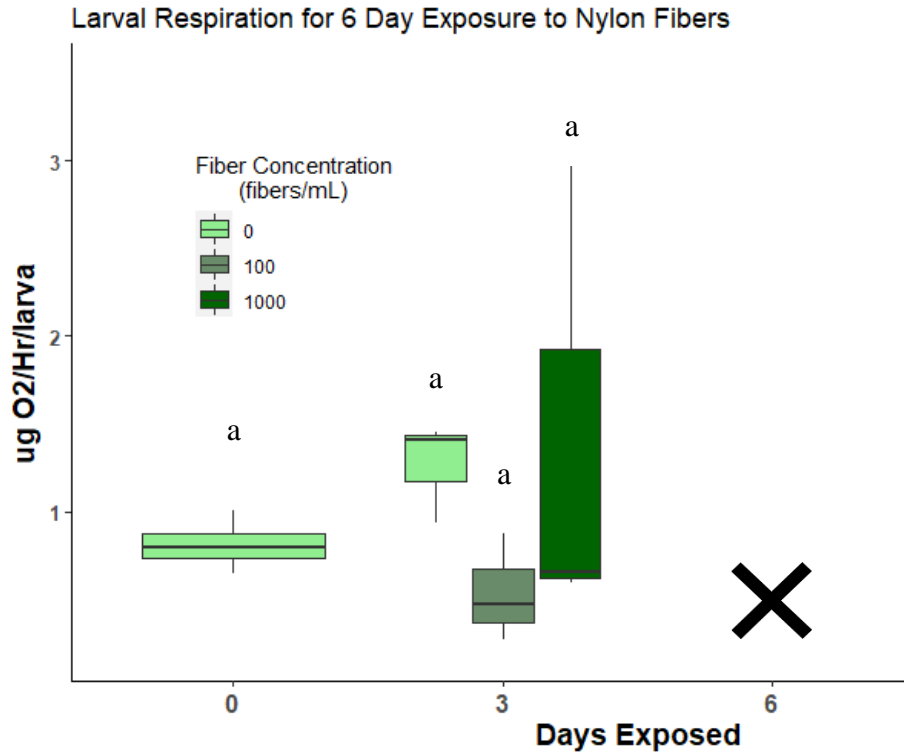


Figure 4.9 *Crassostrea virginica* (*C. virginica*) larval respiration rates after a 6-day exposure to 100 and 1000 nylon 6,6 microfibers mL⁻¹ (10 x 10 μm, 10 x 30 μm). Box whisker plot shows median respiration rates and variation with inter-quartile range, and min-max values. Statistical differences in the mean rates (two-way ANOVA and Tukey's post hoc tests, $p < 0.05$) are indicated by letters. Significant mortality and setting were seen after 6 days of exposure so day 6 data were excluded.

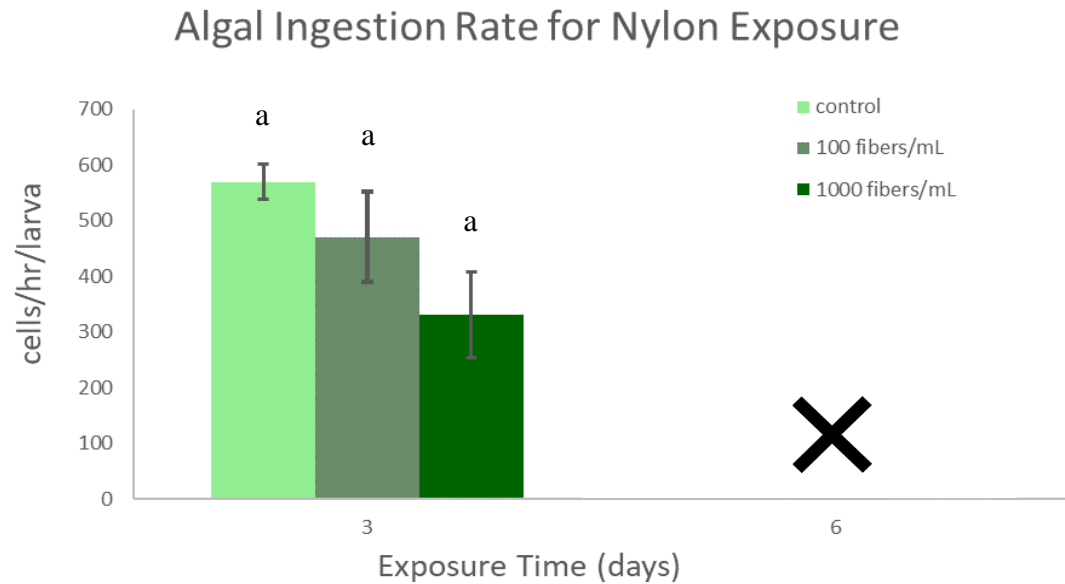


Figure 4.10 *Crassostrea virginica* (*C. virginica*) larval algal ingestion rates after a 6-day exposure to 100 and 1000 nylon 6, 6 microfibers mL^{-1} ($10 \times 10 \mu\text{m}$, $10 \times 30 \mu\text{m}$). Bars are mean respiration rates with standard error. Statistical differences in the mean rates (two-way ANOVA and Tukey's post hoc tests, $p < 0.05$) are indicated by letters. Significant mortality and setting were seen after 6 days of exposure so day 6 data were excluded.

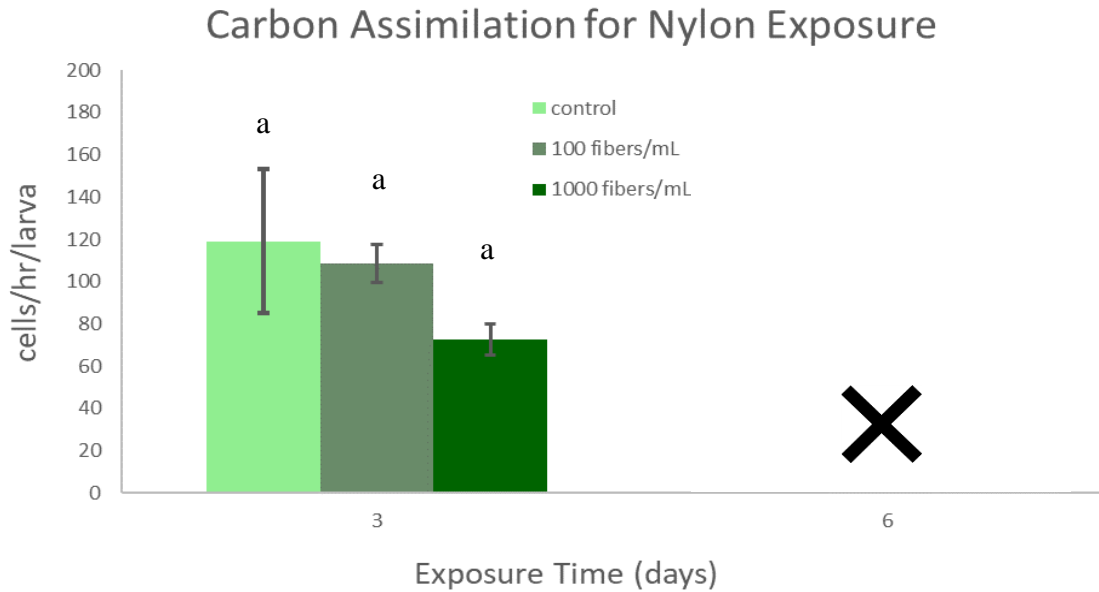


Figure 4.11 *Crassostrea virginica* (*C. virginica*) larval carbon assimilation rates after a 6-day exposure to 100 and 1000 nylon 6, 6 microfibers mL^{-1} ($10 \times 10 \mu\text{m}$, $10 \times 30 \mu\text{m}$). Bars shows mean assimilation rates with standard error. Statistical differences in the mean rates (two-way ANOVA and Tukey's post hoc tests, $p < 0.05$) are indicated by letters. Significant mortality and setting were seen after 6 days of exposure so day 6 data were excluded.

Discussion

This was the first study to examine the effects of microfiber ingestion by larval oysters. At concentrations 10 times the ingestion concentration threshold, only a handful of all larvae observed had ingested microfibers after 6 days of exposure. Results showed that PET and nylon 6,6 microfiber ingestion by *C. virginica* larvae had minor physiological effects at low and high microfiber concentrations (Figures 4.4 - 4.11). Exposure time and microfiber concentration both affected larval physiological responses. Larvae exposed to PET microfibers, had reduced respiration rates in both treatments but only the 100-microfiber mL^{-1} treatment was significantly lower and the high fiber treatment suffered a significant growth penalty after 6 days.

However, algal ingestion and carbon assimilation rates were unaffected. In the nylon exposure experiments, data were limited to only 3 days of exposure because of significant mortality and setting in all treatments after 6 days. There were dose-dependent reductions of algal ingestion and carbon assimilation rates after 3 days but they were not significant. There were no differences in larval growth or respiration rates.

Observations strongly support the hypothesis that the larval brood used for the nylon exposure were stressed before the start of the experiment. Larvae from both experiments started around the same size (Table S4.2) but larvae in the PET exposure grew while the larvae in the nylon exposure did not. Control larvae from the nylon exposure did not grow after 3 days, which is inconsistent with the literature. Under normal conditions, *C. virginica* larvae typically grow tens of microns a day (Helm & Bourne, 2004; Kennedy, 1996; McFarland et al., 2020). Larvae in the nylon experiment ingested fewer algal cells and assimilated less carbon across all treatments compared to the PET exposure. Finally, control larval respiration rates did not increase after 3 days.

The initial conditions for the nylon exposure created a multi-stressor exposure. Larvae used in the nylon experiments were likely stressed from unknown sources at the beginning of the exposure and then exposed to nylon microfibers. Even under these conditions, no significant differences in larval physiology were observed after 3 days of exposure to standard nylon microfibers.

Because of the differences of initial brood condition, comparisons of physiological responses between polymer types should be done cautiously.

Respiration rates across all treatments were in the same range (0.52 ± 0.05 to $2.87 \pm 0.66 \mu\text{g O}_2 \text{ Hr}^{-1} \text{ larva}^{-1}$, Table S4.2). They were also similar to values found in the literature (0.65 to $1.64 \mu\text{g O}_2 \text{ Hr}^{-1} \text{ larva}^{-1}$) (Chapter 3; McFarland et al. 2020) Larger differences in physiological responses in the PET exposure were seen after 6 days so, it is possible that any significant effects from the ingestion of nylon fibers were not captured by the shortened exposure time.

Physiological responses to low microplastic concentrations (~ 100 particles mL^{-1}) were similar to other oyster larval exposures in the literature. *C. virginica* larvae exposed to 2 and 6 μm PS microbeads showed no differences in growth, respiration rates, and algal ingestion and carbon assimilation rates (Chapter 3). *C. gigas* larval growth and feeding was not affected by an 8-day exposure to 1 and 10 μm PS microbeads (Cole & Galloway, 2015). However, larvae showed different responses to particle type, when exposed to the same high concentration (1000 particles mL^{-1}) for the same amount of time (Chapter 3). *C. virginica* larvae exposed to PS microbeads for 6 days showed no differences in mean larval length, respiration rates, or algal ingestion or carbon assimilation rates (Chapter 3). While larvae in these experiments had reduced respiration in the low PET fiber treatment and had a significant growth penalty in the high PET fiber treatment after 6 days. Finally, a 24-hour exposure to 1000 PS microbeads mL^{-1} showed significantly reduced algal ingestion in *C. gigas* larvae (Cole & Galloway, 2015). While there were reductions in algal ingestion in both fiber exposures, none were significant.

Prior studies have not examined microfiber exposure effects on any life stage of oysters but a few have used zooplankton and other bivalve species. Adult mussels

exposed to nylon microfibers ($\sim 186 \text{ mL}^{-1}$, $10 \times 30 \text{ }\mu\text{m}$, nylon 6,6), ingested 22.0 ± 6.4 particles mg^{-1} of digestive tissue after 7 days (Cole et al., 2020). Individuals initially showed a significant oxidative stress response but, after 7 days, that activity returned to normal. Also measurements of immune response and genotoxicity showed no significant changes (Cole et al., 2020). Nylon microfibers, at the same low concentration as my experiment ($100 \text{ fibers mL}^{-1}$), reduced clearance rates and shifted algal cell ingestion preferences in adult copepods (Coppock et al., 2019). Finally, exposures to PET microfibers (0.22 or $4,483 \text{ } 50\text{-}\mu\text{m fibers mL}^{-1}$, 0.11 or $2,233 \text{ } 100\text{-}\mu\text{m fibers mL}^{-1}$) caused DNA damage, necrosis, increased acetylcholine hydrolysis activity, and ROS and nitric oxide production in adult Mediterranean mussels (Choi et al., 2021). These responses could explain the growth penalty seen in my high fiber PET treatment, coupled with no significant decrease in algal ingestion or carbon assimilation. Individuals could be reallocating energy from growth to cell maintenance and immune responses (Choi et al., 2021).

Microfibers show minimal impacts on larval oyster physiology at concentrations higher than expected in the environment. Current maximum environmental concentrations for small microplastics are estimated to be 0.1 to 40 particles mL^{-1} (Bergmann et al., 2017; Brandon et al., 2020). There are no reliable methods to accurately collect, identify, and quantify microplastics $< 100 \text{ }\mu\text{m}$ and few studies filter and collect particles $< 63 \text{ }\mu\text{m}$. However, decreasing mesh net or filter size increased the number of microplastics collected, especially microfibers (Covernton et al., 2019; Lindeque et al., 2020).

Conclusion

Limited effects from microfiber ingestion are seen at the ingestion threshold concentration for *C. virginica* larvae and the multi-stressor interaction observed in the nylon exposure did not produce significant larval physiological responses. The concentrations used in these experiments are higher than environmental concentrations estimated for this size class. With current estimates of environmental concentrations, microfibers are unlikely to be a risk to oyster larvae. However, environmental sampling methods for microplastics < 100 µm are unreliable and particles concentrations in the ingestible size range of oyster larvae are unknown. With plastic pollution predicted to increase in the near future and improvements in environmental sampling of small microplastics, concentrations of small microplastics in the environment might reach oyster larval ingestion thresholds. Therefore, laboratory exposures examining sublethal effects of microplastics are important to continue. Further studies should examine longer exposure times and multi-stressor interactions.

Supporting Information

Table S4.1 Modified Artificial Seawater

To dH₂O add the following per 200 L for 15 ± PSU:

Salts	Amount
400 mM NaCl	2.3375 kg
20 mM MgSO ₄ •7H ₂ O	492.5 g
10 mM CaCl ₂	111 g
1.7 mM KBr	20.25 g
10 mM KCl	74.5 g
20 mM MgCl ₂ •6H ₂ O	406.3 g
0.404 mM H ₃ BO ₃	2.5 g

Table S4.2 Data means (\pm SE) for physiological measurements of *Crassostrea virginica* (*C. virginica*) larvae after exposure to polyethylene terephthalate (PET) or nylon 6,6 microfibers.

Experiment	Day	Measurement type	Treatment (beads mL ⁻¹)	Mean \pm SE
PET exposure	0	Growth (μm)	Control	159.97 \pm 3.21
		Respiration ($\mu\text{g O}_2 \text{ Hr}^{-1} \text{ larva}^{-1}$)	Control	0.52 \pm 0.05
	3	Growth (μm)	Control	193.46 \pm 5.06
			100	208.67 \pm 2.26
			1000	203.63 \pm 2.35
		Respiration ($\mu\text{g O}_2 \text{ Hr}^{-1} \text{ larva}^{-1}$)	Control	0.87 \pm 0.11
			100	1.38 \pm 0.09
			1000	1.31 \pm 0.23
		Algal clearance ($\mu\text{L Hr}^{-1} \text{ larva}^{-1}$)	Control	
			100	X
			1000	
		Algal ingestion (cells Hr ⁻¹ larva ⁻¹)	Control	
			100	X
			1000	
	Carbon assimilation (cells Hr ⁻¹ larva ⁻¹)	Control	358.78 \pm 46.70	
		100	486.49 \pm 51.99	
		1000	446.97 \pm 42.97	
	6	Growth (μm)	Control	226.10 \pm 19.48
			100	240.35 \pm 1.69
			1000	214.03 \pm 6.84
		Respiration ($\mu\text{g O}_2 \text{ Hr}^{-1} \text{ larva}^{-1}$)	Control	2.87 \pm 0.66
			100	1.60 \pm 0.13
			1000	2.12 \pm 0.24
		Algal clearance ($\mu\text{L Hr}^{-1} \text{ larva}^{-1}$)	Control	40.97 \pm 11.54
100			36.21 \pm 10.61	
1000			28.92 \pm 3.86	
Algal ingestion (cells Hr ⁻¹ larva ⁻¹)		Control	1229.07 \pm 346.27	
		100	1086.30 \pm 318.43	
		1000	867.56 \pm 115.88	
Carbon assimilation (cells Hr ⁻¹ larva ⁻¹)	Control	567.46 \pm 152.72		
	100	512.62 \pm 144.84		
	1000	487.96 \pm 37.18		

Nylon exposure	0	Growth (μm)	Control	170.73 ± 3.19
		Respiration ($\mu\text{g O}_2 \text{ Hr}^{-1} \text{ larva}^{-1}$)	Control	0.81 ± 0.04
	3	Growth (μm)	Control	158.55 ± 0.45
			100	161.52 ± 5.32
			1000	164.51 ± 0.75
		Respiration ($\mu\text{g O}_2 \text{ Hr}^{-1} \text{ larva}^{-1}$)	Control	1.27 ± 0.17
			100	0.54 ± 0.18
			1000	1.48 ± 0.86
		Algal clearance ($\mu\text{L Hr}^{-1} \text{ larva}^{-1}$)	Control	18.98 ± 1.06
			100	15.68 ± 2.71
			1000	11.03 ± 2.57
		Algal ingestion ($\text{cells Hr}^{-1} \text{ larva}^{-1}$)	Control	569.42 ± 31.86
			100	470.50 ± 81.30
			1000	330.86 ± 77.21
		Carbon assimilation ($\text{cells Hr}^{-1} \text{ larva}^{-1}$)	Control	119.10 ± 34.23
100	108.61 ± 9.17			
1000	72.72 ± 7.32			

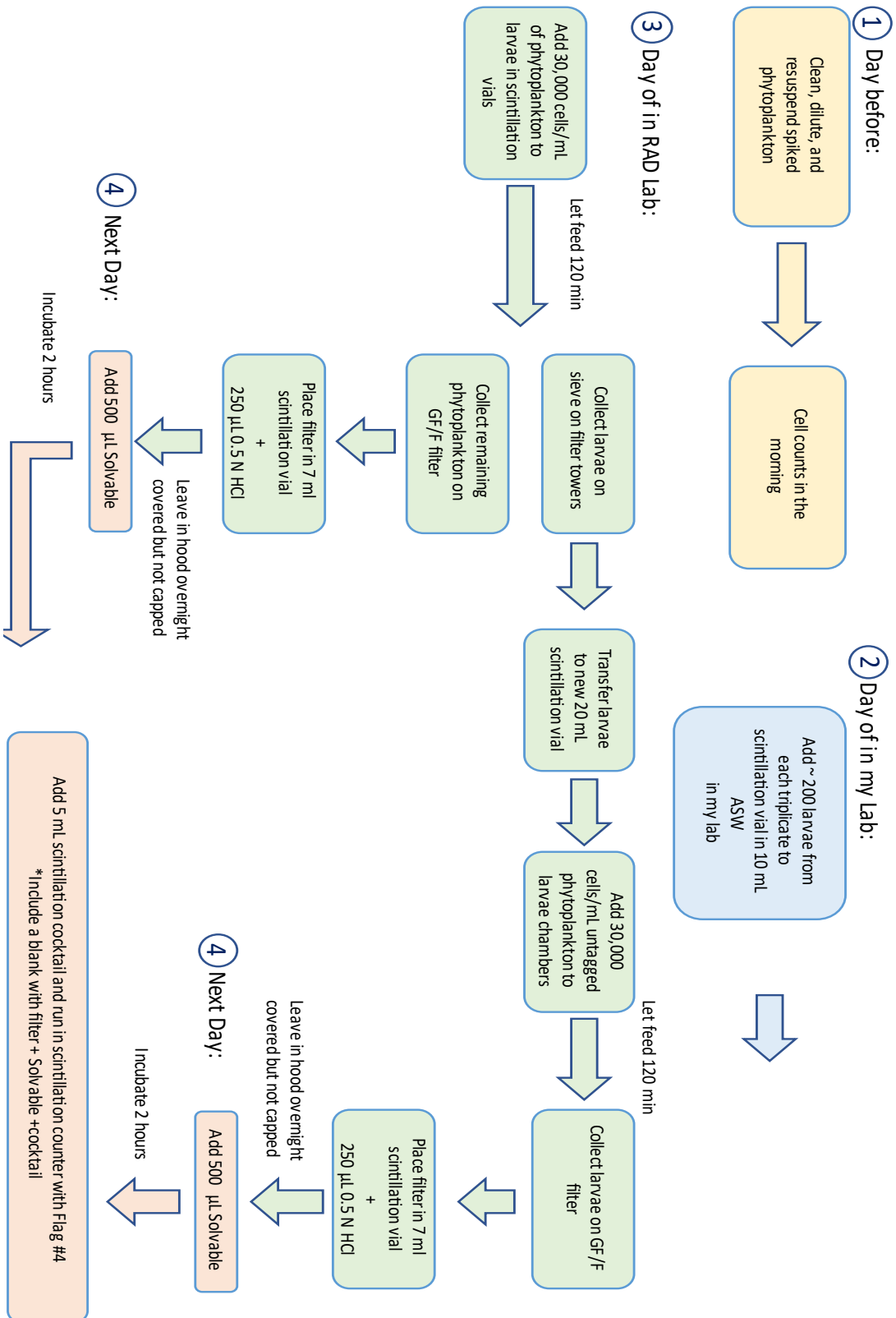


Figure S4.1 Conceptual diagram for ¹⁴C radio-labelled phytoplankton method steps.

Chapter 5: A Paraffin Microtomy Method for Improved and Efficient Production of Standardized Plastic Microfibers¹

Abstract

Microfibers are one of the most abundant microplastic particle types found in the environment, where they cause negative impacts on organisms and possibly on human health. Microfibers should be included in a wide range of laboratory studies, however, microfibers for scientific studies are not commercially available. Current methods to make microfibers generally create particles with large size ranges and poor precision, and efficient production of particles $\leq 100 \mu\text{m}$ is difficult. Laboratory studies of the biological and toxicological effects and chemical interactions of microfibers require uniform, small microfibers in sufficient numbers for environmentally relevant experiments. We developed a novel fiber embedding technique and modified a seminal cryomicrotomy method to produce precise microfibers in quantities suitable for environmentally relevant concentrations. Polyethylene terephthalate (PET) and nylon fibers were strategically wound onto a spindle, embedded in paraffin wax, and sectioned using a standard paraffin microtome. After processing with a suitable organic solvent to remove the wax, microfiber size distributions were assessed. The small microfibers (10 - 42 μm) were accurate to the target lengths with excellent precision and a production rate ≥ 13.5 times higher than previous methods. As a proof of application, 3 lengths of

¹ Revised manuscript submitted to Environmental Toxicology and Chemistry

manufactured PET fibers were stained with Nile red and exposed to Eastern oyster larvae (*Crassostrea virginica*) for 24 h. Larvae ingested the smaller fiber lengths (14 and 28 μ m), and the Nile red-stained fibers were visible and distinguishable in the guts of the larvae. This experiment was the first to demonstrate ingestion of plastic particles other than microspheres by oyster larvae. The present method facilitates the use of small microfibers in laboratory experiments allowing for a more complete understanding of microplastic effects in the environment.

Introduction

Microplastics are ubiquitous in the environment (Karbalaie et al., 2018), are predicted to increase in abundance (Geyer, 2020), and pose risks to organisms and human health (Campanale et al., 2020; Karbalaie et al., 2018). They occur in all environmental compartments, including water (Bergmann et al., 2015; Li et al., 2018), soil (Piehl et al., 2018), air (Cox et al., 2019; Wright et al., 2020), and organisms (de Sá et al., 2018; Lusher et al., 2017). They are also found in human consumables (Kosuth et al., 2018; Mason et al., 2018; Prata et al., 2020).

Microplastics cause endocrine disruptions in adult Japanese medaka, reproductive effects in the Pacific mole crab, impaired development in oyster larvae and juvenile fish, and increased mortality in Pacific mole crabs and juvenile glassfish (Bringer, Thomas, et al., 2020; Horn et al., 2020; Naidoo & Glassom, 2019; Rochman et al., 2014). They also change behaviors of cold water copepods and transport harmful bacteria, such as *Vibrio* spp., and other pathogenic microorganisms (Cole et al., 2019; Walkinshaw et al., 2020). Oysters filter large volumes of water and, are therefore exposed to a high number of microplastics. Ingestion of microspheres by adult

oysters reduced oocyte number and diameter, decreased sperm velocity, and larvae from exposed parents, showed reduced D-larval yield and slower development (Sussarellu et al., 2016). Oyster embryos exposed to microspheres showed malformations, reduced growth, and abnormal swimming behavior, while ingestion of 1 μm microspheres by oyster larvae showed reduced algal ingestion rates (Bringer, Cachot, et al., 2020; Cole & Galloway, 2015).

Microplastics contain and adsorb toxic, persistent, and bioaccumulative chemicals, such as plasticizers, polychlorinated biphenyls, polycyclic aromatic hydrocarbons, polybrominated diphenyl ethers, and heavy metals (Lusher et al., 2017; Rochman et al., 2013). These chemicals are harmful to organisms and because of their affinity for plastic polymers, microplastics can serve as vectors for these pollutants (Koelmans et al., 2016). Conversely, microplastics can also be sinks for such contaminants, depending on the chemical, existing environmental concentrations, organismal concentrations, microplastic polymer, surface area and shape, other organic particles, and environmental conditions (Koelmans et al., 2013; Nobre et al., 2020; Rainieri et al., 2018; Thaysen et al., 2018). It is necessary to have environmentally relevant particle types with well-defined shapes and surface areas, to be able to test chemical partitioning.

Environmental microplastics include a variety of polymers, morphologies, colors, sizes, and additives. The most common particle types found in the environment are fragments and fibers (Lindeque et al., 2020; Rist et al., 2020). Smaller microplastics are also more abundant in the environment than larger microplastics (Brandon et al., 2020; Lindeque et al., 2020; Rist et al., 2020) and pose

high risks to lower trophic organisms (Walkinshaw et al., 2020). Studies have shown that microfibers $\leq 100 \mu\text{m}$ affect organisms. For example, microfibers accumulated in the guts of zebrafish in greater quantities than fragments or beads, causing intestinal mucosal damage, increased intestine permeability and inflammation, disrupted metabolism, and altered intestinal microbiota (Qiao et al., 2019). Copepods ingested small polyethylene terephthalate (PET) and nylon 6, 6 fibers, which reduced ingestion of algal prey species, resulting in 40% reduction of ingested biomass, and shifting prey selection away from sizes similar to microplastics (Cole et al., 2019; Coppock et al., 2019). Finally, copepods exposed to nylon fibers molted prematurely (Cole et al., 2019).

While microbeads, pre-production nurdles, and irregularly shaped fragments are commercially available for experimental applications, microfibers are not. The lack of standardized microfibers, one of the most abundant microplastics observed in the environment, limits environmental representation of laboratory studies and limits comparisons between studies. Microfibers for laboratory exposure experiments are generally manufactured by each individual lab through hand cutting fibers using some type of blade and/or grinding or milling of larger fibers (Jemec et al., 2016; Ma et al., 2020). These methods require serial sieving of the microfibers into imperfect and non-uniform size classes (Paul-Pont et al., 2018). They produce non-standard particles with large, unpredictable size distributions, cannot make small ($\leq 100 \mu\text{m}$) fibers expediently in adequate quantities for environmentally realistic concentrations; produced fiber length means, standard deviations, or size distributions are rarely reported (Jemec et al., 2016; Ma et al., 2020; Paul-Pont et al., 2018; Romanó de Orte

et al., 2019). Robust control of particle shapes and size distributions are crucial prerequisites for laboratory experiments with microplastics (Paul-Pont et al., 2018), and many have sought better standard microplastic particles for laboratory use (Connors et al., 2017; Murphy, 2017). The only prior method for making sufficient quantities of uniform microfibers $\leq 100 \mu\text{m}$ for laboratory experiments used a cryogenic microtome to thinly slice embedded multifilament polymer fibers (Cole, 2016). This method is more precise than other methods, is appropriate for laboratory experiments, and produces microfibers that are easily distinguishable from airborne contaminants (Christoforou et al., 2020). Although it generates high quality experimental microfibers, the cryomicrotomy method is time consuming and requires the use of a relatively uncommon instrument: a cryogenic microtome (Christoforou et al., 2020; Cole, 2016). The production limitations and the limited availability of cryogenic microtomes reduce the applicability of cryomicrotomy for widespread use in laboratory experiments.

Here we describe a novel fiber embedding technique and a modified cutting method using paraffin microtomy, to improve the availability, efficiency, and productivity of cutting plastic microfibers of uniform lengths for experimental use. We also show a preliminary proof of application by exposing larvae of the Eastern oyster (*Crassostrea virginica*) to the manufactured microfibers. Oysters are selective particle feeders and if they are actively selecting for microfibers, one of the most abundant particle types found in coastal ecosystems, then microfibers could pose risks to oyster larvae in the environment (Lindeque et al., 2020; Ward, Rosa, et al., 2019). This is a novel application because microfiber exposure experiments have been

limited to juvenile and adult oysters, and experiments with oyster larvae have been restricted to microspheres (Bringer, Cachot, et al., 2020; Cole & Galloway, 2015; Thomas et al., 2020; Ward, Zhao, et al., 2019).

Materials and Methods

Fiber selection

The fiber manufacturer and polymers were chosen for direct comparison to the cryomicrotomy method and to polymer prevalence in the environment (Cole, 2016; Geyer et al., 2017; Mishra et al., 2019; Paul-Pont et al., 2018). Polyethylene terephthalate (PET or polyester) fibers are commonly used in textiles, and nylon (polyamide) is another common polymer used in textiles, fishing gear, and other maritime equipment (Browne et al., 2011; Mishra et al., 2019). Both polymers are prevalent in the environment and have shown negative effects on aquatic organisms, such as changes in molting behavior and prey selectivity of juvenile copepods (Cole et al., 2019) and decreased filtration capacity and filtration rates of mussels (Christoforou et al., 2020; Woods et al., 2018). For the development of the paraffin microtomy method described here, spools of multifilament synthetic fibers (polyethylene terephthalate-ES305710, nylon 6,6-AM325705) were purchased commercially from Goodfellow Corporation (<https://www.goodfellow.com/>).

Fiber winding and paraffin embedding

Multifilament polymer fibers were wound onto a custom wooden spindle to create 2 parallel bands of fibers. About 960 lengths (480 full spindle rotations) of the multifilament fibers were wound around the wooden dowels of the spindle, which

were 75 mm apart, resulting in 2 bands of parallel fibers about 30 mm wide (Figure 5.1A). The fiber was wound precisely onto the spindle in a single layer, with space between each length, ensuring that each fiber was completely embedded in paraffin wax for support during microtomy. This design also minimized the number of fibers that were cut instantaneously during microtomy, decreasing blade wear and promoting clean cuts. Details of the custom fiber winding instrument are provided in the Supporting Information (Figures S5.1-S5.3). The spindle and wound fibers were placed in a custom aluminum foil and wood mold that was filled with liquid paraffin wax. The spindle was placed so the wound fibers were diagonal across the paraffin wax block, allowing for a larger number of fibers to be cut in each slice during microtomy (Figure 5.1B, 5.1E).

After the wax solidified, the central section of parallel fibers was excised from the spindle, resulting in a 65 mm longitudinal block of embedded fibers (Figure 5.1C). This large paraffin block was then subdivided transversely into narrow blocks (10 - 11 mm thickness) to fit the microtome cassettes (Figure 5.1D, 5.1E). Individual transverse blocks were mounted and affixed to standard plastic microtome cassettes using a small amount of molten paraffin wax. The blocks were oriented on the cassettes so the fibers lengths were perpendicular to the microtome blade. Excess perimeter wax was carefully trimmed from the mounted blocks with a razor blade, minimizing the volume of paraffin wax to be dissolved from collected sections in later steps (Figure 5.1F).

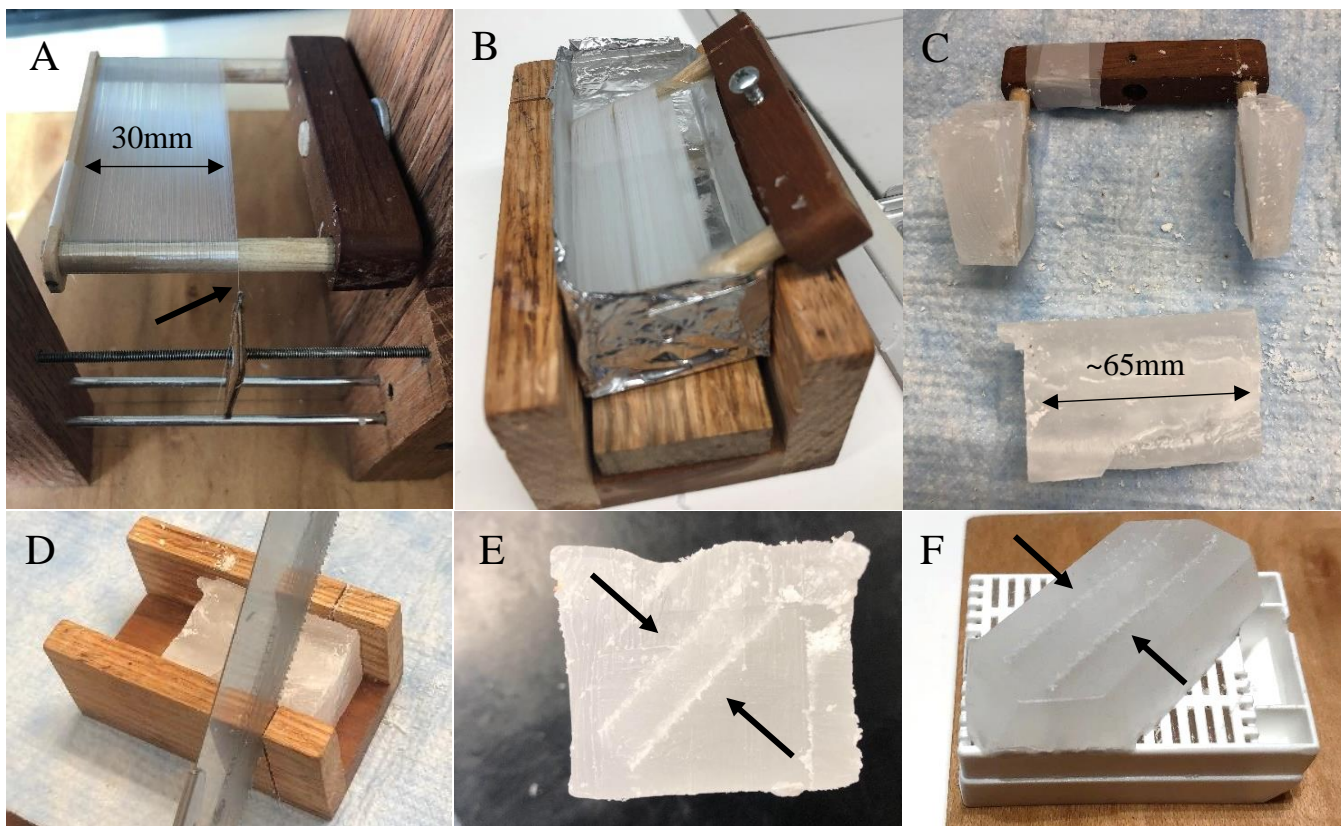


Figure 5.1 Creating paraffin-embedded parallel fibers for cutting with a microtome A) A 30 mm wide band of multifilament fiber precisely wound around the wooden spindle without overlap. B) Spindle with wound fibers immersed diagonally in a custom rectangular mold filled with molten paraffin wax. Maximum band width of multifilament fibers and mold dimensions constrained by microtome cassette dimensions. C) Central section of paraffin-embedded fibers excised from the wooden spindle creating a block about 65 mm long; black line also indicates orientation of fibers. D) Cutting the long 65 mm block into 10 to 11 mm blocks using the wooden mold as a miter box and a fine Japanese saw. E) A thin 10 mm block, with diagonally embedded fibers, cut to fit the microtome cassette; Arrows indicate diagonal white lines, which are stacks of parallel fibers that lie perpendicular to the cutting plane of the microtome blade. F) A thin block of embedded fibers mounted on a microtomy cassette, with excess wax trimmed.

Microfiber cutting

The blocks were then sectioned according to the desired microfiber lengths (10, 14, 28, 30, 42, 100 μm) using a standard paraffin microtome (Microm HM-330).

Microfiber lengths were chosen based on the size range of particles that are routinely

ingested by planktotrophic larvae of *C. virginica* (10, 14, 28, 30, 42 μm). The definition of a microfiber is considered a length : diameter aspect ratio of 3:1 (Cole, 2016). We acknowledge that the lengths of some particles in the present manuscript do not meet this definition, but we were specifically targeting particles that might be ingestible by oyster larvae. For simplicity, all particles generated by the present method are referred to as “microfibers”. Nylon fibers with 100 μm lengths were cut for direct comparison to reported results from the cryogenic microtome method (Cole, 2016). Due to our microtome’s maximum section thickness limitation (65 μm), 100 μm fiber lengths had to be cut by manually advancing the paraffin block twice at 50 μm .

Post-microtomy processing

The blocks were sectioned and a maximum of 150 sections were collected in 50-mL polypropylene centrifuge tubes, where xylene was added to dissolve the paraffin wax. The total number of sections was determined by the desired number of microfibers. Centrifuge tubes with > 100 sections were placed in a 60°C water bath for 5-minute intervals. Once the wax had dissolved by visual inspection, the tubes were centrifuged to pellet the microfibers and the supernatant was aspirated and discarded. Three washes with xylene were used to dissolve and remove any residual paraffin wax. The xylene was then solvent exchanged with 100% (v/v) ethanol (3 washes) followed by a single solvent exchange with 70% (v/v) ethanol for long-term storage without bacterial growth (Chambers et al., 2006). The washes for each ethanol concentration were conducted with centrifugation and supernatant removal between steps. Microfibers were stored concentrated in 70% (v/v) ethanol, in the

dark at 4°C for future experiments. Further details of fiber sectioning and post-cutting processing are provided in the Supplemental Information (Figure S5.4, S5.5).

Immediately prior to microfiber exposure experiments, aliquots of microfibers in ethanol were placed into new polypropylene tubes and solvent exchanged with acetone for staining with the fluorescent dye, Nile red. Nile red was added to the microfiber-acetone solution and microfibers were stained (Maes et al., 2017). The microfibers were then washed 3 times with artificial seawater (1 µm-filtered, 15 psu) that included 0.1% (v/v) Tween 20 during the first wash.

Microfiber analysis

Expected concentrations of microfibers were calculated from the number of filaments in the purchased multifilament fiber, the amount of continuous fiber wound around the spindle, the number of embedded fibers within a microtomy section, and the number of microtomy sections collected. Following production and processing, microfiber dimensions and numbers were evaluated microscopically. Concentrations were determined by diluting small aliquots of each stock microfiber suspension and counting the number of microfibers in a known volume using a light microscope (Olympus IX73 Research Inverted Microscope) and a Sedgewick-Rafter slide. Lengths were measured using a Nikon Eclipse E600 microscope with an AmScope MU800B digital camera and AmScope software version 3.7. Airborne and other particle contamination was also assessed when examining microfibers to quantify their concentrations.

Sources of particle contamination are airborne particles or particles on the surfaces that the blocks and sections came into contact with. Therefore,

contamination was minimized during production and processing by using standard clean lab practices. New aluminum foil for the paraffin mold was used, the microtome and surrounding area was cleaned before use, the fiber-embedded sections were collected in sterile tubes, tubes were uncapped for as little as possible, sterile glass pipets were used for solvent exchanges, and solvent exchange steps were conducted in a fume hood to minimize airborne contamination

Statistical analysis

Statistical analysis was performed to examine the precision of microfiber lengths compared to the target lengths. According to the central limit theorem, data means are approximately normal for large sample sizes (> 40) and parametric tests can be used (Elliott & Woodward, 2007). Sample sizes were 111 for each cut fiber length. Levene's test for homoscedasticity showed heterogeneous variance so a Welch's ANOVA was conducted followed by the Games-Howell post hoc test. Statistical results from the parametric tests were verified using the non-parametric Kruskal-Wallis and Dunn tests. Statistical analyses were performed in R Studio version 1.1.423 and significance was reported at $p \leq 0.01$.

Proof of application

As a proof of application and to examine if microfiber selection and ingestion by oyster larvae were possible, *C. virginica* larvae were exposed to each manufactured PET microfiber length for 24 h. Each PET fiber length stock solution was vortexed on high for 30 s, and small aliquots (25 μ L) of each were transferred to separate sterile 15-mL tubes. Exposures were run in duplicate. Microfibers were

stained with Nile red and cleaned as described in the “Post-cutting processing” section. Larvae (300 per tube, > 224 μm diameter) were placed in the 15-mL tubes containing one PET microfiber length (14, 28, or 42 μm). Larvae were fed once, at the beginning, with a mixture of phytoplankton (120,000 cells mL^{-1} , 60% *Chaetoceros muelleri* and 40% *Tetraselmis chuii*). After larvae and phytoplankton were added to the tubes containing one length of Nile red-stained microfibers, each tube was filled to 15 mL with 15-salinity artificial seawater. Final concentrations of larvae were 20 mL^{-1} and final concentrations of microfibers for each PET fiber length were 727 mL^{-1} for 14 μm , 467 mL^{-1} for 28 μm , and 1,390 mL^{-1} 42 μm . High concentrations of microfibers were used to give the best possible chance for microfiber ingestion. Tubes were rotated on a plankton wheel for 24 h at 1 rotation per minute to keep all particles and larvae suspended. After 24 h, larvae were observed under a Zeiss Axio Imager 2 Research Fluorescent Microscope (Ex/Em: 485/515nm) and imaged with a Photometrics CoolSnap HQ2 Camera. Zen image processing software (2012) was used to examine microfiber ingestion. Larval exposures to the 42 μm -length microfibers were conducted three times, with different broods of larvae, to confirm ingestion results.

Results

The present method was successful in creating PET and nylon 6, 6 microfibers of all attempted fiber lengths (Table 5.1, Figure 5.2). Mean microfiber cut lengths were within 2 μm of the target lengths and had low standard deviations, except for the 100 μm microfibers. Mean microfiber cut lengths (10, 14, 28, 30, 42, 100 μm) were statistically different as indicated by a Welch’s ANOVA and the Games-Howell post

hoc test with $p < 0.01$ (Figure 5.3, S5.6). The boxplot including the 100 μm data and a comparison to 100 μm nylon lengths from Cole 2016 can be found in the supporting information (Figure S5.6). The present method was less precise for microfiber lengths of 100 μm because of instrument limitations and human error using a less-accurate method of manual block advancement, as opposed to the paraffin embedding and cutting techniques. Microfibers did not show signs of physical abnormalities or deterioration from the interaction with xylene (Figure 5.2). Cut microfibers were easily distinguishable from other particles and contamination was minimal as very few particles were observed in any of the concentrated microfiber solutions during microscopic microfiber length and concentration analysis.

Table 5.1 Microfiber target lengths and mean cut lengths for polyethylene terephthalate (PET) and nylon 6, 6.

Fiber Polymer	Diameter (μm)	Target length (μm)	Mean cut length ($\mu\text{m} \pm \text{SD}$)
PET	14	14	14.72 ± 4.83
		28	28.43 ± 3.63
		42	41.35 ± 3.51
Nylon 6, 6	10	10	11.78 ± 5.14
		30	30.19 ± 2.92
		100	108.29 ± 24.35

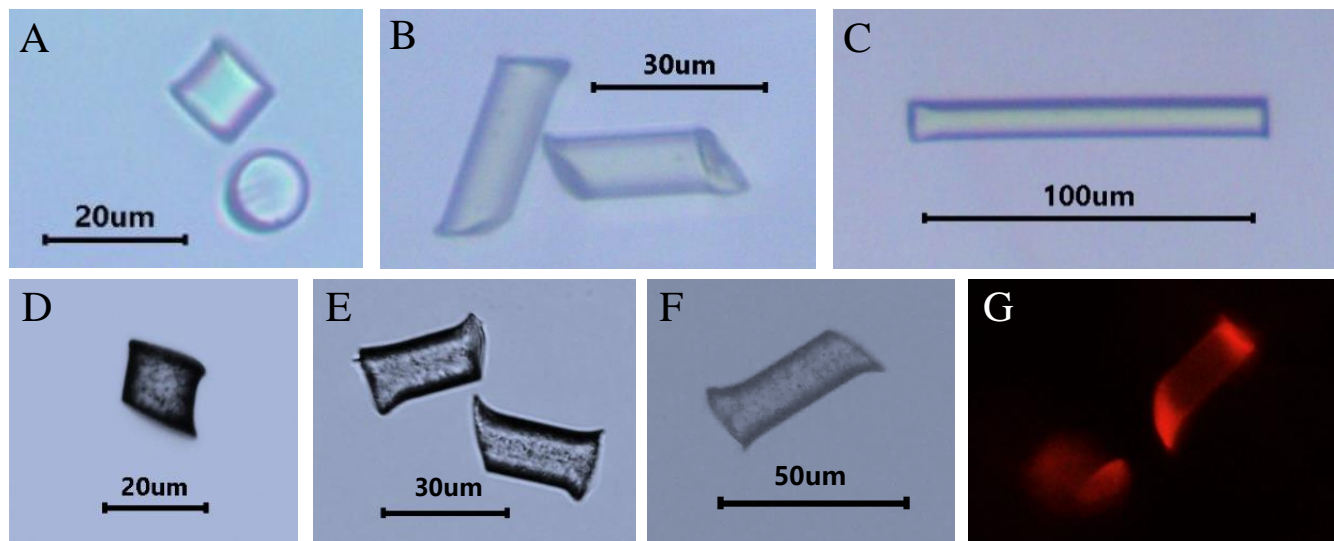


Figure 5.2 Nylon 6, 6 and polyethylene terephthalate (PET) manufactured microfibers imaged using a Nikon Eclipse E600 microscope with an AmScope MU800B digital camera. A) Nylon 10 x 10 μm ; B) Nylon 30 x 10 μm ; C) Nylon 100 x 10 μm ; D) PET 14 x 14 μm ; E) PET 28 x 14 μm ; F) PET 42 x 14 μm ; G) PET 42 x 14 μm microfibers stained with Nile red under fluorescent light (Ex/Em 480/600nm) using an Olympus IX73 inverted microscope.

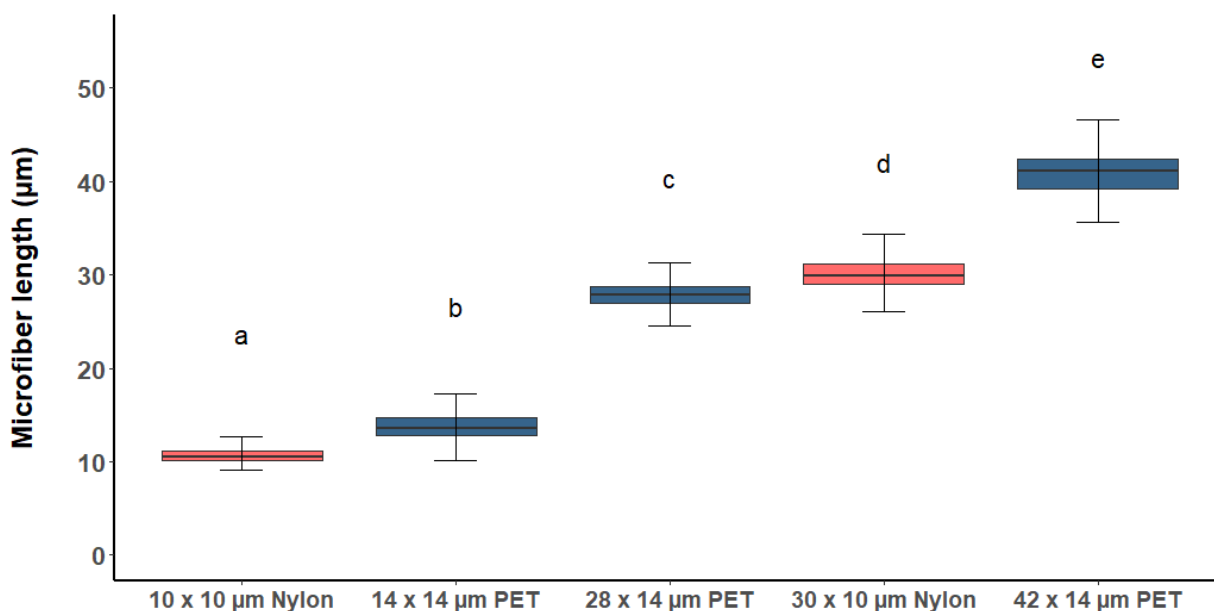


Figure 5.3 The length distributions of cut nylon 6, 6 and polyethylene terephthalate (PET) microfibers for target lengths of 10 and 30 μm (nylon 6, 6, diameter 10 μm , pink boxes) and 14, 28, and 42 μm (PET, diameter 14 μm , blue boxes). Box whisker

plots demonstrate variation in data with median, inter-quartile range, and min-max values. Letters signify statistical significance in mean microfiber length (Welch's ANOVA and Games-Howell post-hoc test $p < 0.01$).

Microfibers were produced in high numbers for PET: 2.51×10^6 (14 μm), 2.66×10^6 (28 μm), and 7.92×10^6 (42 μm) particles from 150, 150, and 440 sections respectively. Equally large numbers of nylon microfibers were manufactured: 10.52×10^6 (10 μm), 14.64×10^6 (30 μm), and 0.45×10^6 (100 μm) particles from 595, 595, and 25 sections respectively. Total effort to produce all microfibers was 4 days.

Larvae of *C. virginica* were able to ingest PET fibers of 14 μm and 28 μm lengths, but not those of 42 μm (Figure 5.4). The manufactured and Nile red-stained PET fibers were easily distinguishable in their fluorescence emissions from the 2 species of phytoplankton used to feed the larvae.

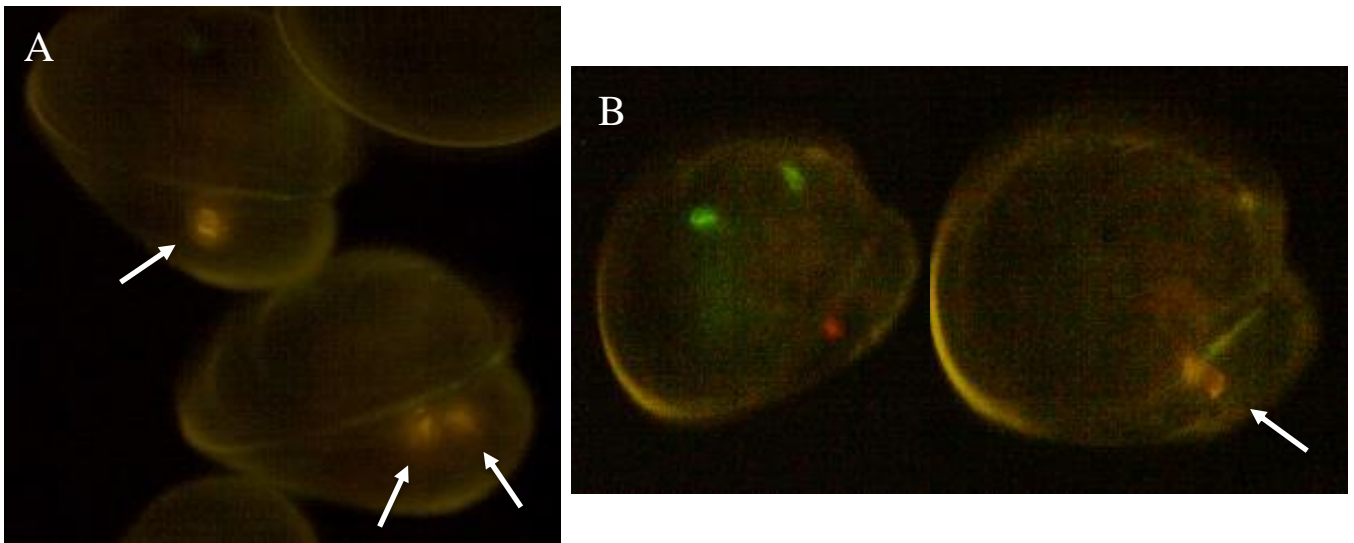


Figure 5.4 Manufactured polyethylene terephthalate (PET) microfibers ingested by *Crassostrea virginica* larvae, indicated by white arrows. A) 14 x 14 μm PET fibers fluoresce yellow/orange in the guts of two larvae; B) 28 x 14 μm PET fiber fluoresces

yellow/orange in the gut of one larva. *Chaetoceros muelleri* and *Tetraselmis chuii* cells fluoresce red and green respectively.

Discussion

Overall, the present method provides an efficient way to create large quantities and accurate lengths of PET and nylon microfibers for use as standardized particles in microplastic laboratory experiments. In addition, a proof of application experiment was the first to show that plastic particles other than microspheres were selected and ingested by *C. virginica* larvae. Manufacturing standard and precise microfibers for laboratory-based experiments is important for comparing studies, for targeting specific lengths and interactions, reducing uncertainty in estimations, and for testing microplastic extraction methods. Precise fiber winding and the diagonal fiber placement in the paraffin blocks allows for a high production rate, at least 13.5 times as many particles h⁻¹ than the seminal cryomicrotomy method, making it more efficient (Cole, 2016). The present method creates microfibers of similar characteristics to those manufactured by the previous method, but with more precision in cutting medium length microfibers (28 - 42 μm) and demonstrates utility at cutting microfibers ≤ 40 μm in length. The paraffin microtomy method also successfully creates microfibers with lengths of 42 to 100 μm.

Paraffin method assessment

Accessibility. Our method improves the creative cryomicrotomy method by substituting a standard paraffin microtome and modifying the fiber embedding method. Standard paraffin microtomes are simpler to use because processing takes

place at room temperature. The cryomicrotomy method requires the user to work quickly and to frequently return the embedded fibers to a freezer to ensure the solvent block stays solid and the fibers secure (Cole, 2016). Another benefit of using a standard paraffin microtome is that they are more widely available than cryogenic microtomes. The standard paraffin microtome requires minimal training for proficiency in fiber cutting. Paraffin blocks containing embedded plastic fibers are stored at standard laboratory room temperatures, and are quickly available for microtomy to cut additional microfibers of specific lengths.

Accuracy and precision. The reported paraffin microtomy method successfully produced accurate and precise mean cut lengths for the majority of microfiber lengths attempted (Table 5.1). Mean cut lengths varied 2 μm or less from the target lengths (10, 14, 28, 30, 42 μm) with small standard deviations, indicating that fibers were securely embedded in paraffin wax and cut cleanly by the microtome blade. Standard deviations for medium cut-lengths (28 ± 3.63 , 30 ± 2.92 , and 42 ± 3.51 μm) were smaller compared to those reported for the 40 ± 12.4 μm nylon microfibers produced by the cryomicrotomy method (Cole, 2016). The cryomicrotomy method did not cut fiber lengths shorter than 40 μm . Statistical analyses showed that all mean cut fiber lengths were statistically significant, even for target lengths that were close together, indicating that the present method created microfibers with high precision. Besides the cryomicrotomy method, there are no other methods described in the literature that produce sufficient quantities of precise microfibers ≤ 100 μm . For example, one method that manually cut fibers using scissors, a fiber slicer, and multiple fixed blades could only produce mean microfiber lengths ≥ 116 μm , with large standard

deviations (28 - 192 μm) and large size ranges, perpetuating the issue of non-standard particles (Ma et al., 2020). The ability to create precise microfiber lengths is useful for targeting organismal size ingestion ranges and observing organismal particle selectivity and interactions. It also provides the ability to create known size distributions of particles to better emulate environmental samples. Finally, it allows for more accurate calculations of microfiber surface area, reducing uncertainty in chemical distribution constants and other measurements reliant on surface area.

Paraffin microtomy successfully created microfibers with lengths longer than 42 μm . Even using a manual procedure for cutting 100 μm lengths, because of instrument specific limitations, the mean cut length and standard deviation ($108.29 \pm 24.35 \mu\text{m}$) closely encompassed the target length (Figure S5.6). Larger variability in cutting 100 μm lengths is not likely due to the process for securely embedding the fibers, the use of paraffin wax over a frozen embedding medium, or to imprecise cutting of embedded fibers by the microtome. The greater length variability for our 100 μm microfibers was likely due to human error while manually advancing the paraffin block to accommodate instrument limitations (maximum section thickness of 65 μm). Microtomy performance for longer microfiber lengths (> 65 μm) could be improved by using paraffin microtomes with greater maxima section thickness, or by developing more accurate techniques for manually advancing paraffin blocks.

Procedures for minimizing particle contamination were successful, since very few non-manufactured particles were seen in the microfiber stock solutions when concentrations were assessed. When work surfaces and instruments are thoroughly cleaned before processing, the biggest sources of particle contamination are from

airborne particles landing in the molten paraffin wax as it solidifies or from airborne particles landing on the blocks and sections during the cutting process. Keeping the blocks covered and clean, and quickly collecting the cut sections into polypropylene tubes was successful in minimizing apparent airborne contamination. To minimize airborne particle contamination further, air filters could be used in the laboratory. For visible particles that reach the post processing stages in polypropylene tubes, glass pipets can be used during the washing steps to aspirate unwanted particles.

Efficiency. The production of microfibers matched or exceeded the quantities desired for experiments. Through preliminary calculations using the winding instrument and wooden spindle dimensions, we estimated that about 6.32×10^6 $42 \mu\text{m}$ -long PET microfibers could be cut using 440 microtome sections from two fiber-embedded blocks with $\sim 7.92 \times 10^6$ $42 \mu\text{m}$ -long microfibers actually cut. Using 150 sections each from one 10mm block yielded 2.66×10^6 $28 \mu\text{m}$ -long and 2.507×10^6 $14 \mu\text{m}$ -long PET particles. After embedding, extra fiber paraffin blocks can be conveniently stored indefinitely at room temperature, expediting production of additional microfibers as needed.

The present method provides a more efficient way of cutting microfibers and better standard particles for laboratory experiments. Creating 6 blocks of embedded fibers took 5 to 6 h, depending on the desired number of microfibers, with the winding of fibers around the wooden spindle requiring the most labor. Fiber cutting on the microtome and post-cutting processing took 2 to 4 h. The production rate of about $792,000$ $42 \mu\text{m}$ -long microfibers h^{-1} was > 13.5 times the rate of the previously published microtomy method for a similar size microfiber ($58,500$ $40 \mu\text{m}$ microfibers

h^{-1}) (Cole, 2016). Production rates for particles $< 42 \mu\text{m}$ in the present method were $>792,000$ microfibers h^{-1} . While a manual cutting method has higher efficiency than the cryomicrotomy method, that approach is limited to long microfibers (300 ± 192 and $116 \pm 28 \mu\text{m}$) and is less precise (Cole, 2016; Ma et al., 2020). Our paraffin microtomy method is more efficient than any other published method for producing standard microfibers, reducing the amount of time needed to produce large quantities of microfibers for large volume, long exposure, or multiple experiments.

Considerations. Our fiber spacing and diagonal placement of the fibers in the paraffin block created a clean cut without pulling the fibers out of place. However, we did see microfibers with angled cuts (Figure 5.2) similar to the microfibers made using the cryomicrotomy method (Cole, 2016). This is likely due to the loosely twisted nature of the individual filaments in the multifilament fibers that were used in both methods. We occasionally saw tails or microfibers that were 2 to 3 times the desired target length possibly due to fiber shearing. It is possible to increase the spacing slightly between the fibers during winding to make sure they are even more securely embedded in the paraffin to prevent this.

The paraffin saturation point in xylene limits the number of sections that can be placed in polypropylene tubes for paraffin extraction. We determined that putting about 100 to 150 sections in a 50-mL tube with 45 mL of xylene (60°C water bath in 5-minute intervals if necessary) was sufficient to dissolve all of the paraffin. Some microfibers were lost in the process of consolidating the microfiber pellets into one tube after they were sufficiently washed with xylene to completely dissolve the paraffin wax. Microfiber loss can be reduced by minimizing transfers from tube to

tube in post-cutting processing. It is also relatively easy to account for loss, if multiple tubes are needed, by cutting a small number of extra sections. Each section contains an estimated 13,440 to 14,400 particles, based on the number of filaments and original amount of fiber length wound onto the spindle. The cryomicrotomy method requires scraping of the produced microfibers from a filter into a long-term storage container (Cole, 2016). The present method eliminates that step by doing solvent exchanges, reducing microfiber losses.

Because of the post-microtomy processing with organic solvents, chemical compatibilities of embedded fiber polymers must be considered. Xylene is the most common solvent used to dissolve paraffin wax, but other solvents are also available (Alwahaibi et al., 2018; Shields & Heinbockel, 2019). Xylene is compatible with the most common polymers used to make fibers (PET, nylon, and polypropylene) for the short interaction time required, covering the majority of applications (Camlab Ltd., 2007; CP Lab Safety, n.d.). Alternative organic solvents include isopropanol (absolute), toluene, benzene, terpenes, and proprietary mixtures of aliphatic hydrocarbons or proprietary mixtures of aliphatic hydrocarbons and D-limonene, but proprietary solvents must be tested for polymer compatibility (Shields & Heinbockel, 2019). Specifically, toluene is compatible with low density- and high density-polyethylene (Camlab Ltd., 2007).

Proof of application

This experiment was the first to expose oyster larvae to plastic particles other than microspheres. Oyster larvae have been shown to ingest microspheres with diameters ranging from 0.16 μm to 27.4 μm (Baldwin & Newell, 1991; Bringer,

Thomas, et al., 2020; Cole & Galloway, 2015). When exposed to 3 different lengths of manufactured PET microfibers, *C. virginica* larvae readily ingested the shorter fibers (14, 28 μm), but did not ingest the 42 μm -long fibers in any of the three exposure experiments for this length. This fiber size is likely too large for the larvae to select and ingest. Oysters are selective filter feeders but are also anatomically constrained by the size of their feeding structures, and the largest reported phytoplankton cells ingested are 30 μm (Baldwin & Newell, 1991; Ward, Rosa, et al., 2019). Observing microfibers in the larval guts means that oyster larvae actively selected those particles at multiple stages of the selection and ingestion processes. This indicates the potential for effects on the larval life stage of oysters in the environment because microfibers are one of the most abundant particle types found in coastal ecosystems, and, although the concentrations of microplastics < 100 μm are not well understood, microplastics < 100 μm are estimated to be more abundant than larger microplastics (Lindeque et al., 2020).

The Nile red-stained PET microfibers fluoresced yellow/orange and were visible through the translucent larval shells (Figure 5.4). Nile red-stained PET microfibers were also distinguishable in fluorescence color and morphology from the 2 species of phytoplankton used to feed the larvae. This ingestion experiment demonstrates the utility of manufactured microfibers using the present method and shows novel ingestion of microfibers by oyster larvae.

Conclusions

Currently, microplastic studies have had limited standardization of methods and particles used for laboratory experiments. Ideally, particles manufactured for

laboratory experiments would reflect the variety in size, shape, polymer, and weathering through milling of larger plastics (Paul-Pont et al., 2018). Although the milling of larger fibers to produce suitable quantities of small fibers $\leq 100 \mu\text{m}$ for laboratory experiments is unrealistic, our method vastly improves microfiber standardization while allowing for post-processing particle manipulation to better reflect environmental microfibers. It creates standardized microfibers in an efficient and cost-effective way so laboratory-based experiments can be comparable and repeatable. It creates precise microfibers to study factors where having an accurate estimate of surface area is crucial, such as distribution constants of chemicals. The present method also provides the ability to target specific sizes of microfibers or to create a range of particle lengths at a known distribution to simulate the environment and examine organismal selectivity, to examine microfiber distribution and fate in the environment and to examine microbiome interactions. Finally, it provides small microfibers to test microplastic extraction methods for environmental samples. Once produced, these microfibers can be weathered to more accurately model environmental plastic microfibers.

In conclusion, our work makes an important step toward conducting repeatable, comparable, and more environmentally relevant laboratory-based microplastic experiments by creating standardized plastic microfibers. Standardized particles provide a better understanding of chemical, metal, and biological distributions on microplastics. Our paraffin microtomy method makes it easier to incorporate microfibers into laboratory-based studies, providing a more accurate picture of the environmental risks of microplastics.

Supporting Information

Images of the fiber winding instrument (Figure S5.1-S5.3), images depicting microtome cutting (Figure S5.4) and post-cutting processing of microfibers (Figure S5.5), and a figure of the fiber length distributions including 100 μm data (Figure S5.6).

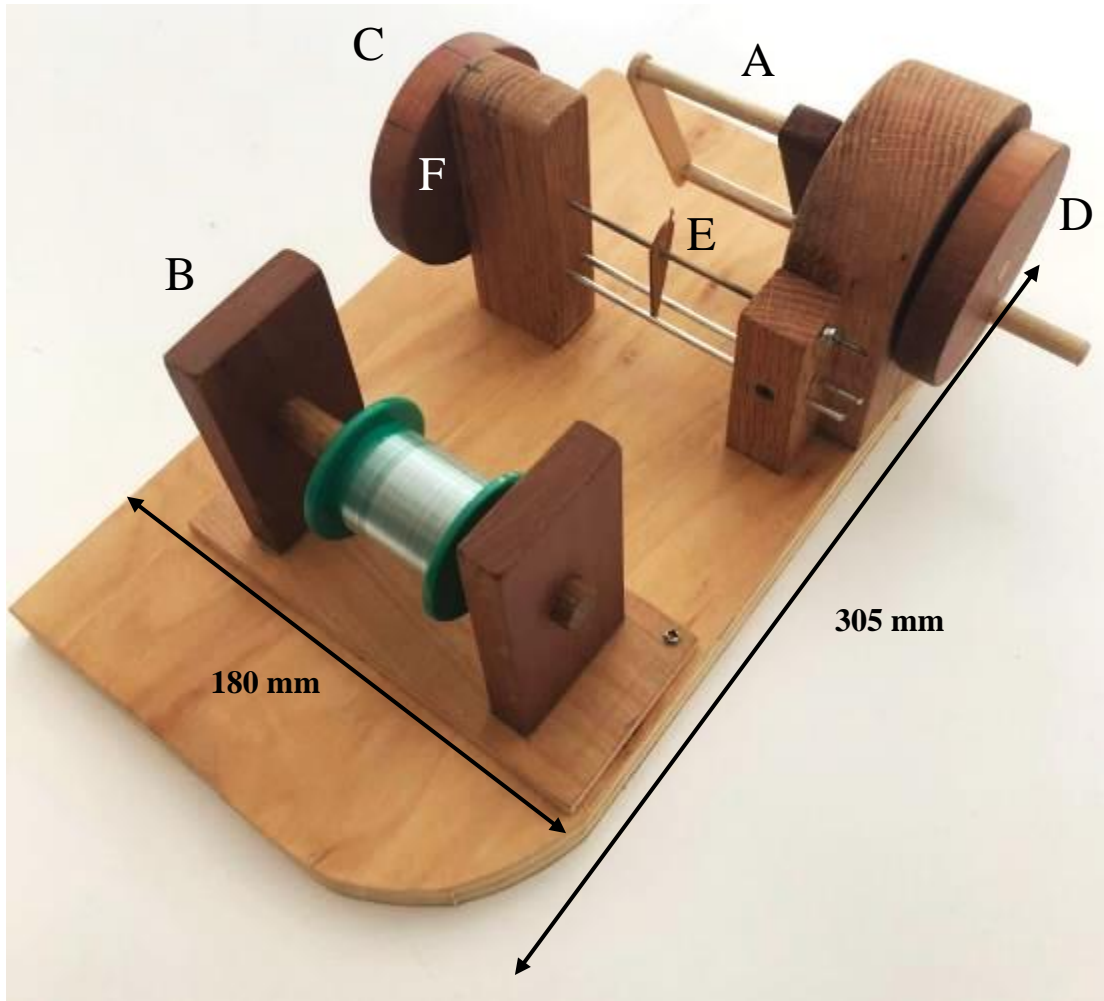


Figure S5.1 Semi-aerial view of the fiber winding instrument from the crank (right) side. The multifilament polymer fibers were precisely wound onto a wooden spindle (A) using a fiber spool dispenser (B) and fiber guide level-wind assembly (C). The spindle is attached to a crank wheel (D). The fiber guide level-wind assembly (C) consists of a fiber guide traveler (E) on a threaded drive shaft, attached to an operation wheel (F), and 2 guide rods.

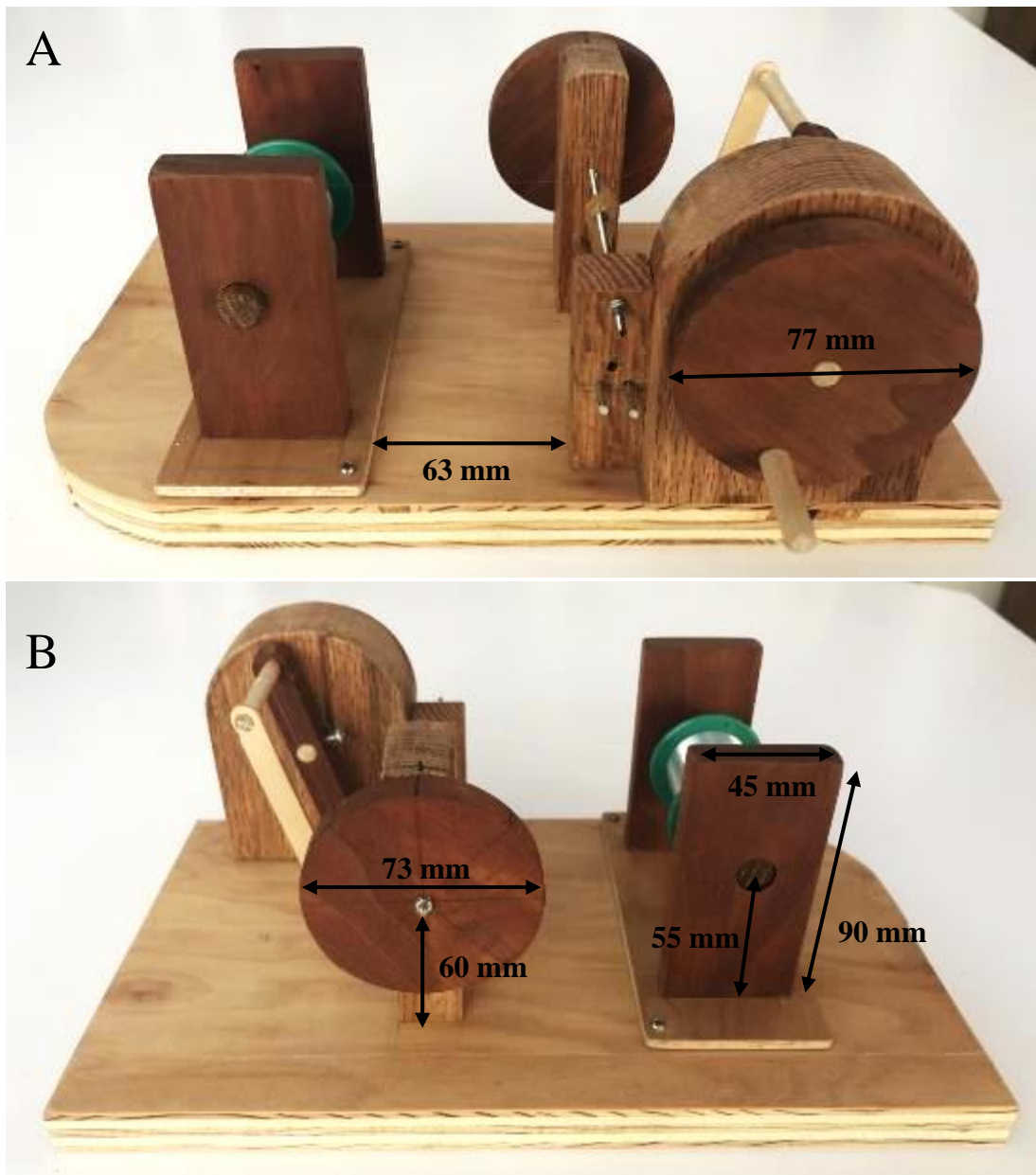


Figure S5.2 Side views of the fiber winding instrument. A) Right side view. The crank wheel is attached to the wooden spindle and 1 full rotation adds 2 lengths of parallel fibers to the spindle. B) Left side view. The operation wheel advances the fiber guide traveler, which precisely winds the fibers onto the spindle. The operation wheel is sectioned into eights, so for each $1/8^{\text{th}}$ advance of the wheel, the fiber guide traveler moves $63 \mu\text{m}$ along the threaded drive shaft rod. For each full rotation of the crank wheel (in A), the operation wheel is rotated $1/8^{\text{th}}$, until the desired amount of fiber lengths are wound on the spindle. The fiber spool dispenser is parallel to the fiber guide level-wind assembly so fibers are wound precisely. The spool is free to move laterally with the fiber guide traveler and the fiber must be taught throughout the winding process.

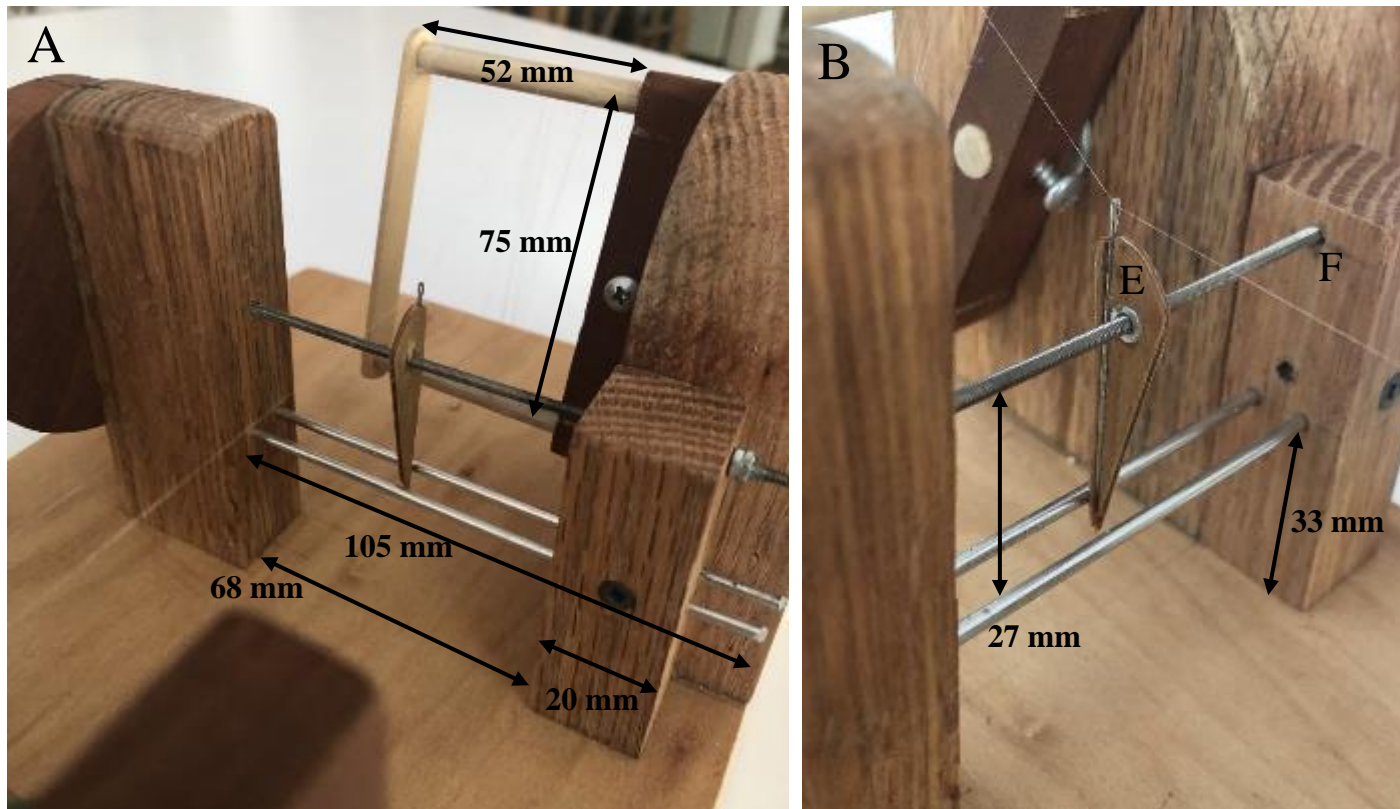


Figure S5.3 A) Close up view of the fiber guide level-wind assembly. Spindle dimensions are constrained by microtome cassette dimensions. B) The fiber guide traveler (E) is made of 2 mm-thick plywood with a 45 mm sewing needle and a small nut to run along the threaded drive shaft (F). The 2 non-threaded rods keep the fiber guide traveler vertical to properly wind the fiber onto the spindle. Precise control of the horizontal movement of the traveler unit with its needle-eye fiber guide, is achieved by rotating the operation wheel which rotates the fine-threaded drive shaft rod (F). The threaded drive shaft passes through the small, threaded nut embedded in the traveler unit. Each $1/8^{\text{th}}$ advance of the operation wheel in Figure S2 B moves the fiber guide traveler to the right by about $63 \mu\text{m}$, ensuring the fibers are not overlapping and there is space between each length to securely embed the fibers. Alternate thread pitches or divisions of the operation wheel can be used to adjust the spacing between the precisely wound fiber lengths on the spindle.

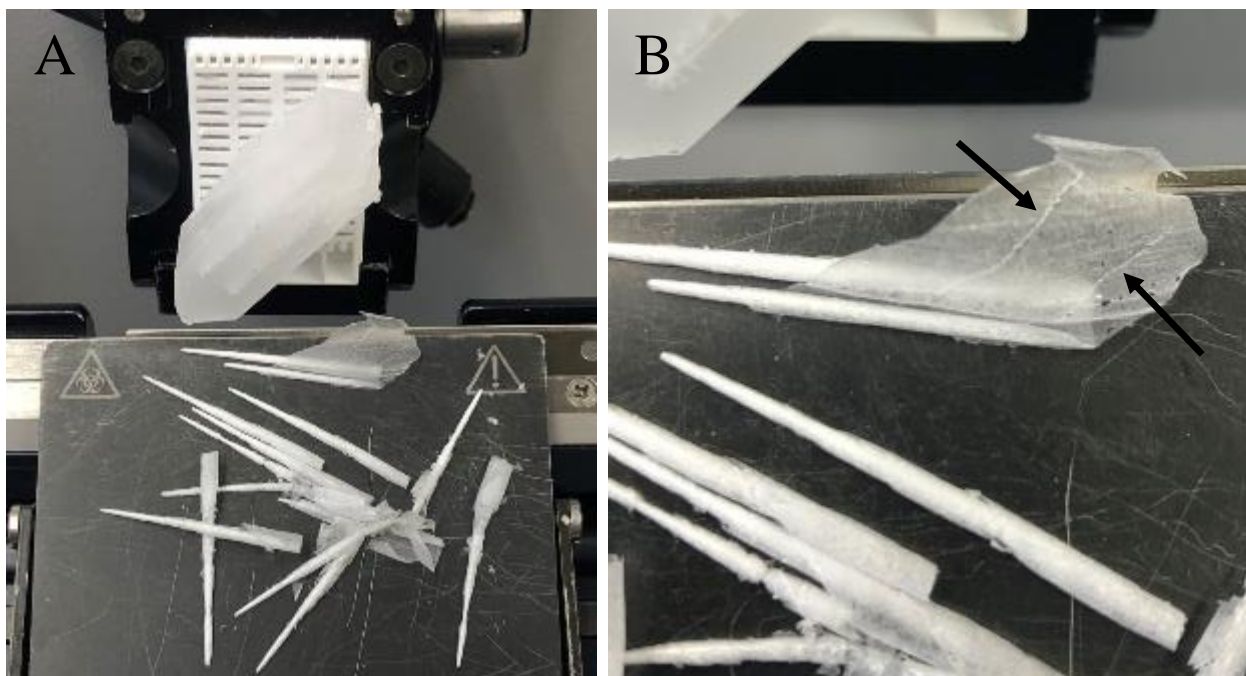


Figure S5.4 A) Sectioning of the paraffin-embedded fiber block using a standard paraffin microtome (Microm HM-330). Sections cut from the trapezoidal block face curl into conical tubes. B) One section of embedded microfibers, arrows indicate the line of stacked embedded microfibers.

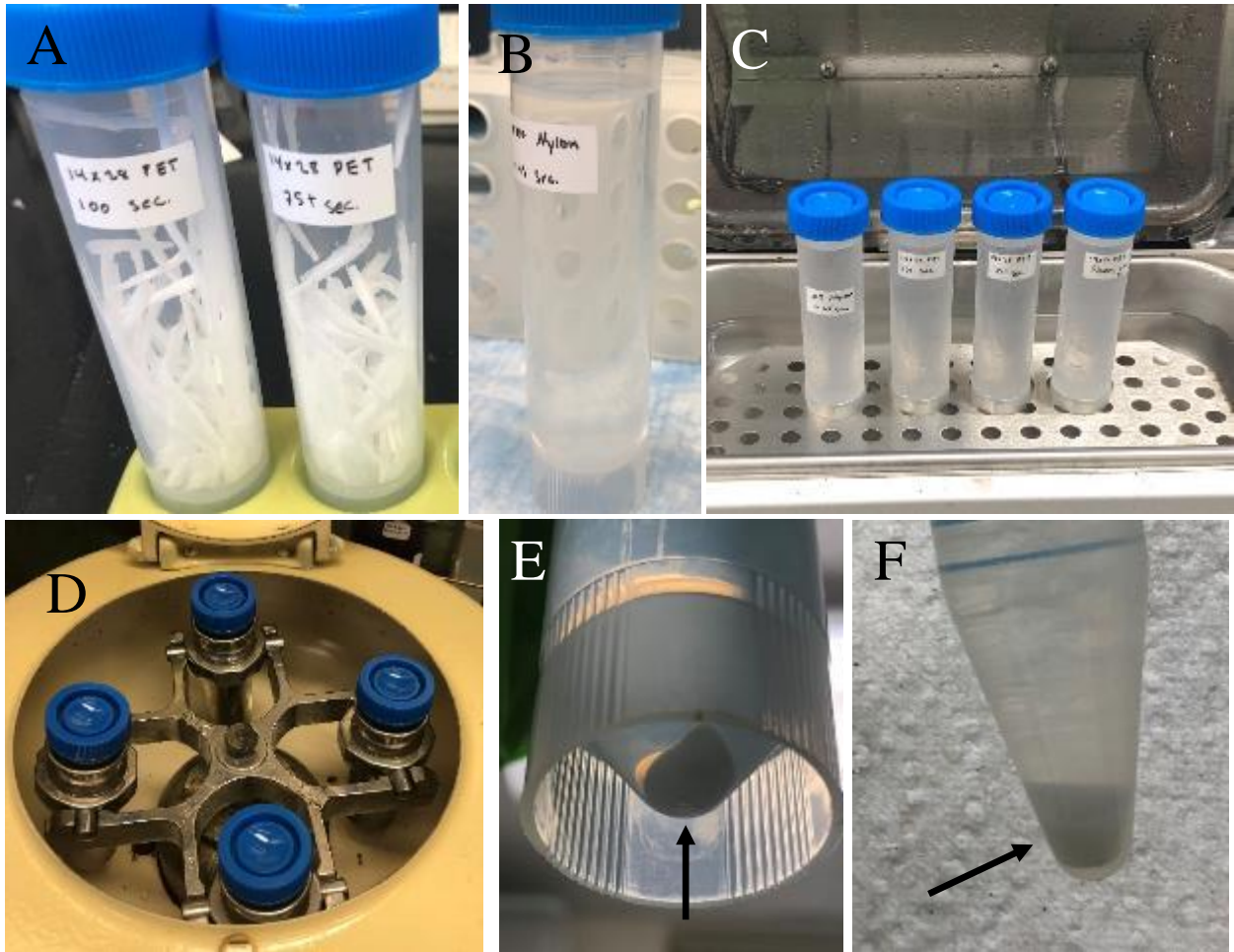


Figure S5.5 Post-cutting processing of microfibers. A) 75 - 150 microfiber-embedded sections of the same thickness were collected in polypropylene centrifuge tubes. B) Dissolving the paraffin wax in the centrifuge tubes using xylene. C) Tubes with > 100 sections were placed in 60°C water bath for 5-minute intervals to fully dissolve paraffin wax. D) Once most of the wax was dissolved, tubes were centrifuged to pellet the released microfibers. E) Pelleted microfibers after centrifugation and supernatant removal. Steps D and E were repeated 3 times with xylene. Xylene was solvent exchanged with 100% (v/v) ethanol and steps D and E were repeated 3 times with 100% ethanol. F) Microfibers of the same length were consolidated into 1 centrifuge tube and 100% ethanol was solvent exchanged for 70% (v/v) ethanol for long-term storage.

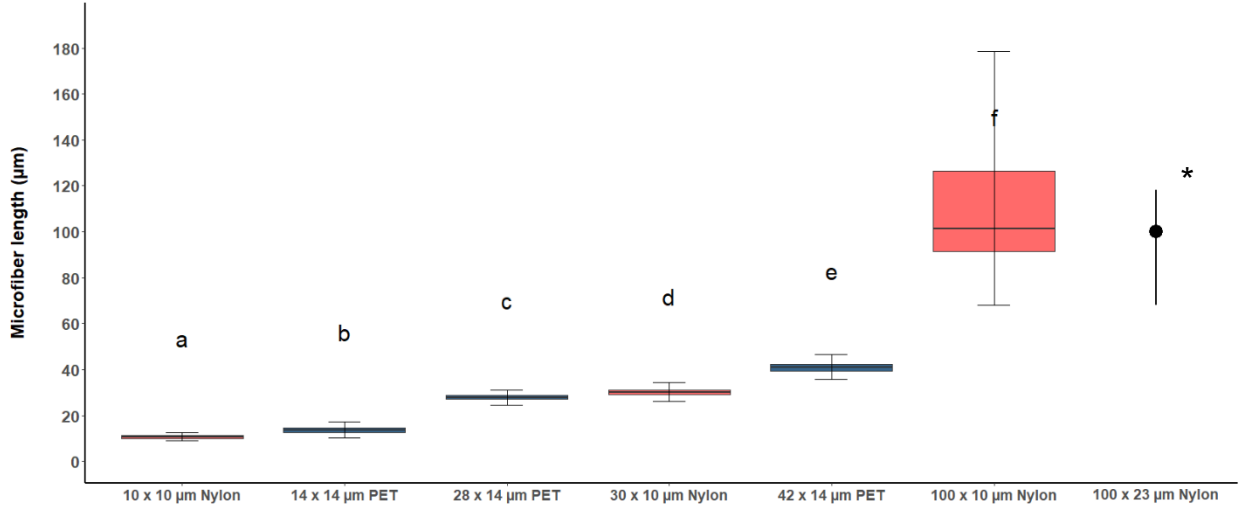


Figure S5.6 The length distributions of cut nylon 6, 6 and polyethylene terephthalate (PET) microfibers for target lengths of 10, 30, and 100 μm (nylon 6, 6, diameter 10 μm , pink boxes) and 14, 28, and 42 μm (PET, diameter 14 μm , blue boxes). Box whisker plots demonstrate variation in data with median, inter-quartile range, and min-max values. Letters signify statistical significance in mean microfiber length (Welch's ANOVA and Games-Howell post-hoc test $p < 0.01$). * Indicates estimated 100 μm nylon microfiber length mean and min-max values from Cole 2016 Figure 2 for comparison to our 100 μm lengths.

Chapter 6: Conclusions

Over the last decade, plastic pollution has become a major global issue. Microplastics have been found in every environment examined and in many species. However, fundamental interactions between microplastics and organisms are not well understood. In the Chesapeake Bay and other coastal environments, oysters are important ecologically, and as a wild-catch fishery and in aquaculture. Consequently, understanding the risks and impacts microplastics have on oysters is important for their management. It was important to use model microplastics because the questions posed in each research chapter of this dissertation have not been examined before and this fundamental research is necessary before more complex experiments are conducted.

To assess the impacts of microplastics on oysters, I used the larval life stage of *C. virginica* and examined a variety of interactions and effects. Examining the interactions and effects of microplastics on oyster larvae involved two stages. The initial examination of factors affecting the uptake of microplastics and the ability for oyster larvae to egest plastics was an important first step. Subsequent evaluation of physiological effects from the ingestion of different types of microplastics provided insight into any deleterious effects to larval oysters. The importance of oysters and the growing environmental contamination of microplastics provide a rationale for the following dissertation questions. How do microplastic and food availability affect *C. virginica* larval ingestion and egestion of particles? What are the threshold ingestion concentrations? Do larvae reach an ingestion saturation of microplastics? Once

ingested, do microplastics affect larval physiology? Are there different physiological responses when larvae are exposed to different microplastic particle types?

Food availability was not a factor in microplastic ingestion for *C. virginica* larvae but microplastic availability was important. As microplastic exposure concentrations increased, larvae ingested more plastics. Ingestion saturations for the two microbead sizes were 5295 beads mL⁻¹ for 2 µm particles and 65,297 beads mL⁻¹ for 6 µm particles. Environmental microplastic concentrations are orders of magnitude lower than these concentrations, so it is likely that under current conditions, or even with modest increases, my observations of minimal effects on oyster larvae will be relevant for now. *C. virginica* were able to egest microbeads but not fully after 24 hours. Other filter feeding larvae required 8 days for complete egestion of microplastic particles (Capolupo et al., 2018). This relatively long time scale could allow for sorption or desorption of organic chemicals in the gut, either increasing or reducing their exposure to harmful chemicals.

Even though *C. virginica* larvae readily ingest microplastics, minimal effects on physiology were seen. *C. virginica* larvae were exposed to PS microbeads and standard manufactured PET and nylon microfibers. There were no effects from PS microbead exposure after 6 days. Only after 6 days of exposure to PET microfibers at high concentrations did larvae show a significant growth penalty. Initial conditions in the nylon microfiber exposure created a multi-stressor exposure. While dose-dependent reductions of algal ingestion and carbon assimilation rates were observed after 3 days, they were not significant. Even under increased stress, larval physiology was not significantly affected.

Microbeads are useful tools for conducting laboratory exposures because they are standardized and they are commercially available, however, microbeads are one of the least common particle types found in the environment. Microfibers are one of the most common particle types found in coastal ecosystems but they are not commercially available or easy to manufacture in the size range available for oyster larvae to ingest. I developed a novel a paraffin embedding technique and modified a microtomy method to manufacture small standardized microfibers for laboratory use. My method produced standard microfibers in an efficient manner. Standard particles are necessary for laboratory experiments because they allow scientists to determine distribution constants of chemicals and metals and other experiments where surface area needs to be well defined. Standard particles also allow for accurate validation of digestion and recovery methods. My method for manufacturing microfibers will help research incorporate these common particle types in laboratory experiments. These particles were used in some of the exposures examining physiological effects of microplastic ingestion on oyster larvae.

Combined, the chapters indicate that oyster larvae are at low direct risk from microplastic pollution. Ingestion threshold concentrations ranged from 20 and 50 microbeads mL^{-1} for 2 and 6 μm bead diameters respectively to about 100 fibers mL^{-1} for PET and nylon fibers (10 to 30 μm in length). No effects on the physiology of *C. virginica* larvae were observed at these concentrations and only minimal effects were seen at 10 times these concentrations. Microplastic concentrations in the Chesapeake Bay are orders of magnitude lower than exposure concentrations in this research (Bikker et al., 2020; Yonkos et al., 2014). However, these studies only looked at

surface trawls and used mesh nets (330 μm), likely underestimating microplastic concentrations and missing the entire ingestible range for oyster larvae. When finer mesh nets are used, microplastic concentrations can be 10-fold greater (Lindeque et al., 2020) and when using 5 μm filters, sea surface contamination reached about 43 particles mL^{-1} in near shore samples (Brandon et al., 2020). Larvae have many challenges in the wild, including predation, low pH, toxins from harmful algal blooms, and diseases. Compared to these other major stressors, microplastic contamination is not a critical concern for oyster larvae at the current estimated environmental concentrations. However, increases in microplastic contamination, changes in environmental or individual factors, or under certain circumstances, microplastics have the potential to induce effects not observed in this research.

This work was the first step in understanding microplastic risks to oyster larvae. It provided fundamental knowledge on the interactions and effects of model microplastics and this knowledge is a stepping stone for more complex and environmentally relevant exposures. The main limitation of this work is that all exposure experiments were conducted with pristine virgin microplastics. In reality, plastics used in commercial products have many chemical additives and dyes and plastic particles sorb organic chemicals and metals from the environment. These leachates and sorbed chemicals have shown impacts on organisms. Microplastics are also substrates for bacterial communities, some harmful to organisms like *Vibrio* spp. Microplastics are a complex suite of contaminants and further studies should evaluate the interactions and effects of a variety of microplastics on oysters, including

different shapes, sizes, surface functionalities, polymer types, chemical additives, and sorbed chemicals and biofilms.

Future research examining the effects of climate change and microplastics will be important moving forward because multi-stressor interactions, such as microplastic ingestion coupled with disease exposure, increased temperature, decreased salinity, and increased ocean acidification, could pose risks to oysters. As sampling, identification, and quantitation techniques for small microplastic improve, laboratory exposure experiments and environmental sampling will converge, providing a better understanding of the actual environmental risks of microplastics to oyster larvae and other zooplankton.

Bibliography

- Alwahaibi, N., Aljaradi, S., & Alazri, H. (2018). Alternative to xylene as a clearing agent in histopathology. *Journal of Laboratory Physicians*, *10*(2), 189–193. https://doi.org/10.4103/JLP.JLP_111_17
- Andrady, A. L. (2011). Microplastics in the marine environment. *Marine Pollution Bulletin*, *62*(8), 1596–1605. <https://doi.org/10.1016/j.marpolbul.2011.05.030>
- Arora, M., Anil, A. C., Leliaert, F., Delany, J., & Mesbahi, E. (2013). *Tetraselmis indica* (Chlorodendrophyceae, Chlorophyta), a new species isolated from salt pans in Goa, India. *European Journal of Phycology*, *48*(1), 61–78. <https://doi.org/10.1080/09670262.2013.768357>
- Baechler, B. R., Granek, E. F., Hunter, M. V., & Conn, K. E. (2020). Microplastic concentrations in two Oregon bivalve species: Spatial, temporal, and species variability. *Limnology and Oceanography Letters*, *5*(1), 54–65. <https://doi.org/10.1002/lol2.10124>
- Bahr, L. M., & Lanier, W. P. (1981). *The ecology of intertidal oyster reefs of the South Atlantic Coast: A community profile*.
- Baldwin, B. S. (1995). Selective particle ingestion by oyster larvae (*Crassostrea virginica*) feeding on natural seston and cultured algae. *Marine Biology*, *123*(1), 95–107. <https://doi.org/10.1007/BF00350328>
- Baldwin, B. S., & Newell, R. I. E. (1991). Omnivorous feeding by planktotrophic larvae of the Eastern oyster *Crassostrea virginica*. *Marine Ecology Progress Series*, *78*(3), 285–301. <https://doi.org/10.3354/meps078285>
- Barboza, L. G. A., Dick Vethaak, A., Lavorante, B. R. B. O., Lundebye, A. K., & Guilhermino, L. (2018). Marine microplastic debris: An emerging issue for food security, food safety and human health. *Marine Pollution Bulletin*, *133*(May), 336–348. <https://doi.org/10.1016/j.marpolbul.2018.05.047>
- Barnes, D. K. A., Galgani, F., Thompson, R. C., & Barlaz, M. (2009). Accumulation and fragmentation of plastic debris in global environments. *Philosophical Transactions of the Royal Society B: Biological Sciences*, *364*(1526), 1985–1998. <https://doi.org/10.1098/rstb.2008.0205>
- Barnes, D. K. A., Walters, A., & Gonçalves, L. (2010). Macroplastics at sea around Antarctica. *Marine Environmental Research*, *70*(2), 250–252. <https://doi.org/10.1016/j.marenvres.2010.05.006>
- Barrows, A. P. W., Cathey, S. E., & Petersen, C. W. (2018). Marine environment microfiber contamination: Global patterns and the diversity of microparticle origins. *Environmental Pollution*, *237*, 275–284. <https://doi.org/10.1016/j.envpol.2018.02.062>
- Bergmann, M., Gutow, L., & Klages, M. (2015). Marine anthropogenic litter. In *Marine Anthropogenic Litter*. <https://doi.org/10.1007/978-3-319-16510-3>

- Bergmann, M., Wirzberger, V., Krumpfen, T., Lorenz, C., Primpke, S., Tekman, M. B., & Gerdt, G. (2017). High Quantities of Microplastic in Arctic Deep-Sea Sediments from the HAUSGARTEN Observatory. *Environmental Science and Technology*, 51(19), 11000–11010. <https://doi.org/10.1021/acs.est.7b03331>
- Bikker, J., Lawson, J., Wilson, S., & Rochman, C. M. (2020). Microplastics and other anthropogenic particles in the surface waters of the Chesapeake Bay. *Marine Pollution Bulletin*, 156(January), 111257. <https://doi.org/10.1016/j.marpolbul.2020.111257>
- Brahney, J., Hallerud, M., Heim, E., Hahnenberger, M., & Sukumaran, S. (2020). Plastic rain in protected areas of the United States. *Science*, 368(6496), 1257–1260. <https://doi.org/10.1126/science.aaz5819>
- Brandon, J. A., Freibott, A., & Sala, L. M. (2020). Patterns of suspended and salp- ingested microplastic debris in the North Pacific investigated with epifluorescence microscopy. *Limnology and Oceanography Letters*, 5(1), 46–53. <https://doi.org/10.1002/lol2.10127>
- Bringer, A., Cachot, J., Prunier, G., Dubillot, E., Clérandeau, C., & Hélène Thomas. (2020). Experimental ingestion of fluorescent microplastics by Pacific oysters, *Crassostrea gigas*, and their effects on the behaviour and development at early stages. *Chemosphere*, 254, 1–10. <https://doi.org/10.1016/j.chemosphere.2020.126793>
- Bringer, A., Thomas, H., Prunier, G., Dubillot, E., Bossut, N., Churlaud, C., Clérandeau, C., Le Bihanic, F., & Cachot, J. (2020). High density polyethylene (HDPE) microplastics impair development and swimming activity of Pacific oyster D-larvae, *Crassostrea gigas*, depending on particle size. *Environmental Pollution*, 260. <https://doi.org/10.1016/j.envpol.2020.113978>
- Browne, M. A. (2015). Sources and pathways of microplastics to habitats. In M. Bergmann, L. Gutow, & M. Klages (Eds.), *Marine Anthropogenic Litter* (pp. 229–244). Springer. <https://doi.org/10.1007/978-3-319-16510-3>
- Browne, M. A., Crump, P., Niven, S. J., Teuten, E., Tonkin, A., Galloway, T., & Thompson, R. (2011). Accumulation of microplastic on shorelines worldwide: Sources and sinks. *Environmental Science and Technology*, 45(21), 9175–9179. <https://doi.org/10.1021/es201811s>
- Browne, M. A., Dissanayake, A., Galloway, T. S., Lowe, D. M., & Thompson, R. C. (2008). Ingested microscopic plastic translocates to the circulatory system of the mussel, *Mytilus edulis* (L.). *Environmental Science and Technology*, 42(13), 5026–5031. <https://doi.org/10.1021/es800249a>
- Browne, M. A., Galloway, T., & Thompson, R. (2007). Microplastic—an emerging contaminant of potential concern? *Integrated Environmental Assessment and Management*, 3(4), 559–561. <https://doi.org/https://doi.org/10.1002/ieam.5630030412>
- Bucci, K., Tulio, M., & Rochman, C. M. (2020). What is known and unknown about the effects of plastic pollution: A meta-analysis and systematic review.

- Ecological Applications*, 30(2), 1–16. <https://doi.org/10.1002/eap.2044>
- Burge, D. R. L., & Edlund, M. (2017). *Chaetoceros muelleri*. Diatoms of North America. https://diatoms.org/species/chaetoceros_muelleri
- Camlab Ltd. (2007). *Plastic chemical and condition compatibility chart*. https://sitefiles.camlab.co.uk/RTP_instructions/Plasticcomp.pdf
- Campanale, C., Massarelli, C., Savino, I., Locaputo, V., & Uricchio, V. F. (2020). A detailed review study on potential effects of microplastics and additives of concern on human health. *International Journal of Environmental Research and Public Health*, 17(4). <https://doi.org/10.3390/ijerph17041212>
- Capolupo, M., Franzellitti, S., Valbonesi, P., Lanzas, C. S., & Fabbri, E. (2018). Uptake and transcriptional effects of polystyrene microplastics in larval stages of the Mediterranean mussel *Mytilus galloprovincialis*. *Environmental Pollution*, 241, 1038–1047. <https://doi.org/10.1016/j.envpol.2018.06.035>
- Castillo, A. B., Al-Maslamani, I., & Obbard, J. P. (2016). Prevalence of microplastics in the marine waters of Qatar. *Marine Pollution Bulletin*, 111(1–2), 260–267. <https://doi.org/10.1016/j.marpolbul.2016.06.108>
- Chambers, S. T., Peddie, B., & Pithie, A. (2006). Ethanol disinfection of plastic-adherent micro-organisms. *Journal of Hospital Infection*, 63(2), 193–196. <https://doi.org/10.1016/j.jhin.2006.01.009>
- Chesapeake Bay Foundation. (n.d.). *Eastern Oysters*. Retrieved June 6, 2020, from <https://www.cbf.org/about-the-bay/more-than-just-the-bay/chesapeake-wildlife/eastern-oysters/>.
- Chialanza, M. R., Sierra, I., Pérez Parada, A., & Fornaro, L. (2018). Identification and quantitation of semi-crystalline microplastics using image analysis and differential scanning calorimetry. *Environmental Science and Pollution Research*, 25(17), 16767–16775. <https://doi.org/10.1007/s11356-018-1846-0>
- Cho, Y., Shim, W. J., Jang, M., Han, G. M., & Hong, S. H. (2019). Abundance and characteristics of microplastics in market bivalves from South Korea. *Environmental Pollution*, 245, 1107–1116. <https://doi.org/10.1016/j.envpol.2018.11.091>
- Choi, J. S., Kim, K., Hong, S. H., Park, K. Il, & Park, J. W. (2021). Impact of polyethylene terephthalate microfiber length on cellular responses in the Mediterranean mussel *Mytilus galloprovincialis*. *Marine Environmental Research*, 168(September 2020), 105320. <https://doi.org/10.1016/j.marenvres.2021.105320>
- Christoforou, E., Dominoni, D. M., Lindström, J., Stilo, G., & Spatharis, S. (2020). Effects of long-term exposure to microfibers on ecosystem services provided by coastal mussels. *Environmental Pollution*, 115184. <https://doi.org/10.1016/j.envpol.2020.115184>
- Cole, M. (2016). A novel method for preparing microplastic fibers. *Scientific Reports*, 6(October), 1–7. <https://doi.org/10.1038/srep34519>

- Cole, M., Coppock, R., Lindeque, P. K., Altin, D., Reed, S., Pond, D. W., Sørensen, L., Galloway, T. S., & Booth, A. M. (2019). Effects of nylon microplastic on feeding, lipid accumulation, and moulting in a coldwater copepod. *Environmental Science and Technology*, 53(12), 7075–7082. <https://doi.org/10.1021/acs.est.9b01853>
- Cole, M., & Galloway, T. S. (2015). Ingestion of nanoplastics and microplastics by Pacific oyster larvae. *Environmental Science and Technology*, 49(24), 14625–14632. <https://doi.org/10.1021/acs.est.5b04099>
- Cole, M., Liddle, C., Consolandi, G., Drago, C., Hird, C., Lindeque, P. K., & Galloway, T. S. (2020). Microplastics, microfibrils and nanoplastics cause variable sub-lethal responses in mussels (*Mytilus* spp.). *Marine Pollution Bulletin*, 160(April), 1–10. <https://doi.org/10.1016/j.marpolbul.2020.111552>
- Cole, M., Lindeque, P., Fileman, E., Halsband, C., Goodhead, R., Moger, J., & Galloway, T. S. (2013). Microplastic ingestion by zooplankton. *Environmental Science and Technology*, 47(12), 6646–6655. <https://doi.org/10.1021/es400663f>
- Cole, M., Lindeque, P., Halsband, C., & Galloway, T. S. (2011). Microplastics as contaminants in the marine environment: A review. *Marine Pollution Bulletin*, 62(12), 2588–2597. <https://doi.org/10.1016/j.marpolbul.2011.09.025>
- Connors, K. A., Dyer, S. D., & Belanger, S. E. (2017). Advancing the quality of environmental microplastic research. *Environmental Toxicology and Chemistry*, 36(7), 1697–1703. <https://doi.org/10.1002/etc.3829>
- Coppock, R. L., Galloway, T. S., Cole, M., Fileman, E. S., Queirós, A. M., & Lindeque, P. K. (2019). Microplastics alter feeding selectivity and faecal density in the copepod, *Calanus helgolandicus*. *Science of the Total Environment*, 687, 780–789. <https://doi.org/10.1016/j.scitotenv.2019.06.009>
- Coughlan, J. (1969). The estimation of filtering rate from the clearance of suspensions. *Marine Biology*, 2(4), 356–358. <https://doi.org/10.1007/BF00355716>
- Covernton, G. A., Pearce, C. M., Gurney-Smith, H. J., Chastain, S. G., Ross, P. S., Dower, J. F., & Dudas, S. E. (2019). Size and shape matter: A preliminary analysis of microplastic sampling technique in seawater studies with implications for ecological risk assessment. *Science of the Total Environment*, 667, 124–132. <https://doi.org/10.1016/j.scitotenv.2019.02.346>
- Cox, K. D., Covernton, G. A., Davies, H. L., Dower, J. F., Juanes, F., & Dudas, S. E. (2019). Human consumption of microplastics. *Environmental Science and Technology*, 53(12), 7068–7074. <https://doi.org/10.1021/acs.est.9b01517>
- Cózar, A., Martí, E., Duarte, C. M., García-de-Lomas, J., Van Sebille, E., Ballatore, T. J., Eguíluz, V. M., Ignacio González-Gordillo, J., Pedrotti, M. L., Echevarría, F., Troublè, R., & Irigoien, X. (2017). The Arctic Ocean as a dead end for floating plastics in the North Atlantic branch of the Thermohaline Circulation. *Science Advances*, 3(4), 1–9. <https://doi.org/10.1126/sciadv.1600582>

- CP Lab Safety. (n.d.). *Chemical Compatibility Chart*. Retrieved July 21, 2020, from <https://www.calpaclab.com/chemical-compatibility-charts/>
- Crossman, J., Hurley, R. R., Futter, M., & Nizzetto, L. (2020). Transfer and transport of microplastics from biosolids to agricultural soils and the wider environment. *Science of the Total Environment*, *724*, 138334. <https://doi.org/10.1016/j.scitotenv.2020.138334>
- Dawson, A. L., Kawaguchi, S., King, C. K., Townsend, K. A., King, R., Huston, W. M., & Bengtson Nash, S. M. (2018). Turning microplastics into nanoplastics through digestive fragmentation by Antarctic krill. *Nature Communications*, *9*(1), 1–8. <https://doi.org/10.1038/s41467-018-03465-9>
- de Sá, L. C., Oliveira, M., Ribeiro, F., Rocha, T. L., & Futter, M. N. (2018). Studies of the effects of microplastics on aquatic organisms: What do we know and where should we focus our efforts in the future? *Science of the Total Environment*, *645*, 1029–1039. <https://doi.org/10.1016/j.scitotenv.2018.07.207>
- Deksheniaks, M. M., Hofmann, E. E., Klinck, J. M., & Powell, E. N. (1996). Modeling the vertical distribution of oyster larvae in response to environmental conditions. *Marine Ecology Progress Series*, *136*(1–3), 97–110. <https://doi.org/10.3354/meps136097>
- Desforges, J. P. W., Galbraith, M., Dangerfield, N., & Ross, P. S. (2014). Widespread distribution of microplastics in subsurface seawater in the NE Pacific Ocean. *Marine Pollution Bulletin*, *79*(1–2), 94–99. <https://doi.org/10.1016/j.marpolbul.2013.12.035>
- Easterling, D. R., Kunkel, K. E., Arnold, J. R., Knutson, T., LeGrande, A. N., Leung, L. R., Vose, R. S., Waliser, D. E., & Wehner, M. . (2017). Preipitation Change in the United States. In D. J. Wuebbles, D. W. Fahey, K. A. Hibbard, D. J. Dokken, B. C. Stewart, & T. K. Maycock (Eds.), *Climate Science Special Report: Fourth National Assessment, Volume 1* (pp. 207–230). U.S. Global Change Research Program. <https://doi.org/10.7930/J0H993CC>
- Eerkes-Medrano, D., Thompson, R. C., & Aldridge, D. C. (2015). Microplastics in freshwater systems: A review of the emerging threats, identification of knowledge gaps and prioritisation of research needs. *Water Research*, *75*, 63–82. <https://doi.org/10.1016/j.watres.2015.02.012>
- Elliott, A. C., & Woodward, W. A. (2007). *Statistical analysis quick reference guidebook: With SPSS examples*. Sage Publications, Inc.
- Eriksen, M., Lebreton, L. C. M., Carson, H. S., Thiel, M., Moore, C. J., Borerro, J. C., Galgani, F., Ryan, P. G., & Reisser, J. (2014). Plastic Pollution in the World's Oceans: More than 5 Trillion Plastic Pieces Weighing over 250,000 Tons Afloat at Sea. *PLoS ONE*, *9*(12), 1–15. <https://doi.org/10.1371/journal.pone.0111913>
- Free, C. M., Jensen, O. P., Mason, S. A., Eriksen, M., Williamson, N. J., & Boldgiv, B. (2014). High-levels of microplastic pollution in a large, remote, mountain lake. *Marine Pollution Bulletin*, *85*(1), 156–163. <https://doi.org/10.1016/j.marpolbul.2014.06.001>

- Gall, S. C., & Thompson, R. C. (2015). The impact of debris on marine life. *Marine Pollution Bulletin*, 92(1–2), 170–179. <https://doi.org/10.1016/j.marpolbul.2014.12.041>
- Gallager, S. M., Waterbury, J. B., & Stoecker, D. K. (1994). Efficient grazing and utilization of the marine cyanobacterium *Synechococcus* sp. by larvae of the bivalve *Mercenaria mercenaria*. *Marine Biology*, 119(2), 251–259. <https://doi.org/10.1007/BF00349564>
- Gaspar, T. R., Chi, R. J., Parrow, M. W., & Ringwood, A. H. (2018). Cellular bioreactivity of micro- and nano-plastic particles in oysters. *Frontiers in Marine Science*, 5(OCT), 1–8. <https://doi.org/10.3389/fmars.2018.00345>
- Geyer, R. (2020). Production, use, and fate of synthetic polymers. In T. M. Letcher (Ed.), *Plastic waste and recycling: Environmental impact, societal issues, prevention, and solutions* (pp. 13–32). Elsevier Inc.
- Geyer, R., Jambeck, J. R., & Law, K. L. (2017). Production, use, and fate of all plastics ever made. *Science Advances*, 3(7), 25–29. <https://doi.org/10.1126/sciadv.1700782>
- Gonçalves, C., Martins, M., Sobral, P., Costa, P. M., & Costa, M. H. (2019). An assessment of the ability to ingest and excrete microplastics by filter-feeders: A case study with the Mediterranean mussel. *Environmental Pollution*, 245, 600–606. <https://doi.org/10.1016/j.envpol.2018.11.038>
- Ha, J., & Yeo, M. K. (2018). The environmental effects of microplastics on aquatic ecosystems. *Molecular and Cellular Toxicology*, 14(4), 353–359. <https://doi.org/10.1007/s13273-018-0039-8>
- Hartmann, N. B., Rist, S., Bodin, J., Jensen, L. H. S., Schmidt, S. N., Mayer, P., Meibom, A., & Baun, A. (2017). Microplastics as vectors for environmental contaminants: Exploring sorption, desorption, and transfer to biota. *Integrated Environmental Assessment and Management*, 13(3), 488–493. <https://doi.org/10.1002/ieam.1904>
- Helm, M. M., & Bourne, N. (2004). *Hatchery culture of bivalves: A practical manual* (A. Lovatelli (ed.)). FAO Fisheries Department.
- Hermabessiere, L., Dehaut, A., Paul-Pont, I., Lacroix, C., Jezequel, R., Soudant, P., & Duflos, G. (2017). Occurrence and effects of plastic additives on marine environments and organisms: A review. *Chemosphere*, 182, 781–793. <https://doi.org/10.1016/j.chemosphere.2017.05.096>
- Horn, D. A., Granek, E. F., & Steele, C. L. (2020). Effects of environmentally relevant concentrations of microplastic fibers on Pacific mole crab (*Emerita analoga*) mortality and reproduction. *Limnology and Oceanography Letters*, 5(1), 74–83. <https://doi.org/10.1002/lol2.10137>
- Isensee, B. K., & Valdes, L. (2015). *GSRD 2015 Brief Marine Litter: Microplastics*.
- Jambeck, J. R., Geyer, R., Wilcox, C., Siegler, T. R., Perryman, M., Andrady, A., Narayan, R., & Law, K. L. (2015). Plastic waste inputs from land into the ocean.

- American Association for the Advancement of Science*, 347(6223), 768–771.
<https://doi.org/https://doi.org/10.1126/science.1260352>
- Jemec, A., Horvat, P., Kunej, U., Bele, M., & Kržan, A. (2016). Uptake and effects of microplastic textile fibers on freshwater crustacean *Daphnia magna*. *Environmental Pollution*, 219, 201–209.
<https://doi.org/10.1016/j.envpol.2016.10.037>
- Kach, D. J., & Ward, J. E. (2008). The role of marine aggregates in the ingestion of picoplankton-size particles by suspension-feeding molluscs. *Marine Biology*, 153(5), 797–805. <https://doi.org/10.1007/s00227-007-0852-4>
- Karbalaei, S., Hanachi, P., Walker, T. R., & Cole, M. (2018). Occurrence, sources, human health impacts and mitigation of microplastic pollution. *Environmental Science and Pollution Research*, 25(36), 36046–36063.
<https://doi.org/10.1007/s11356-018-3508-7>
- Kennedy, V. S. (1996). Biology of Larvae and Spat. In V. S. Kennedy & R. I. E. Newell (Eds.), *The Eastern Oyster: Crassostrea virginica* (pp. 371–421). Maryland Sea Grant College.
- Kennedy, V. S., & Breisch, L. L. (1983). Sixteen Decades of Political Management of the Oyster Fishery in Maryland's Chesapeake Bay. *Journal of Environmental Management*, 164(1332), 153–171.
- Koelmans, A. A., Bakir, A., Burton, G. A., & Janssen, C. R. (2016). Microplastic as a vector for chemicals in the aquatic environment: Critical review and model-supported reinterpretation of empirical studies. *Environmental Science and Technology*, 50(7), 3315–3326. <https://doi.org/10.1021/acs.est.5b06069>
- Koelmans, A. A., Besseling, E., Wegner, A., & Foekema, E. M. (2013). Plastic as a carrier of POPs to aquatic organisms: A model analysis. *Environmental Science and Technology*, 47(14), 7812–7820. <https://doi.org/10.1021/es401169n>
- Kooi, M., Reisser, J., Slat, B., Ferrari, F. F., Schmid, M. S., Cunsolo, S., Brambini, R., Noble, K., Sirks, L. A., Linders, T. E. W., Schoeneich-Argent, R. I., & Koelmans, A. A. (2016). The effect of particle properties on the depth profile of buoyant plastics in the ocean. *Scientific Reports*, 6(September), 1–10.
<https://doi.org/10.1038/srep33882>
- Kosuth, M., Mason, S. A., & Wattenberg, E. V. (2018). Anthropogenic contamination of tap water, beer, and sea salt. *PLoS ONE*, 13(4), 1–18.
<https://doi.org/10.1371/journal.pone.0194970>
- Langdon, C. J., & Newell, R. I. E. (1996). Digestion and nutrition in larvae and adults. In V. S. Kennedy & R. I. E. Newell (Eds.), *The Eastern Oyster: Crassostrea virginica* (pp. 231–270). Maryland Sea Grant College.
- Lau, W. W. Y., Shiran, Y., Bailey, R. M., Cook, E., Stuchtey, M. R., Koskella, J., Velis, C. A., Godfrey, L., Boucher, J., Murphy, M. B., Thompson, R. C., Jankowska, E., Castillo, A. C., Pilditch, T. D., Dixon, B., Koerselman, L., Kosior, E., Favoino, E., Gutberlet, J., ... Palardy, J. E. (2020). Evaluating

- scenarios toward zero plastic pollution. *Science*, 369(6509), 1455–1461.
<https://doi.org/10.1126/SCIENCE.ABA9475>
- Lenz, R., Enders, K., & Nielsen, T. G. (2016). Microplastic exposure studies should be environmentally realistic. *Proceedings of the National Academy of Sciences of the United States of America*, 113(29), E4121–E4122.
<https://doi.org/10.1073/pnas.1606615113>
- Li, J., Liu, H., & Paul Chen, J. (2018). Microplastics in freshwater systems: A review on occurrence, environmental effects, and methods for microplastics detection. *Water Research*, 137, 362–374. <https://doi.org/10.1016/j.watres.2017.12.056>
- Lindeque, P. K., Cole, M., Coppock, R. L., Lewis, C. N., Miller, R. Z., Watts, A. J. R., Wilson-McNeal, A., Wright, S. L., & Galloway, T. S. (2020). Are we underestimating microplastic abundance in the marine environment? A comparison of microplastic capture with nets of different mesh-size. *Environmental Pollution*, 114721. <https://doi.org/10.1016/j.envpol.2020.114721>
- Liu, Z., Yu, P., Cai, M., Wu, D., Zhang, M., Huang, Y., & Zhao, Y. (2019). Polystyrene nanoplastic exposure induces immobilization, reproduction, and stress defense in the freshwater cladoceran *Daphnia pulex*. *Chemosphere*, 215, 74–81. <https://doi.org/10.1016/j.chemosphere.2018.09.176>
- Lozano, R. L., & Mouat, J. (2009). *Marine litter in the North-East Atlantic Region: Assessment and priorities for response*.
- Lusher, A. (2015). Microplastics in the marine environment: Distribution, interactions and effects. In M. Bergmann, L. Gutow, & M. Klages (Eds.), *Marine anthropogenic litter* (pp. 245–307). <https://doi.org/10.1007/978-3-319-16510-3>
- Lusher, A., Hollman, P., & Mandoza-Hill, J. . J. (2017). Microplastics in fisheries and aquaculture. In *FAO Fisheries and Aquaculture Technical Paper* (Vol. 615, Issue July). <https://doi.org/dmd.105.006999> [pii]\r10.1124/dmd.105.006999
- Ma, C., Li, L., Chen, Q., Lee, J., Gong, J., & Shi, H. (2020). Application of internal persistent fluorescent fibers in tracking microplastics in vivo processes in aquatic organisms. *Journal of Hazardous Materials*, June, 123336.
<https://doi.org/10.1016/j.jhazmat.2020.123336>
- Maes, T., Jessop, R., Wellner, N., Haupt, K., & Mayes, A. G. (2017). A rapid-screening approach to detect and quantify microplastics based on fluorescent tagging with Nile Red. *Scientific Reports*, 7(November 2016), 1–10.
<https://doi.org/10.1038/srep44501>
- Maryland Department of Natural Resources. (2018). *A Stock Assessment of the Eastern Oyster, Crassostrea virginica, in the Maryland waters of Chesapeake Bay*.
- Mason, S. A., Welch, V. G., & Neratko, J. (2018). Synthetic polymer contamination in bottled water. *Frontiers in Chemistry*, 6(September).
<https://doi.org/10.3389/fchem.2018.00407>
- McFarland, K., Plough, L. V., Nguyen, M., & Hare, M. P. (2020). Are bivalves

- susceptible to domestication selection? Using starvation tolerance to test for potential trait changes in eastern oyster larvae. *PLoS ONE*, *15*(6 June), 1–20. <https://doi.org/10.1371/journal.pone.0230222>
- Mishra, S., Rath, C. charan, & Das, A. P. (2019). Marine microfiber pollution: A review on present status and future challenges. *Marine Pollution Bulletin*, *140*(November 2018), 188–197. <https://doi.org/10.1016/j.marpolbul.2019.01.039>
- Moore, C. J. (2008). Synthetic polymers in the marine environment: A rapidly increasing, long-term threat. *Environmental Research*, *108*(2), 131–139. <https://doi.org/10.1016/j.envres.2008.07.025>
- Murphy, M. (2017). *Microplastics Expert Workshop Report*. https://www.epa.gov/sites/production/files/2018-03/documents/microplastics_expert_workshop_report_final_12-4-17.pdf
- Naidoo, T., & Glassom, D. (2019). Decreased growth and survival in small juvenile fish, after chronic exposure to environmentally relevant concentrations of microplastic. *Marine Pollution Bulletin*, *145*(June), 254–259. <https://doi.org/10.1016/j.marpolbul.2019.02.037>
- National Oceanic and Atmospheric Administration Marine Debris Program. (2017). Report on Marine Debris as a potential Pathway for Invasive species. In *National Oceanic and Atmospheric Administration Marine Debris Program*. <https://doi.org/10.1016/B978-0-12-805247-1.00024-1>
- Newell, R. I. E. (1988). Ecological changes in Chesapeake Bay: Are they the result of overharvesting the American oyster, *Crassostrea virginica*? *Understanding the Estuary Advances in Chesapeake Bay Research*, *129*, 536–546.
- Nobre, C. R., Moreno, B. B., Alves, A. V., de Lima Rosa, J., da Rosa Franco, H., Abessa, D. M. de S., Maranhão, L. A., Choueri, R. B., Gusso-Choueri, P. K., & Pereira, C. D. S. (2020). Effects of microplastics associated with Triclosan on the oyster *Crassostrea brasiliana*: An integrated biomarker approach. *Archives of Environmental Contamination and Toxicology*, 101–110. <https://doi.org/10.1007/s00244-020-00729-8>
- Pace, D. A., Marsh, A. G., Leong, P. K., Green, A. J., Hedgecock, D., & Manahan, D. T. (2006). Physiological bases of genetically determined variation in growth of marine invertebrate larvae: A study of growth heterosis in the bivalve *Crassostrea gigas*. *Journal of Experimental Marine Biology and Ecology*, *335*(2), 188–209. <https://doi.org/10.1016/j.jembe.2006.03.005>
- Paul-Pont, I., Tallec, K., Gonzalez-Fernandez, C., Lambert, C., Vincent, D., Mazurais, D., Zambonino-Infante, J. L., Brotons, G., Lagarde, F., Fabioux, C., Soudant, P., & Huvet, A. (2018). Constraints and priorities for conducting experimental exposures of marine organisms to microplastics. *Frontiers in Marine Science*, *5*(JUL), 1–22. <https://doi.org/10.3389/fmars.2018.00252>
- Piehl, S., Leibner, A., Löder, M. G. J., Dris, R., Bogner, C., & Laforsch, C. (2018). Identification and quantification of macro- and microplastics on an agricultural farmland. *Scientific Reports*, *8*(1), 1–9. <https://doi.org/10.1038/s41598-018->

- Pierce, K. E., Harris, R. J., Larned, L. S., & Pokras, M. A. (2004). Obstruction and starvation associated with plastic ingestion in a Northern Gannet *Morus bassanus* and a Greater Shearwater *Puffinus gravis*. *Marine Ornithology*, 32(2), 187–189.
- Plastics Europe. (2016). Plastics – the Facts 2016: An analysis of European plastics production, demand and waste data. In *Plastics – the Facts 2016*.
www.plasticseurope.de/informations
- Plastics Europe. (2018). Plastics – the Facts: An analysis of European plastics production, demand and waste data. In *Plastics – the Facts 2018*.
- Poulain, M., Mercier, M. J., Brach, L., Martignac, M., Routaboul, C., Perez, E., Desjean, M. C., & Ter Halle, A. (2019). Small Microplastics As a Main Contributor to Plastic Mass Balance in the North Atlantic Subtropical Gyre. *Environmental Science and Technology*, 53(3), 1157–1164.
<https://doi.org/10.1021/acs.est.8b05458>
- Prata, J. C., Paço, A., Reis, V., da Costa, J. P., Fernandes, A. J. S., da Costa, F. M., Duarte, A. C., & Rocha-Santos, T. (2020). Identification of microplastics in white wines capped with polyethylene stoppers using micro-Raman spectroscopy. *Food Chemistry*, 331(December 2019), 127323.
<https://doi.org/10.1016/j.foodchem.2020.127323>
- Priester, A. (2016). *Effects of salinity on settlement and metamorphosis of the Eastern Oyster (Crassostrea virginica)*. University of Maryland, College Park.
- Qiao, R., Deng, Y., Zhang, S., Wolosker, M. B., Zhu, Q., Ren, H., & Zhang, Y. (2019). Accumulation of different shapes of microplastics initiates intestinal injury and gut microbiota dysbiosis in the gut of zebrafish. *Chemosphere*, 236, 124334. <https://doi.org/10.1016/j.chemosphere.2019.07.065>
- Rainieri, S., Conlledo, N., Larsen, B. K., Granby, K., & Barranco, A. (2018). Combined effects of microplastics and chemical contaminants on the organ toxicity of zebrafish (*Danio rerio*). *Environmental Research*, 162(September 2017), 135–143. <https://doi.org/10.1016/j.envres.2017.12.019>
- Revel, M., Châtel, A., Perrein-Ettajani, H., Bruneau, M., Akcha, F., Sussarellu, R., Rouxel, J., Costil, K., Decottignies, P., Cognie, B., Lagarde, F., & Mouneyrac, C. (2020). Realistic environmental exposure to microplastics does not induce biological effects in the Pacific oyster *Crassostrea gigas*. *Marine Pollution Bulletin*, 150(September 2019). <https://doi.org/10.1016/j.marpolbul.2019.110627>
- Rist, S., Vianello, A., Winding, M. H. S., Nielsen, T. G., Almeda, R., Torres, R. R., & Vollertsen, J. (2020). Quantification of plankton-sized microplastics in a productive coastal arctic marine ecosystem. *Environmental Pollution*, 266, 115248. <https://doi.org/10.1016/j.envpol.2020.115248>
- Rochman, C. M., Brookson, C., Bikker, J., Djuric, N., Earn, A., Bucci, K., Athey, S., Huntington, A., McIlwraith, H., Munno, K., Frond, H. De, Kolomijeca, A., Erdle, L., Grbic, J., Bayoumi, M., Borrelle, S. B., Wu, T., Santoro, S.,

- Werbowski, L. M., ... Hung, C. (2019). Rethinking microplastics as a diverse contaminant suite. *Environmental Toxicology and Chemistry*, 38(4), 703–711. <https://doi.org/10.1002/etc.4371>
- Rochman, C. M., Hoh, E., Hentschel, B. T., & Kaye, S. (2013). Long-term field measurement of sorption of organic contaminants to five types of plastic pellets: Implications for plastic marine debris. *Environmental Science and Technology*, 47(3), 1646–1654. <https://doi.org/10.1021/es303700s>
- Rochman, C. M., Kurobe, T., Flores, I., & Teh, S. J. (2014). Early warning signs of endocrine disruption in adult fish from the ingestion of polyethylene with and without sorbed chemical pollutants from the marine environment. *Science of the Total Environment*, 493, 656–661. <https://doi.org/10.1016/j.scitotenv.2014.06.051>
- Rochman, C. M., Tahir, A., Williams, S. L., Baxa, D. V., Lam, R., Miller, J. T., Teh, F. C., Werorilangi, S., & Teh, S. J. (2015). Anthropogenic debris in seafood: Plastic debris and fibers from textiles in fish and bivalves sold for human consumption. *Scientific Reports*, 5(August), 1–10. <https://doi.org/10.1038/srep14340>
- Romanó de Orte, M., Clowez, S., & Caldeira, K. (2019). Response of bleached and symbiotic sea anemones to plastic microfiber exposure. *Environmental Pollution*, 249, 512–517. <https://doi.org/10.1016/j.envpol.2019.02.100>
- Salaberria, I., Nadvornik-Vincent, C., Monticelli, G., Altin, D., & Booth, A. M. (2020). Microplastic dispersal behavior in a novel overhead stirring aqueous exposure system. *Marine Pollution Bulletin*, 157(June), 111328. <https://doi.org/10.1016/j.marpolbul.2020.111328>
- Science Advice for Policy by European Academies (SAPEA). (2019). A Scientific Perspective on Microplastics in Nature and Society | SAPEA. In *Evidence Review Report* (Issue 4). <https://doi.org/10.26356/microplastics>
- Shields, V. D. C., & Heinbockel, T. (2019). Introductory Chapter: Histological microtechniques. In T. Heinbockel & V. D. C. Shields (Eds.), *Histology* (p. 14). IntechOpen. <https://doi.org/10.5772/intechopen.75080>
- Shim, W. J., Hong, S. H., & Eo, S. E. (2017). Identification methods in microplastic analysis: A review. *Analytical Methods*, 9(9), 1384–1391. <https://doi.org/10.1039/c6ay02558g>
- Smith, M., Love, D. C., Rochman, C. M., & Neff, R. A. (2018). Microplastics in Seafood and the Implications for Human Health. *Current Environmental Health Reports*, 5(3), 375–386. <https://doi.org/10.1007/s40572-018-0206-z>
- Sussarellu, R., Suquet, M., Thomas, Y., Lambert, C., Fabioux, C., Pernet, M. E. J., Goïc, N. Le, Quillien, V., Mingant, C., Epelboin, Y., Corporeau, C., Guyomarch, J., Robbens, J., Paul-Pont, I., Soudant, P., & Huvet, A. (2016). Oyster reproduction is affected by exposure to polystyrene microplastics. *Proceedings of the National Academy of Sciences of the United States of America*, 113(9), 2430–2435. <https://doi.org/10.1073/pnas.1519019113>

- Taltec, K., Huvet, A., Di Poi, C., González-Fernández, C., Lambert, C., Petton, B., Le Goïc, N., Berchel, M., Soudant, P., & Paul-Pont, I. (2018). Nanoplastics impaired oyster free living stages, gametes and embryos. *Environmental Pollution*, 242(March 2019), 1226–1235. <https://doi.org/10.1016/j.envpol.2018.08.020>
- Tekman, M. B., Krumpfen, T., & Bergmann, M. (2017). Marine litter on deep Arctic seafloor continues to increase and spreads to the North at the HAUSGARTEN observatory. *Deep-Sea Research Part I: Oceanographic Research Papers*, 120, 88–99. <https://doi.org/10.1016/j.dsr.2016.12.011>
- Textile Exchange. (2020). *Preferred fiber & materials market report 2020*. 103. https://textileexchange.org/wp-content/uploads/2020/06/Textile-Exchange_PREFERRED-Fiber-Material-Market-Report_2020.pdf%0Ahttps://textileexchange.org/2020-preferred-fiber-and-materials-market-report-pfmr-released/
- Thaysen, C., Stevack, K., Ruffolo, R., Poirier, D., De Frond, H., De Vera, J., Sheng, G., & Rochman, C. M. (2018). Leachate from expanded polystyrene cups is toxic to aquatic invertebrates (*Ceriodaphnia dubia*). *Frontiers in Marine Science*, 4(FEB), 1–9. <https://doi.org/10.3389/fmars.2018.00071>
- Thomas, M., Jon, B., Craig, S., Edward, R., Ruth, H., John, B., Dick, V. A., Heather, L. A., & Matthew, S. (2020). The world is your oyster: low-dose, long-term microplastic exposure of juvenile oysters. *Heliyon*, 6(1). <https://doi.org/10.1016/j.heliyon.2019.e03103>
- Thompson, R. C., Swan, S. H., Moore, C. J., & Vom Saal, F. S. (2009). Our plastic age. *Philosophical Transactions of the Royal Society B: Biological Sciences*, 364(1526), 1973–1976. <https://doi.org/10.1098/rstb.2009.0054>
- Thompson, R. J., Newell, R. I. E., Kennedy, V. S., & Mann, R. (1996). Reproductive processes and early development. In V. S. Kennedy & R. I. E. Newell (Eds.), *The Eastern Oyster: Crassostrea virginica* (pp. 335–370). Maryland Sea Grant College.
- U.S. Army Corps of Engineers. (2019). *Chesapeake Bay Oyster Recovery, MD and VA* (p. 3). <https://cdm16021.contentdm.oclc.org/digital/collection/p16021coll11/id/3450>.
- Van Cauwenberghe, L., & Janssen, C. R. (2014). Microplastics in bivalves cultured for human consumption. *Environmental Pollution*, 193, 65–70. <https://doi.org/10.1016/j.envpol.2014.06.010>
- Waite, H. R., Donnelly, M. J., & Walters, L. J. (2018). Quantity and types of microplastics in the organic tissues of the eastern oyster *Crassostrea virginica* and Atlantic mud crab *Panopeus herbstii* from a Florida estuary. *Marine Pollution Bulletin*, 129(1), 179–185. <https://doi.org/10.1016/j.marpolbul.2018.02.026>
- Walkinshaw, C., Lindeque, P. K., Thompson, R., Tolhurst, T., & Cole, M. (2020). Microplastics and seafood: lower trophic organisms at highest risk of

- contamination. *Ecotoxicology and Environmental Safety*, 190(August 2019), 110066. <https://doi.org/10.1016/j.ecoenv.2019.110066>
- Wallace, R. K. (2001). Cultivating the eastern oyster, *Crassostrea virginica*. In *Southern Regional Aquaculture Center* (Issue 432).
- Ward, J. E., Rosa, M., & Shumway, S. E. (2019). Capture, ingestion, and egestion of microplastics by suspension-feeding bivalves : a 40-year history. *Anthropocene Coasts*, 49(June), 39–49.
- Ward, J. E., Zhao, S., Holohan, B. A., Mladinich, K. M., Griffin, T. W., Wozniak, J., & Shumway, S. E. (2019). Selective ingestion and egestion of plastic particles by the blue mussel (*Mytilus edulis*) and Eastern oyster (*Crassostrea virginica*): Implications for using bivalves as bioindicators of microplastic pollution. *Environmental Science and Technology*, 53(15), 8776–8784. <https://doi.org/10.1021/acs.est.9b02073>
- Weber, A., Jeckel, N., Weil, C., Umbach, S., Brennholt, N., Reifferscheid, G., & Wagner, M. (2021). Ingestion and Toxicity of Polystyrene Microplastics in Freshwater Bivalves. *Environmental Toxicology and Chemistry*, 40(8), 2247–2260. <https://doi.org/10.1002/etc.5076>
- Wilberg, M. J., Livings, M. E., Barkman, J. S., Morris, B. T., & Robinson, J. M. (2011). Overfishing, disease, habitat loss, and potential extirpation of oysters in upper Chesapeake Bay. *Marine Ecology Progress Series*, 436, 131–144. <https://doi.org/10.3354/meps09161>
- Woodall, L. C., Sanchez-Vidal, A., Canals, M., Paterson, G. L. J., Coppock, R., Sleight, V., Calafat, A., Rogers, A. D., Narayanaswamy, B. E., & Thompson, R. C. (2014). The deep sea is a major sink for microplastic debris. *Royal Society Open Science*, 1(4). <https://doi.org/10.1098/rsos.140317>
- Woods, M. N., Stack, M. E., Fields, D. M., Shaw, S. D., & Matrai, P. A. (2018). Microplastic fiber uptake, ingestion, and egestion rates in the blue mussel (*Mytilus edulis*). *Marine Pollution Bulletin*, 137(October), 638–645. <https://doi.org/10.1016/j.marpolbul.2018.10.061>
- World Economic Forum. (2016). *The New Plastics Economy: Rethinking the future of plastics* (Issue January). http://www3.weforum.org/docs/WEF_The_New_Plastics_Economy.pdf
- Wright, S. L., Ulke, J., Font, A., Chan, K. L. A., & Kelly, F. J. (2020). Atmospheric microplastic deposition in an urban environment and an evaluation of transport. *Environment International*, 136(November 2019), 105411. <https://doi.org/10.1016/j.envint.2019.105411>
- Yonkos, L. T., Friedel, E. A., Perez-Reyes, A. C., Ghosal, S., & Arthur, C. D. (2014). Microplastics in four estuarine rivers in the chesapeake bay, U.S.A. *Environmental Science and Technology*, 48(24), 14195–14202. <https://doi.org/10.1021/es5036317>
- Zhao, S., Zhu, L., Wang, T., & Li, D. (2014). Suspended microplastics in the surface

water of the Yangtze Estuary System, China: First observations on occurrence, distribution. *Marine Pollution Bulletin*, 86(1–2), 562–568.
<https://doi.org/10.1016/j.marpolbul.2014.06.032>